NAVAL POSTGRADUATE SCHOOL

MONTEREY, CALIFORNIA

THESIS

NORTH PACIFIC – NORTH AMERICAN CIRCULATION AND PRECIPITATION ANOMALIES ASSOCIATED WITH THE MADDEN–JULIAN OSCILLATION

by

Adam J. Stepanek

March 2006

Thesis Co-Advisors: Tom Murphree
Carlyle Wash

Approved for public release; distribution is unlimited

THIS PAGE INTENTIONALLY LEFT BLANK

REPORT DOCUMENTATION PAGE			Form Approved OMB No. 0704-0188
Public reporting burden for this collection of information is estimated to average 1 hour per response, including the time for reviewing instruction, searching existing data sources, gathering and maintaining the data needed, and completing and reviewing the collection of information. Send comments regarding this burden estimate or any other aspect of this collection of information, including suggestions for reducing this burden, to Washington headquarters Services, Directorate for Information Operations and Reports, 1215 Jefferson Davis Highway, Suite 1204, Arlington, VA 22202-4302, and to the Office of Management and Budget, Paperwork Reduction Project (0704-0188) Washington DC 20503.			
1. AGENCY USE ONLY *(Leave blank)*	**2. REPORT DATE** March 2006	**3. REPORT TYPE AND DATES COVERED** Master's Thesis	
4. TITLE AND SUBTITLE: North Pacific – North American Circulation and Precipitation Anomalies Associated with the Madden-Julian Oscillation		**5. FUNDING NUMBERS**	
6. AUTHOR(S) Adam J. Stepanek			
7. PERFORMING ORGANIZATION NAME(S) AND ADDRESS(ES) Naval Postgraduate School Monterey, CA 93943-5000		**8. PERFORMING ORGANIZATION REPORT NUMBER**	
9. SPONSORING /MONITORING AGENCY NAME(S) AND ADDRESS(ES) N/A		**10. SPONSORING/MONITORING AGENCY REPORT NUMBER**	
11. SUPPLEMENTARY NOTES The views expressed in this thesis are those of the author and do not reflect the official policy or position of the Department of Defense or the U.S. Government.			
12a. DISTRIBUTION / AVAILABILITY STATEMENT Approved for public release; distribution is unlimited		**12b. DISTRIBUTION CODE**	

13. ABSTRACT (maximum 200 words)

The Madden-Julian Oscillation (MJO) has been associated with extreme precipitation events in western North America. However, the mechanisms for, and predictability of these associations are not clear. We have examined the influence of the MJO on North Pacific - North America (NPNA) circulation and precipitation anomalies. We constructed composites of MJO events determined from the Wheeler RMM1/RMM2 index of MJO activity. Our analyses were based on NCEP reanalysis data. We focused our investigations on the impacts on NPNA circulation and precipitation of: (1) the location and amplitude of the MJO; (2) the season of MJO occurrence; and (3) concurrent El Niño (EN) or La Niña (LN) events.

We found that the NPNA response to MJO activity is sensitive to the location of both the convective and subsidence components of the MJO, the season of MJO occurrence, and the existence of concurrent EN or LN events. EN or LN events affect the extratropical response to the MJO by altering the equatorial Rossby-Kelvin wave response to the MJO. This affects the anomalous extratropical wave trains initiated by the MJO, and alters the resulting NPNA precipitation anomalies. Our results provide a foundation for improving extended range forecasts of NPNA circulation and precipitation.

14. SUBJECT TERMS Madden-Julian Oscillation, teleconnections, El Niño, La Niña, climatology, precipitation anomalies			**15. NUMBER OF PAGES** 143
			16. PRICE CODE
17. SECURITY CLASSIFICATION OF REPORT Unclassified	**18. SECURITY CLASSIFICATION OF THIS PAGE** Unclassified	**19. SECURITY CLASSIFICATION OF ABSTRACT** Unclassified	**20. LIMITATION OF ABSTRACT** UL

NSN 7540-01-280-5500

Standard Form 298 (Rev. 2-89)
Prescribed by ANSI Std. 239-18

THIS PAGE INTENTIONALLY LEFT BLANK

Approved for public release; distribution is unlimited

NORTH PACIFIC – NORTH AMERICAN CIRCULATION AND PRECIPITATION ANOMALIES ASSOCIATED WITH THE MADDEN-JULIAN OSCILLATION

Adam J. Stepanek
Captain, United States Air Force
B.S., Valparaiso University, 2001

Submitted in partial fulfillment of the
requirements for the degree of

MASTER OF SCIENCE IN METEOROLOGY

from the

NAVAL POSTGRADUATE SCHOOL
March 2006

Author: Adam J. Stepanek

Approved by: Tom Murphree
Thesis Co-Advisor

Carlyle Wash
Thesis Co-Advisor

Phillip Durkee
Chairman, Department of Meteorology

THIS PAGE INTENTIONALLY LEFT BLANK

ABSTRACT

The Madden-Julian Oscillation (MJO) has been associated with extreme precipitation events in western North America. However, the mechanisms for, and predictability of, these associations are not clear. We have examined the influence of the MJO on North Pacific - North America (NPNA) circulation and precipitation anomalies during the boreal winter. We constructed composites of MJO events during 1979-2005 determined from the Wheeler RMM1/RMM2 index of MJO activity. Our analyses of NPNA anomalies were based primarily on the National Centers for Environmental Prediction reanalysis data set. We focused our investigations on the impacts on NPNA circulation and precipitation of: (1) the location and amplitude of the convective and subsidence components of the MJO; (2) the season of MJO occurrence; and (3) concurrent El Nino (EN) or La Nina (LN) events.

We found that the NPNA response to the MJO is sensitive to the location of both the convective and subsidence components of the MJO, the season of MJO occurrence, and to the existence of concurrent EN or LN events. EN or LN events affect the extratropical response to the MJO by altering the equatorial Rossby-Kelvin wave response to the components of the MJO. This in turn affects the anomalous extratropical wave trains initiated by the MJO, and alters the strength and location of the resulting NPNA precipitation anomalies. Our results have allowed us to identify characteristic patterns associated with the MJO that can be related to the location and intensity of extreme NPNA precipitation. MJO events are relatively persistent phenomena. Thus, increased understanding of the mechanisms by which they impact the extratropics has the potential to improve extratropical extended range forecasting. Our results provide a substantial foundation for improving forecasts of NPNA circulation and precipitation.

THIS PAGE INTENTIONALLY LEFT BLANK

TABLE OF CONTENTS

I. INTRODUCTION 1
A. BACKGROUND 1
B. PRIOR STUDIES REGARDING MJO IMPACTS ON THE WESTERN CONUS 4
1. Prior Studies Characterizing MJO Activity 5
2. Prior Studies of NPNA Circulation and Precipitation Anomalies Associated with the MJO 7
C. DESIGN OF THIS STUDY: ISSUES AND HYPOTHESES 12

II. DATA AND METHODS 15
A. DATA 15
1. Atmospheric Variables 15
2. MJO and ENLN Indices 16
B. METHODS 20
1. Regions and Periods 20
2. Methods for Developing Composites 21
3. Methods for Determining Sensitivity of the NPNA Response to MJOs 25
4. Additional Analysis Methods 26
C. WESTERN CONUS REGION SELECTION 27

III. RESULTS 29
A. THE SENSITIVITIES OF MJO TELECONNECTIONS 29
1. Climatology 29
2. Amplitude Based Method versus Case Following Method 31
3. Baseline composites 31
4. Sensitivity of the NPNA Response to the Phase of the MJO 36
5. Sensitivity of the NPNA Response to MJO Amplitude 39
6. Sensitivity of the NPNA Response to the Season of MJO Occurrence 44
7. Sensitivity of the NPNA Response to Concurrent El Niño / La Niña / Neutral Conditions 47
8. Impacts of Applying a Lag to MJO Event Composites 52
B. AN ANALYSIS OF MJO IMPACTS ON PRECIPITATION IN WESTERN NORTH AMERICA 53
1. Three Critical Factors and 48 Composites Approach 53
2. Analysis of Wet and Dry Regimes for Regions Along the Pacific Coast of North America 54
a. California and Desert Southwest 54
b. Pacific Northwest 63
c. British Columbia 72

d. Alaska 80
3. Relationships to Prior Studies 87
C. CASE STUDIES OF INDIVIDUAL EVENTS 89
1. December 2004 – January 2005 90
2. December 1996 – January 1997 92
3. January 1995 95
4. Summary of Individual Case Studies 98
D. ADDITIONAL RESULTS WITH NPNA FORECAST IMPLICATIONS 99
1. Role of the Subsidence Component of the MJO 99
2. Rapid and Smooth Transitions in MJO Phase 101
3. Relationships between MJO Amplitude and MJO Event Days 101
4. Relationships between the MJO and Southwest Asia 103
E. CONCLUSIONS 104
IV. SUMMARY AND CONCLUSIONS 107
A. SUMMARY 107
B. TELECONNECTIONS BETWEEN THE MJO AND NPNA CIRCULATION AND PRECIPITATION 107
C. DYNAMICAL MECHANISMS FOR MJO TELECONNECTIONS 108
D. CONTRIBUTIONS OF THIS STUDY 109
E. IMPLICATIONS FOR DEPARTMENT OF DEFENSE FORECASTING 111
F. RECOMMENDATIONS FOR FUTURE RESEARCH 111
LIST OF REFERENCES 115
INITIAL DISTRIBUTION LIST 119

LIST OF ACRONYMS

ABM	Amplitude Based Method
AFB	Air Force Base
AK	Alaska
AZ	Arizona
BC	British Columbia
BOM	Bureau of Meteorology
CA	California
CDC	Climate Diagnostics Center
CFM	Case Following Method
CONUS	contiguous United States
CPC	Climate Prediction Center
DJF	December, January, and February
DoD	Department of Defense
DSW	Desert Southwest
ENLN	El Niño / La Niña
EOF	empirical orthogonal function
HOA	Horn of Africa
hPa	hectopascals
ICM	Individual Case Method
IDL	international date line
IO	Indian Ocean
JFM	January, February, and March
MEI	Multivariate ENSO Index
MJO	Madden-Julian Oscillation
MS	Mississippi
NA	North America
NAM	North American Monsoon
NATL	north Atlantic
NCAR	National Center for Atmospheric Research
NCEP	National Centers for Environmental Prediction
NCL	NCAR Command Language
NPAC	north Pacific
NM	New Mexico
NPNA	North Pacific – North American
OH	Ohio
OLR	Outgoing Longwave Radiation
OND	October, November, and December
OR	Oregon
PNP	persistent north Pacific
PNW	Pacific Northwest
PRA	precipitation rate anomaly
RMM	Real-time Multivariate MJO

SOI	Southern Oscillation Index
SWA	southwest Asia
WA	Washington

LIST OF FIGURES

Figure 1. Composite OLR anomalies and 850-hPa wind vector anomalies for each of the 8 phases of the MJO as described in the Wheeler index of MJO activity. More details regarding this figure can be found in Chapter II. From Wheeler and Hendon (2004). 6

Figure 2. Graphical depiction of MJO activity based on the RMM1/RMM2 index. This depiction indicates the amplitude, position, and motion of the MJO during December 1996 – March 1997. The colors indicate the different months and the numbers indicate the dates within each month. Note the general strength (weakness) of the MJO in much of December, February, and March (late January). From: http://www.bom.gov.au/bmrc/clfor/cfstaff/matw/maproom/RMM/phasediag.list.htm 18

Figure 3. Approximate regions for which periods of anomalous precipitation were identified in order to assess the impacts of MJO activity on western CONUS precipitation. 28

Figure 4. Long term mean 200-hPa geopotential heights from 1968-2003 for the months of October – March. 30

Figure 5. Index of ENLN activity from 1950 to present. Positive values (red) indicate EN regimes while negative values (blue) indicate LN events. Note the bias towards EN events from 1979 to present. From http://www.cdc.noaa.gov/people/klaus.wolter/MEI/ 30

Figure 6. Baseline composite figure for 200-hPa height anomalies for phase 3 of the MJO (all amplitudes, fall and winter seasons combined, all EN / LN / neutral events included). Blue and red circles indicate centers of MJO anomalous convection and subsidence respectively. Black ovals outline the tropical Rossby wave response to the anomalous convection/subsidence. Black arrows indicate energy propagation through anomalous extratropical wave trains. 32

Figure 7. Baseline composite figure for OLR anomalies. Regions of anomalous convection associated with phase 3 MJO events are outlined in blue, and regions of anomalous subsidence are outlined in red 33

Figure 8. Baseline composite figure for precipitation rate anomalies. Blue circle highlights the anomalously high precipitation across BC and the PNW during associated with anomalously onshore flow from the southwest (cf. Fig. 7). 33

Figure 9. Illustration of the equivalent barotropic structure that occurs throughout the extratropics in terms of height anomalies in terms of 500-hPa height anomalies (top) and 850-hPa height anomalies

(bottom). The ability to infer low-level height anomalies from upper-level height anomalies allows one to interpret the low-level flow characteristics from 200-hPa height anomaly charts. 34
Figure 10. Actual 200-hPa height values for baseline composites (MJO: phase 3 for all amplitudes, all EN / LN / neutral regimes and for ONDJFM).. 35
Figure 11. Actual OLR values for the baseline figures (MJO phase 3 for all amplitudes, all EN / LN / neutral regimes and for ONDJFM). 36
Figure 12. Actual precipitation rates for the baseline composites (MJO: phase 3 for all amplitudes, all EN / LN / neutral regimes and for ONDJFM).. 36
Figure 13. Evolution of baseline OLR anomalies with respect to MJO phase. Phase 1 is in the upper-left corner, with a progression to phase 8 in the lower-right corner. Red circles are indicative of the subsidence component (s) of the MJO and blue circles represent the convective component(s). 37
Figure 14. Evolution of baseline 200-hPa height anomalies with respect to MJO phase. Phase 1 is in the upper-left corner, with a progression to phase 8 in the lower-right corner. Black circles indicate equatorial Rossby wave responses to the anomalous tropical convection / subsidence associated with the MJO. Black arrows indicate the approximate path of energy propagation through extratropical wave trains. 38
Figure 15. Composite OLR anomalies for low (left figure) and high (right figure) amplitude phase 3 MJO events with respect to the baseline OLR anomalies (top figure). These composites illustrate how the OLR anomalies are stronger during high amplitude MJO events when separated from the low amplitude events, albeit slightly in some phases, including phase 3. 40
Figure 16. 200-hPa anomalies for low (left figure) and high (right figure) amplitude phase 3 MJO events with respect to the corresponding baseline figure (top figure). Blue and red circles highlight features discussed in the text. 41
Figure 17. Same as Fig. 15, but for phase 1 composites. Note the stronger anomalous convection (subsidence) over the western IO (Maritime Continent) in the high amplitude case composite than in the low amplitude composite. 42
Figure 18. Same as Fig. 16, but for phase 1 composites. The height anomalies in the low and high amplitude composites have roughly similar overall patterns but different positions, shapes, and orientations. 42
Figure 19. Same as Figs. 15 and 17, but for phase 8 composites. A stronger subsidence component of the MJO is evident in the high amplitude composite. 43
Figure 20. Same as Figs. 16 and 18, but for phase 8 composites. The height anomalies in the low and high amplitude composites have similar overall patterns but different positions, shapes, and orientations. 43

Figure 21. Phase 3 MJO baseline figure (top) for OLR anomalies separated into OND (left) and JFM (right) composites for the purposes of testing the sensitivity of the NPNA response to the season of MJO occurrence. Note the southward shift from fall to winter in the anomalous tropical convection and subsidence components of the MJO. 44
Figure 22. Phase 3 MJO baseline figure (top) for OLR anomalies separated into OND (bottom left) and JFM (bottom right) composites for the purposes of testing the sensitivity of the NPNA response to the season of MJO occurrence. Strong differences in anomaly intensities are evident between the seasons, but the overall anomalous wave train patterns are roughly similar. 45
Figure 23. Same as Fig. 23, but for phase 4. Note the major differences circled in red across the NPAC and NATL regions between the OND and JFM composites. 46
Figure 24. Same as Figs. 23 and 24, but for phase 5. Implications in separating the OND composites from the JFM composites are significant over the western CONUS for this phase by the anomalous flow that would result from the anomalous offshore height patterns. 46
Figure 25. Same as Figs. 23 – 25, but for Phase 8. This phase exhibited the most significant differences from OND to JFM, which is evidenced by a strong anomalous high over the NPAC in fall transitioning to a strong anomalous low in winter. 47
Figure 26. Breakdown of phase 3 MJO events in terms of ENLN background regime. OLR anomalies for: baseline composite (top) LN composite (2nd from top) and EN composite (3rd from top) and neutral composite (neither EN nor LN, bottom). Differences in tropical OLR anomalies are consistent with constructive and destructive interference between convective and subsidence components of the MJO, EN, and LN. Ovals highlight features discussed in text. 49
Figure 27. Schematic of EN (top) and LN (bottom) convective and subsidence components. Blue (red) ovals are indicative of anomalous convection (subsidence) due to ENLN. 50
Figure 28. Same as Figure 28, but for 200-hPa height anomalies. Note the large differences in the strength of the tropical Rossby wave response over southern Asia (black ovals). 51
Figure 29. Precipitation rate anomalies for the five composites with the most positive precipitation rate anomalies for the CA-DSW region. The critical factor conditions for these five composites are shown in Table 7. 56
Figure 30. Precipitation rate anomalies for the five composites with the most negative precipitation rate anomalies for the CA-DSW region. The

critical factor conditions for these five composites are shown in Table 7. 57
Figure 31. 200-hPa height anomalies for the five composites with the most positive precipitation rate anomalies for the CA-DSW region. The critical factor conditions for these five composites are shown in Table 7. 60
Figure 32. 200-hPa height anomalies for the five composites with the most negative precipitation rate anomalies for the CA-DSW region. The critical factor conditions for these five composites are shown in Table 7. 61
Figure 33. Composites of all days in the five composites with the most positive precipitation rate anomalies for the CA-DSW region (Fig. 29) for 200-hPa height anomalies (left) and precipitation rate anomalies (right). Blue arrows and ovals highlight regions of anomalously onshore flow and positive precipitation rates, and red ovals and arrows indicate anomalously offshore flow and negative precipitation rates. 62
Figure 34. Composites of all days in the five composites with the most negative precipitation rate anomalies for the CA-DSW region (Fig. 30) for 200-hPa height anomalies (left) and precipitation rate anomalies (right). Blue arrows and ovals highlight regions of anomalously onshore flow and positive precipitation rates, and red ovals and arrows indicate anomalously offshore flow and negative precipitation rates. 62
Figure 35. Precipitation rate anomalies for the five composites with the most positive precipitation rate anomalies for the PNW region. The critical factor conditions for these five composites are shown in Table 9. 65
Figure 36. Precipitation rate anomalies for the five composites with the most negative precipitation rate anomalies for the PNW region. The critical factor conditions for these five composites are shown in Table 9. 66
Figure 37. 200-hPa height anomalies for the five composites with the most positive precipitation rate anomalies for the PNW region. The critical factor conditions for these five composites are shown in Table 9. 67
Figure 38. 200-hPa height anomalies for the five composites with the most negative precipitation rate anomalies for the PNW region. The critical factor conditions for these five composites are shown in Table 9. 68
Figure 39. Composites of all days in the five composites with the most positive precipitation rate anomalies for the PNW region (Fig. 35) for 200-hPa height anomalies (left) and precipitation rate anomalies (right). Blue arrows and ovals highlight regions of anomalously onshore

flow and positive precipitation rates, and red ovals and arrows indicate anomalously offshore flow and negative precipitation rates. . 70
Figure 40. Composites of all days in the five composites with the most negative precipitation rate anomalies for the PNW region (Fig. 36) for 200-hPa height anomalies (left) and precipitation rate anomalies (right). Blue arrows and ovals highlight regions of anomalously onshore flow and positive precipitation rates, and red ovals and arrows indicate anomalously offshore flow and negative precipitation rates. 71
Figure 41. Precipitation rate anomalies for the five composites with the most positive precipitation rate anomalies for the BC region. The critical factor conditions for these five composites are shown in Table 11..... 73
Figure 42. Precipitation rate anomalies for the five composites with the most negative precipitation rate anomalies for the BC region. The critical factor conditions for these five composites are shown in Table 11..... 74
Figure 43. 200-hPa height anomalies for the five composites with the most positive precipitation rate anomalies for the BC region. The critical factor conditions for these five composites are shown in Table 11..... 75
Figure 44. 200-hPa height anomalies for the five composites with the most negative precipitation rate anomalies for the BC region. The critical factor conditions for these five composites are shown in Table 11..... 76
Figure 45. Composites of all days in the five composites with the most positive precipitation rate anomalies for the BC region (Fig. 41) for 200-hPa height anomalies (left) and precipitation rate anomalies (right). Blue arrows and ovals highlight regions of anomalously onshore flow and positive precipitation rates, and red ovals and arrows indicate anomalously offshore flow and negative precipitation rates. . 78
Figure 46. Composites of all days in the five composites with the most negative precipitation rate anomalies for the BC region (Fig. 42) for 200-hPa height anomalies (left) and precipitation rate anomalies (right). Blue arrows and ovals highlight regions of anomalously onshore flow and positive precipitation rates, and red ovals and arrows indicate anomalously offshore flow and negative precipitation rates. 79
Figure 47. Precipitation rate anomalies for the five composites with the most positive precipitation rate anomalies for the southern AK region. The critical factor conditions for these five composites are shown in Table 13. 82
Figure 48. Precipitation rate anomalies for the five composites with the most negative precipitation rate anomalies for the southern AK region. The critical factor conditions for these five composites are shown in Table 13. 83
Figure 49. 200-hPa height anomalies for the five composites with the most positive precipitation rate anomalies for the southern AK region.

The critical factor conditions for these composites are shown in Table 13. 84
Figure 50. 200-hPa height anomalies for the five composites with the most negative PRAs for the southern AK region. The critical factor conditions for these composites are shown in Table 13. 85
Figure 51. Composites of all days in the five composites with the most positive precipitation rate anomalies for the southern AK region (Fig. 47) for 200-hPa height anomalies (left) and precipitation rate anomalies (right). Blue arrows and ovals highlight regions of anomalously onshore flow and positive precipitation rates, and red ovals and arrows indicate anomalously offshore flow and negative precipitation rates. 86
Figure 52. Composites of all days in the five composites with the most negative precipitation rate anomalies for the southern AK region (Fig. 48) for 200-hPa height anomalies (left) and precipitation rate anomalies (right). Blue arrows and ovals highlight regions of anomalously onshore flow and positive precipitation rates, and red ovals and arrows indicate anomalously offshore flow and negative precipitation rates. 86
Figure 53. Wheeler phase-space diagram for 1 Dec 2004 to 31 Mar 2005 (Dec in brown, Jan in blue). The late December – early January period in which anomalously heavy precipitation occurred in southern CA is highlighted by the red oval. Accounting for a lag of about one week between the development of MJO conditions in the tropics and the development of an NPNA response to those conditions, indicates that the MJO conditions most closely associated with the southern CA precipitation anomaly were: phases 1-4, with low amplitudes in phases 1-3 and moderate amplitudes in phase 4. 91
Figure 54. 200-hPa height anomalies (left) and precipitation rate anomalies (right) for a strong precipitation event over southern California during late December 2004 - early January 2005. Anomalously onshore (offshore) flow and positive (negative) precipitation anomalies are marked by blue (red) arrows (left panel) and ovals (right panel). Black arrows designate the energy propagation through an anomalous extratropical wave train extending from southeast Asia into the NPNA region. 92
Figure 55. Wheeler phase-space diagram for 1 Dec 1996 to 31 Mar 1997 (Dec in red, Jan in green). The December – January period in which anomalously heavy precipitation occurred across central and northern CA is outlined by the red arrow. Accounting for a lag of about one week between the development of MJO conditions in the tropics and the development of an NPNA response to those conditions indicate that intense rainfall periods occurred in the middle to late phases of the MJO. 94

Figure 56. 200-hPa height anomalies (left) and precipitation rate anomalies (right) for a strong precipitation event over central and northern California during late December 1996 – March 1997. Anomalously onshore (offshore) flow and positive (negative) precipitation anomalies are marked by blue (red) arrows (left panel) and ovals (right panel). Black arrows designate the energy propagation through anomalous extratropical wave trains extending from Asia into the NPNA region. 95
Figure 57. Wheeler phase-space diagram for 1 Dec 1994 to 31 Mar 1995 (Jan in green). The January period in which anomalously heavy precipitation occurred in CA is highlighted by the red oval. Accounting for a lag of about one week between the development of MJO conditions in the tropics and the development of an NPNA response to those conditions, indicates that the MJO conditions most closely associated with the positive precipitation anomalies in CA were phases 2-5, with low amplitudes in phases 2-3 and moderate amplitudes in phases 4-5..... 97
Figure 58. 200-hPa height anomalies (left) and precipitation rate anomalies (right) for a strong precipitation event over California during January 1995. Anomalously onshore (offshore) flow and positive (negative) precipitation anomalies are marked by blue (red) arrows (left panel) and ovals (right panel). Black arrows designate the energy propagation through an anomalous extratropical wave train extending from southeast Asia into the NPNA region. 98
Figure 59. 200-hPa height anomaly for a composite of all MJO events with an amplitude of 1.0 or greater, in phase 1, during October-March, and during EN, LN, or neutral conditions. Black oval indicates tropical Rossby wave response to MJO subsidence over the Maritime Continent. Black arrow indicates the propagation of energy through the anomalous extratropical wave train. 100
Figure 60. Average number of event days per phase, based on an average of all phases for MJO events with low amplitude (blue), medium amplitude (purple), and high amplitude (yellow), and analyzed by season: OND (left bars), JFM (middle bars), and October-March (right bars). In both fall and winter, stronger MJOs characteristically take 1-2 days longer to progress through a single MJO phase than do weaker MJOs..... 102
Figure 61. Schematics of low-level anomalous heights and winds flow associated with anomalously dry (left) and wet (right) periods for CA-DSW region. 104
Figure 62. Schematics of low-level anomalous heights and winds flow associated with anomalously dry (left) and wet (right) periods for PNW region. 105

Figure 63. Schematics of low-level anomalous heights and winds flow associated with anomalously dry (left) and wet (right) periods for BC region. 105
Figure 64. Schematics of low-level anomalous heights and winds flow associated with anomalously dry (left) and wet (right) periods for AK region. 106

LIST OF TABLES

Table 1. Approximate locations of MJO convective and subsidence components by longitude, ordered by phase. Regions are approximate, and are derived from Wheeler and Hendon (2004) and are based upon the Real-time Multivariate MJO Indices for DJF. 7

Table 2. Relationships identified by Mo and Higgins (1998) between tropical convection anomalies and U.S. winter precipitation anomalies based on 10-90 day band-pass filtered data. Note the evidence for an anomalous precipitation dipole along the west coast, with wet (dry) conditions in the PNW concurrent with dry (wet) conditions across southern CA and the DSW. 9

Table 3. Tropical Pacific states identified for this study and their corresponding MEI values. These states were used to determine the background conditions under which MJOs occurred during 1979-present. 20

Table 4. Three examples of how MJO events were classified using the Amplitude Based Method for the purpose of creating amplitude based composites. Note how event classifications often contain dates with amplitudes outside of the classification value. 22

Table 5. Example of how MJO events were classified using the Case Following Method for the purpose of creating amplitude based composites. Note that although the MJO event days within phase 4 must meet certain amplitude criteria, the days outside of phase 4 do not to meet any amplitude criteria. 24

Table 6. Relationships between convective and subsidence components of MJO, EN, and LN by the phase of the MJO. Constructive interference means that the convective and subsidence components of the MJO are reinforced by co-located convective and subsidence components of EN or LN. Destructive interference means that the MJO convective and subsidence components are weakened by co-located subsidence and convective components of EN or LN. 52

Table 7. Critical factor conditions for the five wettest and five driest composites for the CA-DSW region. 55

Table 8. Favorable and unfavorable conditions during MJO activity for anomalously wet and dry periods in the CA-DSW region. 63

Table 9. Critical factor conditions for the five wettest and five driest composites for the PNW region. 64

Table 10. Favorable and unfavorable conditions during MJO activity for anomalously wet and dry periods in the PNW region. 71

Table 11. Critical factor conditions for the five wettest and five driest composites for the BC region. 72
Table 12. Favorable and unfavorable conditions during MJO activity for anomalously wet and dry periods in the BC region. 79
Table 13. Critical factor conditions for the five wettest and five driest composites for the AK region. 81
Table 14. Favorable and unfavorable conditions during MJO activity for anomalously wet and dry periods in the AK region. 87
Table 15. Overview comparison of our result with those from prior studies. 89

ACKNOWLEDGMENTS

I would like to thank Prof Tom Murphree and Prof Chuck Wash for their extensive time, patience and wisdom, Lt Col Karl Pfeiffer for his priceless NCL assistance and support, Capt Damon Vorhees for his countless thesis discussions, and to my wife Jill for her many sacrifices over our first nine months of marriage in order that I complete this project and my Master's Degree.

THIS PAGE INTENTIONALLY LEFT BLANK

I. INTRODUCTION

A. BACKGROUND

In order to improve medium to long-range weather forecasts of the extratropics, one must account for climate variations, including remote tropical climate variations, which can affect the behavior of extratropical weather systems. Teleconnections, which are interactions between widely separated parts of the world, can be especially useful in producing such forecasts. Many teleconnections are associated with tropical climate variations, such as El Niño and La Niña (ENLN) events that occur in the tropics but affect many parts of the extratropics.

An example of a tropical climate variation is the Madden-Julian Oscillation (MJO) that occurs at intraseasonal scales and affects the extratropics. The MJO, first recognized by Madden and Julian (Madden and Julian 1971), is approximately a 40-50 day oscillation in tropical convection and circulation that propagates eastward from the western Indian Ocean (IO), into the Pacific, and then further to the east. The oscillation consists of a convective component and a subsidence component, and upper and lower level tropical wind anomalies.

In the winter of 1996–97, a period of intense MJO activity occurred in the tropical IO and Pacific Ocean region. This MJO activity helped to excite and maintain an extratropical wave train that was associated with strong onshore flow into Oregon (OR) and northern California (CA), with a corresponding atmospheric river and pineapple express condition that advected copious amounts of tropical moisture into western North America (NA). The result was catastrophic flooding in the foothills of the Sierra Nevada mountain range, with record levels of flooding near Beale Air Force Base (AFB), as well as in and around Yosemite National Park. Rapidly rising waters from the Feather and Yuba Rivers due to the excessive rainfall resulted in approximately 8,000 civilians taking shelter at Beale AFB, which was located on relatively high ground. United States Air Force personnel provided food, shelter, and medical care in a short notice humanitarian

operation on U.S. soil. Research studies just prior to and after this event indicate that information about on-going MJO activity might be useful in producing better forecasts for much of the North Pacific – North American (NPNA) region, including forecasts for Department of Defense (DoD) operations in this region. Thus, extended range forecasts of the 1996-97 sequence of events might have been improved by using the MJO as a forecast tool, leading to more accurate precipitation and flooding forecasts, and improved emergency management plans.

Although extreme precipitation events in the NPNA region have been shown to be associated with ENLN events, the 1996–97 event occurred during an ENLN neutral year, indicating that climate variations other than ENLN events need to be accounted for in preparing extended range forecasts for the NPNA region. Furthermore, the fact that both ENLN and MJO events can both have major impacts on west coast weather, and can occur at the same time, indicates that the two climate variations phenomena could constructively or destructively interfere with each other in producing NPNA impacts.

Sardeshmukh and Hoskins (1988) found that anomalous tropical convection might initiate an extratropical wave train by creating a Rossby wave source along a subtropical jet. They also found, as other studies have, that the extratropical response was relatively insensitive to the longitude of the anomalous tropical convection. Their results, and those from other studies, also imply that a negative tropical convection anomaly (i.e., one associated with anomalous subsidence) can generate extratropical wave trains similar to those generated by a positive tropical convection anomaly, but opposite in sign. This indicates that MJOs: (1) may generate extratropical wave trains throughout their propagation along the equator, especially in longitudes with a strong subtropical jet; and (2) may do so from both their convective and subsidence components.

Prior studies of the extratropical impacts of the MJO have little to say about the extratropical wave trains and dynamical processes that are associated with MJO activity. Furthermore, there has been a lack of research relating MJO-

induced wave trains to precipitation patterns along the Pacific Coast of the United States while concurrently accounting not just for the phase of the MJO, but also for the strength of the MJO, the role of both the convective and subsidence components of the MJO, and connections between the MJO and ENLN. Our study focused on these topics in an attempt to better explain the role that the MJO plays in influencing weather conditions in the western contiguous U.S. (CONUS) that in turn influence DoD planning and short-term humanitarian operations.

Medium to long-range forecasts, which can be influenced by dynamical processes associated with the MJO, are extremely important to both civilian and DoD planning purposes. Resources can be better used as confidence in weather forecasts increase, and this is especially true in extended-range forecasts and planning. Space shuttle launches, which cost hundreds of millions of dollars to prepare and conduct, are highly sensitive to weather conditions. Having greater confidence in go/no-go weather conditions could help save resources when poor weather conditions have a greater-than-average probability of occurrence. Likewise, civilian issues such as flooding and drought have significant implications to military operations. Regions of the west coast, especially CA and the Desert Southwest (DSW) are highly susceptible to flooding conditions, which may result in military involvement for rescue operations or disaster relief. Exploiting the MJO in forecasting these potential weather conditions has great potential for improving planning and reducing costs before event occurrence, and more efficient resource management after event occurrence.

The use of MJO information in operational forecasting is a relatively new development and the methods for using this information are still being developed and tested. The Climate Prediction Center (CPC) in Boulder currently issues an operational MJO forecast on a weekly basis, indicating locations that stand to be influenced by the MJO on a one to two-week timeframe. Additional information regarding the MJO bulletins issued by CPC can be found at http://www.cpc.ncep.noaa.gov/products/precip/CWlink/MJO/mjo.shtml. These forecasts do not seek to make quantitative forecasts on precipitation, but rather

look to highlight increased risk for above or below average precipitation for areas throughout North America and other parts of the world. The related forecast discussions focus on atmospheric variables that describe the state and evolution of MJO-related features in an attempt to further the understanding of how teleconnections associated with the MJO evolve. Enhancing the understanding of the teleconnections associated with the MJO would make these forecasts more useful, helping to increase the effectiveness of decisions based on these extended-range forecasts

B. PRIOR STUDIES REGARDING MJO IMPACTS ON THE WESTERN CONUS

Previous studies have demonstrated that the MJO influences precipitation across the western CONUS (Bond and Vecchi 2003, Whitaker and Weickmann 2001, Higgins et al. 2000, Jones 2000, Mo 2000), and on the global scale (Hendon and Liebmann 1990, Nogués-Paegle and Mo 1997, Paegle et al. 2000, Hall et al. 2001, Barlow et al. 2005). These studies stem from the breakthrough research by Madden and Julian (1971; see also the follow-on paper, Madden and Julian (1994)). These studies found the oscillation to be a zonal wave number one phenomenon, with an approximate 30-60 day period. The convective anomalies associated with the MJO are most obvious in the IO and Pacific, while the upper-level circulation anomalies are relatively distinct all around the global tropics. A recent paper by Zhang (2005) summed up much of the work performed on the MJO and its associated teleconnections, which continues to become more extensive as researchers realize its potential value of MJO information in extended range forecasting.

Although the work on teleconnections associated with the MJO have been extensive, it is far from exhaustive. Statistically based studies have dominated the MJO teleconnection research over the past decade, leaving many dynamical questions unanswered. A number of subjects regarding the topic have not been addressed in enough detail to increase forecaster confidence to a high level. Results on where precipitation anomalies associated with the MJO occur along

the North American west coast have shown some agreement, but some notable differences. A dipole relationship has been identified where anomalously high (low) precipitation across the Pacific Northwest (PNW) is associated with anomalously low (high) precipitation in southern CA and the DSW. Studies have focused on the location of the convective component of the MJO when relating the MJO to weather conditions in a distant location. However, the role of the amplitude, or strength of the MJO, has been ignored for the most part, as has been the subsidence component of the MJO. Bond and Vecchi (2003) investigated the relationship between the teleconnections associated with the MJO and the season of MJO occurrence, but their results focused solely on Washington (WA) and OR.

The various features of the MJO (e.g., phase, amplitude, season of occurrence, etc.) appear to have the potential to produce significant differences in MJO induced teleconnections to the NPNA. Thus, it is important to systematically investigate the sensitivity of the NPNA response to these MJO features. In addition, it is important to investigate the potential interactions between MJO induced teleconnections and those induced by ENLN. This topic has only been indirectly addressed and only in a few prior studies of the co-existence of MJO and ENLN events (Slingo et al. 1999; Jones 2000; Higgins and Mo 1997).

The following sections focus on prior research into: (1) characterizing MJO activity; and (2) NPNA circulation and precipitation anomalies associated with the MJO.

1. Prior Studies Characterizing MJO Activity

The convective component of the MJO initially develops near the east African coastline and the far western IO. This component then propagates eastward and can be traced in terms of outgoing longwave radiation (OLR) and zonal winds through the IO, into the Maritime Continent, and into the CPAC. Several phases of the MJO have been identified. Figure 1, taken from Wheeler and Hendon (2004) shows the OLR and low-level wind anomalies associated with each phase of the MJO during December, January, and February (DJF).

The MJO is located in phase 1 when the convective component of the MJO is located in the eastern IO, and in phase 8 when the convective component of the MJO is located east of the international date line (IDL). The convective component is usually most intense when it is over or near the Maritime Continent, and can very difficult to identify when it is near east Africa or east of the IDL. Table 1 describes the approximate locations of the convective and subsidence components of the MJO during the boreal winter.

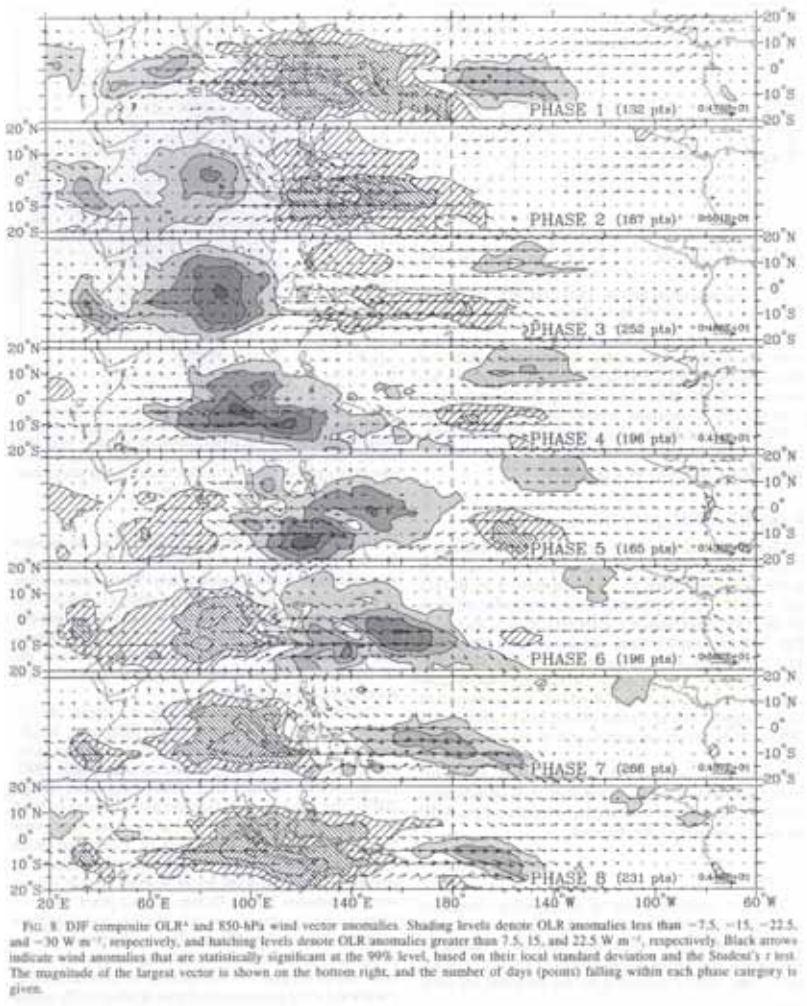

FIG. 8. DJF composite OLR* and 850-hPa wind vector anomalies. Shading levels denote OLR anomalies less than −7.5, −15, −22.5, and −30 W m^{-2}, respectively, and hatching levels denote OLR anomalies greater than 7.5, 15, and 22.5 W m^{-2}, respectively. Black arrows indicate wind anomalies that are statistically significant at the 99% level, based on their local standard deviation and the Student's *t* test. The magnitude of the largest vector is shown on the bottom right, and the number of days (points) falling within each phase category is given.

Figure 1. Composite OLR anomalies and 850-hPa wind vector anomalies for each of the 8 phases of the MJO as described in the Wheeler index of MJO activity. More details regarding this figure can be found in Chapter II. From Wheeler and Hendon (2004).

Phase	Longitude of Convection	Longitude of Subsidence
1	50°E – 80°E; 175°W – 135°W	110°E – 160°E
2	75°E – 105°E	120°E – 175°E
3	75°E – 115°E	155°E – 170°W
4	85°E – 130°E	180° – 160°W
5	110°E – 160°E	50°E – 80°E; 170°W – 135°W
6	130°E – 180°	75°E – 115°E
7	150°E – 160°W	80°E – 120°E
8	180° – 150°W	90°E – 140°E

Table 1. Approximate locations of MJO convective and subsidence components by longitude, ordered by phase. Regions are approximate, and are derived from Wheeler and Hendon (2004) and are based upon the Real-time Multivariate MJO Indices for DJF.

2. Prior Studies of NPNA Circulation and Precipitation Anomalies Associated with the MJO

The interaction between the MJO and NPNA region is based in part on tropical Rossby - Kelvin wave dynamics. Air rising within the convective phase of the MJO creates upper tropospheric anticyclones located poleward and westward of the convection (Matsuno 1966; Gill 1980). In addition, poleward divergent upper tropospheric outflow from the convective region crossing the subtropical jet can create a subtropical Rossby wave source that initiates an

extratropical wave train that extends into the extratropics far from the tropical convective region (Sardeshmukh and Hoskins 1988).

The initiation of the extratropical wave train into the NPNA region is strongly affected by the state of the subtropical jet over the north Pacific. Higgins et al. (2000) noted that as tropical heating related to the MJO convective component moved eastward, there were corresponding changes in the anomalous divergent outflow and subtropical Rossby wave source that were consistent with an observed eastward extension of the north Pacific subtropical jet. Bond and Vecchi (2003) found that teleconnections associated with the MJO across the PNW changed from OND to JFM, apparently due to the evolution of the north Pacific subtropical jet from fall to winter.

Higgins and Mo (1997) investigated how persistent North Pacific (PNP) circulation anomalies are related to intraseasonal and longer term tropical climate variations. Their research focused on some of the mechanisms that generate the circulation anomalies, but did not segregate MJO impacts from those of other tropical climate variations (e.g., ENLN). They found that the tropical anomalies most strongly associated with PNP anomalies occurred more than a week prior to the development of the strongest PNP anomalies. This indicates that the NPNA response lags the tropical forcing by a week or more. It also hints at the possibility that a slowly propagating MJO may be more conducive for setting up an NPNA response than a fast moving MJO.

Mo and Higgins (1998) analyzed anomalies in western U.S. circulation and precipitation patterns using both low pass and band pass filtering of their data. Their study sought to distinguish teleconnections on the intraseasonal scale from those on the interannual scale, but, similar to their 1997 study, did not deal specifically with the MJO. They concluded that tropical intraseasonal (interannual) tropical climate variations are most likely to produce western U.S. precipitation anomalies when the anomalous tropical convection is located at 150-180°E (east of the IDL). Table 2 illustrates these and other results from their study. One of the shortcomings of this study, from the perspective of determining

MJO impacts on the NPNA region, is that it was based heavily on a broad band pass filter spanning 10-90 days. Thus, the MJO anomalies in the tropics and impacts on the extratropics are not clearly distinguished from those occurring at time scales shorter and longer than the MJO scale of 30-60 days.

Longitude of Tropical Convection Anomaly	Regions in U.S. With Above Average Precipitation	Regions in U.S. With Below Average Precipitation
120°E	PNW	CA & DSW
135°E	NONE	CA & OR
150°E	Mid Mississippi (MS) Valley & southern CA	PNW
165°E	NONE	PNW
180°W	DSW & Plains	PNW
165°W	DSW & Plains	PNW
135°W	DSW, Plains, & PNW	Ohio (OH) River Valley
120°W	central Plains & southeastern U.S.	northern CA & OR

Table 2. Relationships identified by Mo and Higgins (1998) between tropical convection anomalies and U.S. winter precipitation anomalies based on 10-90 day band-pass filtered data. Note the evidence for an anomalous precipitation dipole along the west coast, with wet (dry) conditions in the PNW concurrent with dry (wet) conditions across southern CA and the DSW.

Mo (1999) investigated California precipitation during four fall-winter (November-March) periods. She analyzed 10-90 day band pass filtered data using singular spectrum analysis. She identified a 20-25 day mode that was responsible for much of the California intraseasonal variance. She found that the heaviest precipitation over CA was associated with the eastward movement of positive convection anomalies out of the central Pacific and their subsequent decay, and a concurrent development of positive convection anomalies in the IO.

Higgins et al. (2000) related the top 25 extreme precipitation events in coastal regions extending from northern WA to southern CA to tropical intraseasonal oscillations. This study also found evidence for: (1) a dipole in anomalous coastal precipitation, with extreme high (low) precipitation conditions in the PNW often accompanied by extreme low (high) precipitation conditions in the DSW; and (2) abnormally dry conditions inland of the positive coastal precipitation anomalies consistent with troughing over the coast and ridging inland. They concluded that positive precipitation anomalies over the PNW were associated with positive convection anomalies near the Maritime Continent, and that the region of positive west coast precipitation anomalies shifted southward as the tropical convection anomalies progressed eastward into the Pacific, with positive precipitation anomalies in southern CA occurring when the tropical convection anomalies approached 170°E. Finally, they also found evidence that the impacts of the tropical convection anomalies are greater for the northern portions of the west coast (e.g., PNW) than the southern (e.g., southern CA).

Jones (2000) conducted a statistical analysis of circulation patterns, OLR, and precipitation data to investigate the relationship between the MJO and extreme positive precipitation anomalies in CA. He found that positive precipitation events across CA were more common when MJO activity was high. This suggests that the strength of the MJO may be an important factor in understanding, and forecasting, the NPNA response to the MJO. He also identified a slight tendency for positive precipitation anomalies in CA when the MJO convective component was located in the IO. This is in contrast to the findings of Mo and Higgins (1998) who found positive precipitation anomalies in CA when the convective component of the MJO was located near 150°E or 135°W, and negative precipitation anomalies in CA when the convective component of the MJO was located near 120°E (Table 2).

Bond and Vecchi (2003) analyzed the impacts of the MJO on precipitation in WA and OR during October, November, and December (OND) and January, February, and March (JFM). They found that the OND impacts were very different from those for JFM. In particular, they found that in OND, the PNW

tended to have positive (negative) precipitation anomalies when the MJO convective component was near 160-170°E (in the IO). However, they found that in JFM, the PNW tended to have positive (negative) precipitation anomalies when the MJO convective component was near 120°E (near 70°E or 170°E). In addition, the circulation anomalies associated with the OND precipitation anomalies were distinctly different from those associated with similar precipitation anomalies in JFM. They suggested these circulation differences were due to the seasonal southward migration and eastward extension of the north Pacific subtropical jet from OND to JFM.

Lorenz and Hartmann (2006) performed a statistical analysis of circulation and precipitation anomalies in the DSW associated with the MJO during the boreal summer. Their focus was on the effects of the MJO on the North American Monsoon (NAM). MJO activity and teleconnections from the tropics into the NPNA tends to be weaker in the boreal summer. Thus, one would expect the mechanisms by which the MJO affects the NPNA region, and the impacts exerted on the region, to be distinctly different from those in the boreal winter. They concluded that the greatest influence of the MJO on the NAM occurred through anomalous moisture surges from the Gulf of California. The MJO acted as a catalyst in modifying the strength of easterly waves off the coast of Mexico, which in turn triggered the development of surges from the Gulf. They also noted that in New Mexico (NM), which is east of higher terrain, the influence of the MJO was much weaker than in southern CA and Arizona (AZ) due to topographic barriers to the flow of low-level moisture from the Gulf into NM.

In all of these studies, a variety of variables were used, with the most common being OLR and 200-hPa geopotential heights and streamfunction. Some studies used pre-1979 data, while others focused solely on data after 1979 when satellite data was more available. Almost each study had a different method of identifying the MJO periods, and more looked at a variety of intraseasonal, or intraseasonal plus interannual, oscillations rather than the MJO by itself. Some authors used an approach in which periods of active MJO activity were first identified, and then subsequently related to CONUS precipitation, while

other studies used an approach in which periods of extreme precipitation were first identified, and then related back to the state of MJO activity. For our study, we refer to these two methods as *forward* and *backward* approaches, respectively, to denote the time evolution of the teleconnected events being analyzed. Finally, in some studies, a band pass filtering scheme was applied in order to remove synoptic scale phenomena and interannual oscillations, while others used a low pass filter, but did not separate the MJO from longer term oscillations.

C. DESIGN OF THIS STUDY: ISSUES AND HYPOTHESES

Our study was designed to enhance understanding of the NPNA teleconnections associated with the MJO during the boreal winter, with a focus on the MJO as a DoD forecasting tool. We focused on nine main issues.

1. Prior studies have examined the importance of MJO phase, but with different definitions of phase. We chose a well-documented and detailed index that is calculated in near real time and used operationally for analyzing and forecasting the MJO within the tropics (Wheeler and Hendon 2004). We used the eight different MJO phases described by this index to determine the sensitivity of the NPNA response to those phases.

2. The majority of prior studies have neglected to address the strength of the MJO. We conducted an investigation of the sensitivity of the NPNA response to MJO strength.

3. Few prior studies have addressed the sensitivity of the response of the NPNA response to the season of MJO occurrence. We have examined the response using OND, JFM, and Oct-Mar composites.

4. Prior studies have not analyzed how the NPNA response to MJO activity is affected by concurrent ENLN activity. Due to the strong effects of ENLN on western CONUS weather, we separately examined the response to MJO activity when there was a

concurrent El Niño (EN) event, a concurrent La Niña (LN) event, and no concurrent EN or LN event.

5. Many prior studies were based on band pass filtered data in order to isolate the MJO signal. We have analyzed unfiltered data so that: (1) interactions between climate variations at different time scales can be examined (see issue 4, above); and (2) we can more closely approximate the wide range of time scales with which forecasters must contend.

6. Most previous studies have focused on the convective phase of the MJO as the mechanism that drives the anomalous weather in a remote location. We conducted an investigation into whether or not the subsidence component of the MJO plays a role in the generation of the NPNA response.

7. In prior research, very little analysis has been conducted from a forecasting perspective. We performed lagged composites on various phases of the MJO in order to identify predictors of the NPNA response to MJO activity that might be useful in extended range forecasts of NPNA conditions.

8. The majority of previous studies have focused on composites of many separate MJO events and NPNA responses to those events. We conducted studies of individual MJO events and their associated responses to estimate the applicability of composite results to extended range forecasting.

9. Most previous studies were based on statistical analyses, with relatively little attention to the mechanisms that create the NPNA response to MJO activity. We have examined how the extratropical wave train response is generated and maintained by the convective and subsidence components of the MJO, especially via tropical Rossby - Kelvin wave dynamics and extratropical wave generation and propagation processes.

Based on these nine issues, we developed and tested four hypotheses:

1. Teleconnections to the NPNA regions associated with the MJO are sensitive to numerous variables influencing MJO activity, especially the phase of the MJO, the amplitude of the MJO, and the season of MJO occurrence.
2. The NPNA response to MJO activity is sensitive to concurrent ENLN activity
3. Both the convective and subsidence components of the MJO are involved in generating the NPNA response.
4. The RMM1/RMM2 Multivariate MJO index (Wheeler and Hendon 2004) allows forecasters to determine the status of MJO factors that are predictors of the NPNA response to MJO activity.

Deliverable products from this thesis study include: (1) guidance on forecasting precipitation events along the west coast through analyses of the MJO factors that affect NPNA circulation and precipitation in the fall and winter; and (2) graphical illustrations of how these factors affect the NPNA region. Including numerous schematics demonstrating idealized patterns and real-world examples of how MJO influences wave trains affect NPNA weather.

In Chapter II, our data and methods are presented. Chapter III presents our main results, while Chapter IV provides our summary of results, including forecast guidance, discussions and conclusions, and suggestions for future research.

II. DATA AND METHODS

A. DATA

1. Atmospheric Variables

The majority of data used in our study is from the National Center for Environmental Prediction (NCEP) reanalysis data set, which was obtained through the NOAA-CIRES Climate Diagnostics Center (CDC) web site at http://www.cdc.noaa.gov. The NCEP we used consist of atmospheric variables at a 2.5° latitude by 2.5° longitude resolution. Details regarding the reanalysis data can be found in Kalnay et al. (1996) and Kistler et al. (2001). The data can be accessed at http://www.cdc.noaa.gov/cdc/data.nmc.reanalysis.html.

For the purposes of analyzing extratropical wave trains influenced by MJO processes, we focused our analyses on climate anomaly fields, with our long-term means created with a base period of 35 years from 1968 - 2003. We used a combination of geopotential height anomalies at 200, 500, and 850 hectopascals (hPa) to analyze anomalous upper and lower level circulations and wave trains.

We used NOAA Interpolated OLR anomalies (OLRAs) as a proxy for anomalous deep convection in the tropics. The gridded daily OLR dataset, described by Liebmann and Smith (1996), is available at the NOAA-CIRES CDC website at http://www.cdc.noaa.gov/. We used data from 1979 – 2005 in order to weight the dataset toward satellite based data and eliminate periods with known data inconsistencies that occurred prior to 1979, while using working with a multi-decadal period that with numerous examples of MJO, EN, and LN events.

Precipitation rate anomalies (PRAs) from the NCEP reanalysis data were used as a proxy for actual precipitation amounts, and for determining positive and negative precipitation anomalies. The 2.5 x 2.5 degree grid spacing of the precipitation rate data is a shortcoming of this data, since many extreme events occur on the mesoscale. However, we concluded that this dataset was sufficient,

since it allowed us to make the desired conclusions regarding the impacts of large scale circulation anomalies on regional precipitation patterns in the western CONUS.

2. MJO and ENLN Indices

As our index of MJO activity, we used a pre-existing index available online from the Australian Bureau of Meteorology (BOM). This index, maintained by Matthew Wheeler at the BOM and entitled the Real-time Multivariate MJO Series 1 (RMM1) and RMM2, is available on a near real-time basis (Wheeler and Hendon 2004). We chose to base our analyses on the RMM1/RMM2 index throughout this study due to the near-real time availability of the product, as well as because the index has been demonstrated to describe two key aspects of the MJO, location (an indicator of MJO phase) and intensity. The index is based on three variables: 200-hPa zonal winds, 850-hPa zonal winds, and OLR analyzed between 15°S and 15°N, from 1974 to present. Basing the index on three variables instead of one makes the index less vulnerable to bias from non-MJO features, including high-frequency mesoscale phenomena. In addition, this index is increasingly being used the meteorological community as organizations such as the CPC use it in their forecasts. This suggests that the RMM1/RMM2 index will continue to be produced and distributed.

To isolate the MJO from other atmospheric phenomena, the index is based not on the actual values of the three variables, but on the two leading empirical orthogonal functions (EOFs) of the three variables. Together, the two EOFs describe about 25% of the variance. The three atmospheric variables are normalized so that one does not dominate over the others. The use of the two leading EOFs does not eliminate all day-to-day noise, but gives a relatively focused description of the atmospheric variability associated with the MJO.

The OLR data used in the calculation of the index is available within about a day of being collected. The wind data used in the index is not available as soon as the OLR data, but BOM operational model data is used as a temporary proxy for actual zonal wind data. The model data that is used has been highly

correlated with the actual zonal wind values. The use of near-real time data allows the index to be used in near-real time for tropical and extratropical forecasting.

RMM1/RMM2 data is available in both textual and graphical formats, which increases the usefulness of the index in forecasting. Graphical depictions of MJO activity based on the index have been archived for December 1979 - March 1980 to present (Fig. 2). The depictions for the most current 90 days, regardless of month or season, are available from the BOM website. Figure 2 shows an example of a graphical depiction of MJO activity, including a radial axis for MJO amplitude, a unit circle indicating an MJO amplitude of 1.0, and points depicting the strength and location of an individual MJO event. Points closer to the origin indicate weaker MJOs, and vice versa. The location, or phase, of an MJO is indicated by the azimuthal position of the dots, with the dots indicating the location of the convective component with respect to longitude. The numbers next to each dot indicate the date at which the convective component was located at the indicated longitude. The counter-clockwise progression of the dates indicates the eastward propagation of the MJO. The index data is also available in text form for 01 June 1974 to present. All charts and data tables related to the RMM1/RMM2 index, as well as additional information on the index can be seen at http://www.bom.gov.au/bmrc/clfor/cfstaff/matw/maproom/RMM/.

We compared the RMM1/RMM2 index to the CPC MJO index, which is based on pentads of 200-hPa velocity potential and is available dating back to 1978. For the CPC index, daily 200-hPa velocity potential is regressed against ten established patterns constructed by an extended EOF in order to determine both the position and strength of the MJO convective and subsidence components. One advantage of the CPC MJO index is the graphical depiction of both the position and strength of the subsidence component of the MJO, which is not directly available with the RMM1/RMM2 index. Our comparisons of the two indices indicated that the positions of the convective component of the MJO on the RMM1/RMM2 index and the CPC MJO index matched up very well.

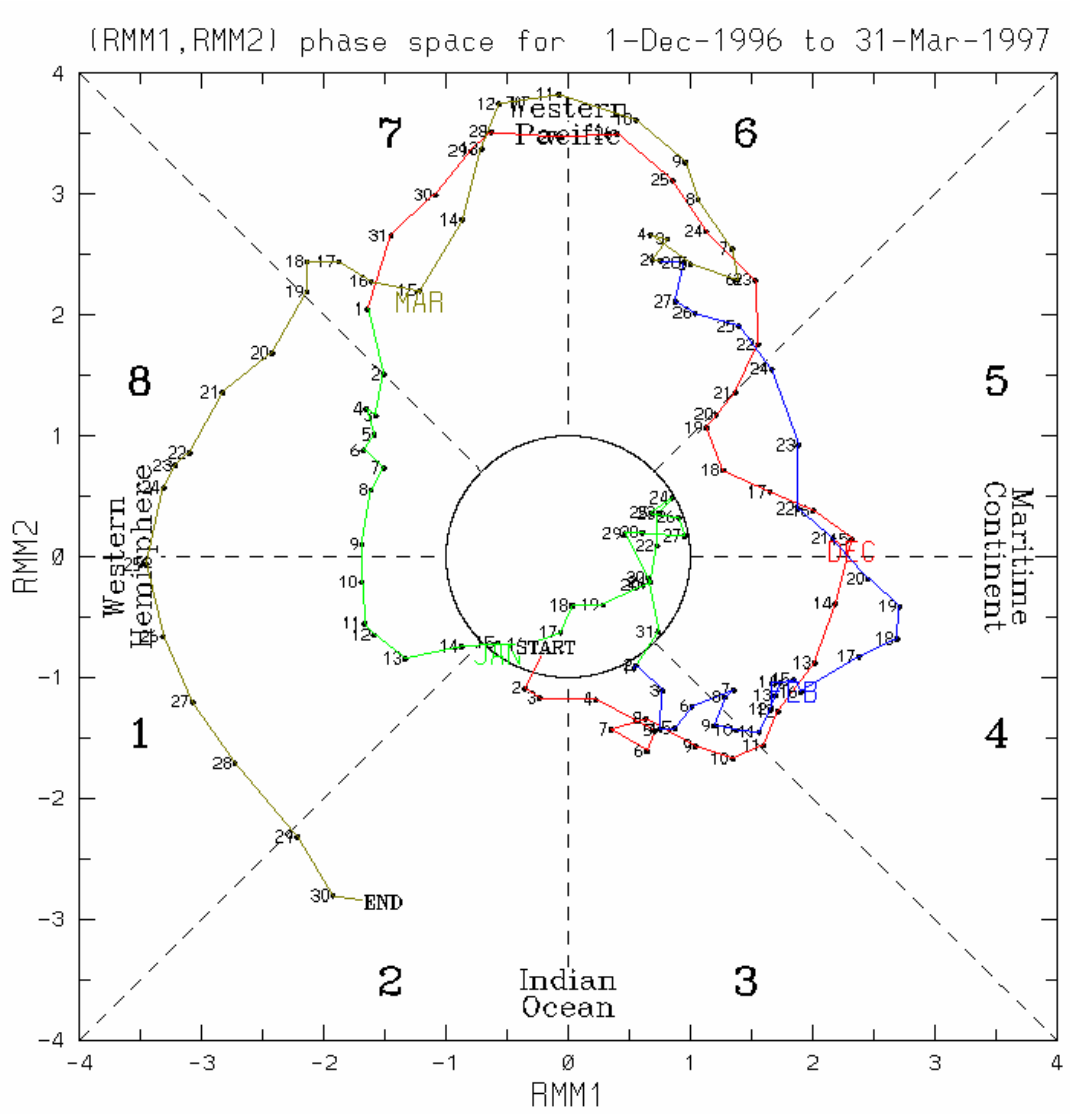

Figure 2. Graphical depiction of MJO activity based on the RMM1/RMM2 index. This depiction indicates the amplitude, position, and motion of the MJO during December 1996 – March 1997. The colors indicate the different months and the numbers indicate the dates within each month. Note the general strength (weakness) of the MJO in much of December, February, and March (late January). From: http://www.bom.gov.au/bmrc/clfor/cfstaff/matw/maproom/RMM/phasediag.list.htm

However, we chose the RMM1/RMM2 index over the CPC index because: (1) the availability of the index data in text; and (2) the CPC index uses only one upper level variable to assess the strength and position of the MJO. Additional details

regarding the CPC MJO Index can be found at http://www.cpc.ncep.noaa.gov/products/precip/CWlink/daily_mjo_index/mjo_index.html.

In order to investigate potential relationships between the MJO and ENLN activity, we compared several different indices of ENLN activity. Although many different indices such as the Southern Oscillation Index (SOI) and NINO3 Index have been frequently used to represent ENLN activity, we chose to utilize the Multivariate ENSO Index (MEI). The MEI is based on six atmospheric and oceanic variables in the tropical Pacific: sea level pressure, zonal surface winds, meridional surface winds, sea surface temperature, surface air temperature, and total cloudiness fraction of the sky (Wolter and Timlin 1993). It is recorded on a bi-monthly scale (e.g. June/July, July/August, December/January, etc). Positive (negative) values of the MEI indicate EN (LN) events, and trends in the numerical data indicate the formation or dissipation of EN or LN events. Updated and historical values of the MEI along with additional information on the index can be found at http://www.cdc.noaa.gov/people/klaus.wolter/MEI/.

In order to use the MEI index to classify MJO events, we needed to define MEI values constituting EN and LN events. We used the MEI values for 1979-present to identify five different states of the tropical Pacific: EN, LN, neutral, positive buffer, and negative buffer. The MEI values corresponding to each condition are shown in Table 3.

One negative aspect to using the MEI is that it is available only at a bi-monthly scale while MJOs have time scales of one to two months. For cases in which an MJO event overlapped two periods with differing MEI values, the average MEI value between the two periods was calculated and assigned to the MJO event. This was a rare occurrence, since ENLN events are relatively low frequency phenomena.

Tropical Pacific State	MEI Values
La Niña Event	MEI ≤ -0.5
Negative Buffer	-0.5 < MEI ≤ -0.4
Neutral Event	-0.4 < MEI < 0.4
Positive Buffer	0.4 ≤ MEI < 0.5
El Niño Event	MEI ≥0.5

Table 3. Tropical Pacific states identified for this study and their corresponding MEI values. These states were used to determine the background conditions under which MJOs occurred during 1979-present.

B. METHODS

1. Regions and Periods

Our research concentrated on times of the year and regions of the globe that are known to be favorable for MJO teleconnections, with the goal of enhancing the current knowledge base for improving DoD weather operations. In order to analyze the global tropical aspects of the MJO, and tropical-extratropical teleconnections into the Northern Hemisphere, we chose a focus region that spanned 20°S to 90°N and 50°E to 110°W. We also did analyses for smaller regions, especially in the northeast Pacific – western CONUS that are described later in this chapter. We focused our attention on the northern fall and winter (October – March), since this is the period in which: (1) MJO activity tends to be high; and (2) tropical-extratropical teleconnections tend to be strong (e.g., Horel and Wallace 1981). We created composites for each month and for several groupings of consecutive months — OND, JFM, and October-March. The multi-month composites were used in order to work with larger datasets and to produce seasonal results.

2. Methods for Developing Composites

In addition to the compositing described in the preceding section, we also composited according to several other factors, including MJO phase, MJO amplitude, and concurrent ENLN state. The basic composting approach we developed is called the Amplitude Based Method (ABM). The ABM is designed to composite together MJO periods with the same phase and similar amplitudes - for example, periods of three or more consecutive days in which the amplitude was greater than or equal to 1.0 while in phase 3. As the MJO is considered weak when the amplitude is less than 1.0, we chose to place our base threshold at 1.0, and further separate high amplitude cases with a base threshold of 1.5. Although it would have been desirable to include a higher threshold to further test the NPNA response to the MJO using the ABM, there was a steadily decreasing number of MJO events, and number of days within each event, as the amplitude threshold was increased. The three consecutive day requirement was used to focus on days with sustained MJO intensity that is most likely to produce persistent and large-scale tropical and extratropical responses. Examples of how the ABM is applied are illustrated in Table 4.

There were some complications in using the ABM. First, some strong MJO events potentially impacting NPNA circulation and precipitation may only have spent one or two days within a given phase, which would have excluded them from being incorporated into the composite. Second, the ABM allows, for a given phase, all days in which the amplitude fell below the threshold to be included in a composite, so long as at least three consecutive days within the phase met or exceeded the threshold (see Table 4). This creates the potential for dates with very weak MJO events to influence the ABM composites. Third, the ABM composites are based on relatively strong events in all eight phases, which may not be the optimal depiction of typical MJOs which are known to be relatively weak in the early phases and late phases and strong in the middle phases (Madden and Julian 1994).

Date	MJO Phase	Amplitude of MJO	Discussion
1979 10 23 1979 10 24 1979 10 25 1979 10 26 1979 10 27 1979 10 28 1979 10 29 1979 10 30	1 1 1 1 1 1 1 1	1.65 1.35 1.24 1.39 1.47 1.55 1.32 1.15	Classified as an amplitude 1.00 event due to the triad of 26-28 October 1979, even though 2 days have amplitudes exceeding 1.50.
1982 11 12 1982 11 13 1982 11 14 1982 11 15 1982 11 16	7 7 7 7 7	0.76 1.00 1.08 1.21 1.39	Classified as an amplitude 1.00 event due to the triad of 14-16 November 1982, even though 1 date has an amplitude less than 1.00 and another has an amplitude above 1.25.
1994 02 01 1994 02 02 1994 02 03 1994 02 04 1994 02 05	2 2 2 2 2	1.24 1.46 1.73 1.72 1.67	Classified as an amplitude 1.50 event due to the triad of 3-5 February 1994, even though one day has an amplitude less than 1.50 and another less than 1.25.

Table 4. Three examples of how MJO events were classified using the Amplitude Based Method for the purpose of creating amplitude based composites. Note how event classifications often contain dates with amplitudes outside of the classification value.

We addressed this third complication with the ABM by developing a second methodology we called the Case Following Method (CFM). The CFM composites events in which the phase 4 MJO amplitude exceeds 1.0 for three or

more consecutive days. The events that are identified through this process are then used to form the composites for all the other seven phases, regardless of the amplitudes in those other phases. This allows the evolution of events that were strong in phase 4 to be analyzed throughout their life cycle, from phase 1 through phase 8. The CFM is intended to give a more realistic depiction of amplitude changes that occur from phase 1 to phase 8. An example of how an MJO event was composited using the CFM is shown in Table 5.

Multiple reasons exist for creating our CFM composites based on phase 4 amplitudes. First, the MJO amplitude is characteristically highest in phase 4. Thus, we were able to create numerous composites from our 26 years of data. In addition, the extratropical Rossby wave response to tropical heating anomalies tends to be large when the anomalies are near the Maritime Continent (the location of the convective component of the MJO in phase 4). The CFM should give a more realistic depiction of the evolution of typical MJO events that are strong during phase 4. This, in turn, should allow a more realistic assessment of the NPNA response to MJO events.

The CFM also has the advantage of being well suited for analyzing the effects of concurrent ENLN events on MJO activity and the extratropical responses to MJOs. Because the same MJO events are used for each phase when constructing the CFM composites, the background state (EN, LN, or neutral) remains the same as well. This facilitates the construction of EN, LN, and neutral composites.

Dates (hypothetical)	MJO Phase	Amplitude of MJO	Discussion
3 Feb 1998	1	0.43	Phase 4 occurred from 11 Feb 1998 to 14 Feb 1998.
4 Feb 1998	1	0.78	
5 Feb 1998	2	1.01	
6 Feb 1998	2	1.21	Event classified as a 1.50, or high amplitude, event due to 3 or more consecutive days within phase 4 above 1.50 in amplitude.
7 Feb 1998	3	0.98	
8 Feb 1998	2	1.01	
9 Feb 1998	3	1.32	
10 Feb 1998	3	1.67	
11 Feb 1998	4	1.56	
12 Feb 1998	4	1.66	
13 Feb 1998	4	1.89	
14 Feb 1998	4	2.02	Note that other phases may have a stronger or weaker amplitude, but are still included in CFM composite for high amplitude events since the events used in the CFM method are based solely on phase 4 amplitude.
15 Feb 1998	5	2.07	
16 Feb 1998	5	1.88	
17 Feb 1998	5	1.45	
18 Feb 1998	5	1.39	
19 Feb 1998	5	1.29	
20 Feb 1998	5	1.03	
21 Feb 1998	5	1.45	
22 Feb 1998	6	1.44	
23 Feb 1998	7	1.21	
24 Feb 1998	8	0.98	
25 Feb 1998	7	0.67	
26 Feb 1998	8	0.65	
27 Feb 1998	8	0.64	

Table 5. Example of how MJO events were classified using the Case Following Method for the purpose of creating amplitude based composites. Note that although the MJO event days within phase 4 must meet certain amplitude criteria, the days outside of phase 4 do not to meet any amplitude criteria.

However, there are some limitations with the CFM. First, the beginning and end of an individual MJO event may be very diffuse and difficult to determine. For instance, some MJO events do not become evident in the data until entering phase 2 or phase 3, some weaken before reaching phase 8, and still others have very weak periods in the middle of the MJO lifecycle. Likewise, slow moving events that linger in a certain phase which may bias the resulting composite toward that event. Another intrinsic problem with the CFM was that

individual MJO cases almost always spanned two or more months, and therefore sometimes resulted in difficulties in creating composites for a specific period of interest. Compositing together different months (e.g. OND, JFM) helped to alleviate this problem while increasing the amount of data contained in each composite, though care had to be taken in ensuring that the same day was not included more than once in each composite.

The third and final key approach we created was the Individual Case Method (ICM), in which individual MJOs were considered rather than composites of many MJOs. The primary reason for including the ICM in our thesis research was to investigate the behavior of individual MJO events for comparison to the results from the composite analyses. These comparisons were used to assess the validity of the composites and to help in the interpretation of individual events.

3. Methods for Determining Sensitivity of the NPNA Response to MJOs

In order to test our hypotheses (chapter I), we developed several methods for selectively analyzing the NPNA response to MJO phase, amplitude, and season of MJO occurrence. In our initial method, we used the ABM with an amplitude threshold of 1.0 to composite together all MJO phase 3 periods during October-November of our 1979 - 2005 study period. These composites included MJOs that occurred during EN, LN, and neutral events. This yielded one set of composites containing the largest possible number of MJO events and days in phase 3. Thus, we designated them the baseline composites.

We then subdivided the baseline composites according to various factors to determine the factors to which the NPNA was most responsive. The resulting smaller composites were based on compositing just the days from the baseline composites:

1. for which the amplitudes were greater than or equal to 1.0 but less than 1.5
2. for which the amplitudes were greater than or equal to 1.5
3. for which the days occurred in OND

4. for which the days occurred in JFM

5. for which the days occurred in an EN period

6. for which the days occurred in a LN period

7. for which the days occurred in a neutral period

These seven additional sets of composites were then compared to the baseline set of composites and to each other to determine the sensitivity of the NPNA response to the factor used to develop the composites. For example, the set 1 composite 200-hPa anomaly fields were compared to those from the baseline composites and from each phase to determine how phase altered the NPNA response.

4. Additional Analysis Methods

In order to investigate MJO impacts on the NPNA region from a forecasting perspective, additional methods were developed. We used lagged analyses to represent the delay in the extratropical response to MJO forcing. Thus, we lagged the extratropical circulation and precipitation rate anomalies with respect to the corresponding MJO dates. We experimented with seven, ten, and 12 day lags and found relatively small differences between them, especially between the seven and ten day lagged results. Based on this result, and results from prior studies (e.g., Higgins and Mo 1997), we used seven days as our standard lag period. The lag analyses were used to investigate the impact of MJO events a week into the future and to estimate the types of NPNA responses that might be predictable.

We also used forward approaches (see chapter I) to determine how specific MJO factors led to subsequent NPNA responses, and backward approaches (see chapter I) to determine how specific NPNA features were related to preceding MJO factors. The ABM and CFM are examples of the forward approach since they are based on specific MJO factors. We used the backward approach in some of our ICM investigations by first identifying the periods of anomalous precipitation in western North America and relating these anomalies back to the properties of the MJO.

Prior MJO studies have used both forward and the backward approaches and both are valid methods of investigating a climate variation such as the MJO and its teleconnections. For example, Jones (2000) employed a backward approach, looking at extreme precipitation events in CA and subsequently relating them to MJO activity. Bond and Vecchi (2003) used a forward approach by compositing the days in which the MJO was active from October through March before relating MJO activity to PNW precipitation data.

We did not do any filtering of the data. This is in contrast to the majority of prior MJO teleconnection studies which have used band or low pass filtering to separate the MJO signal from signals with higher and/or lower frequencies. Band pass filtering designed to isolate the MJO signal is of course advantageous in many respects. However, we chose to do no filtering in order to: (1) assess the interactions between the MJO and other climate variations --- specifically, ENLN; and (2) analyze the combined effects of many simultaneous variations with which forecasters must contend.

C. WESTERN CONUS REGION SELECTION

One of the main goals of our study was to identify the relationships between the MJO and precipitation in the western CONUS. Our preliminary results indicated that the western CONUS precipitation anomalies associated with the MJO were different for different regions of the western CONUS (cf. Higgins et al. 2000; Jones 2000; Bond and Vecchi 2003). Thus, we chose to analyze the precipitation anomalies separately for four major western CONUS regions: southern Alaska, British Columbia, the PNW (Washington and Oregon) and CA and the Desert Southwest (DSW) (Fig. 4). We area averaged the PRAs for the four regions to identify, and composite, periods of positive and negative PRAs. The composites were then used as part of a backward approach to determine the characteristic circulation and precipitation anomalies, and MJO factors, associated with positive and negative PRAs in the four regions.

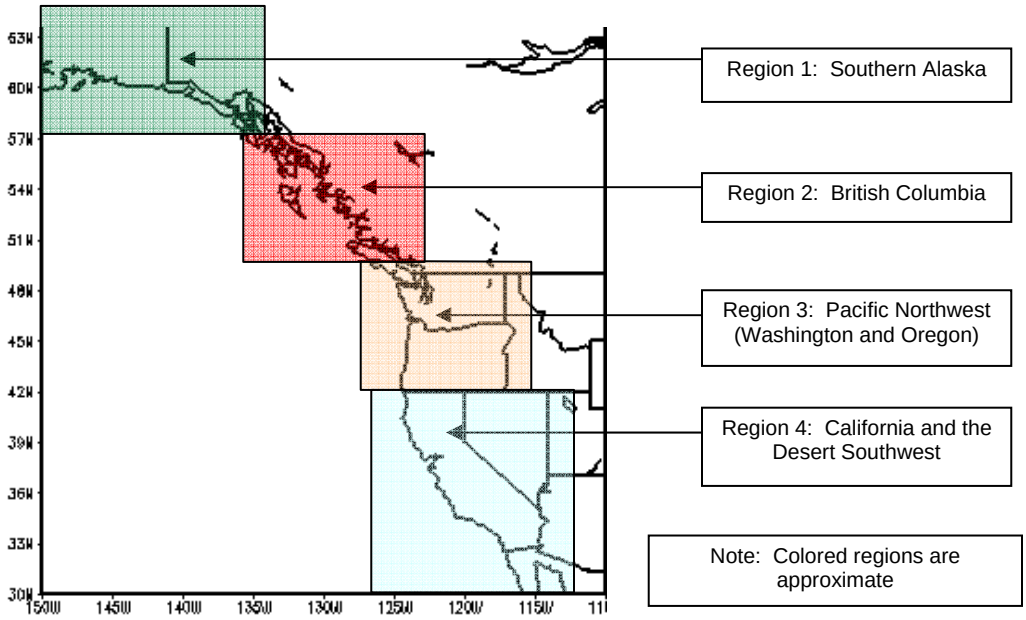

Figure 3. Approximate regions for which periods of anomalous precipitation were identified in order to assess the impacts of MJO activity on western CONUS precipitation.

III. RESULTS

A. THE SENSITIVITIES OF MJO TELECONNECTIONS

We have analyzed the NPNA response to MJO activity to determine the MJO factors and seasonal factors to which the response is most sensitive. We initiated this assessment by establishing baseline composites through which to make comparisons in an effort to establish the most critical variables that affect the MJO induced teleconnections to the NPNA region. Our two main objectives were to identify the: (1) variables that have the greatest influence on the NPNA circulation and precipitation response; and (2) characteristics of MJO induced anomalous precipitation patterns over western North America that can be used to improve extended range forecasting techniques. The results presented in this chapter are based on the MJO methodologies presented in Chapter II, with the initial baseline composite results based on the ABM.

1. Climatology

To understand the results of our climate variation analyses, it is helpful to first review some background climatological issues. The boreal winter months are characterized by an abundance of extratropical weather systems moving across the NPNA region. This is a response to an enhanced jet pattern shifting southward during the fall into the winter months. The southward shift in the track allows tropical moisture to more readily be advected into extratropical synoptic scale systems during the winter than in summer. Figure 4 shows the long-term mean values for 200-hPa geopotential heights for Oct-Mar. An upper-level trough across eastern Asia associated with tight packing of the height contours signifies the location of the core of a strong east Asian – north Pacific jet.

Throughout our period of study (1979-2005), EN events were more prevalent than LN or neutral events. However, enough LN and neutral periods were available to make meaningful comparisons between the differing interannual regimes. As discussed in Chapter II, high MEI indices represent EN events, and low MEI indices indicate LN events (Table 3). During neutral ENSO

conditions, the MEI is close to zero. Figure 5 shows the MEI index over the years of interest, confirming that El Niño events outnumbered La Niña events during our research period.

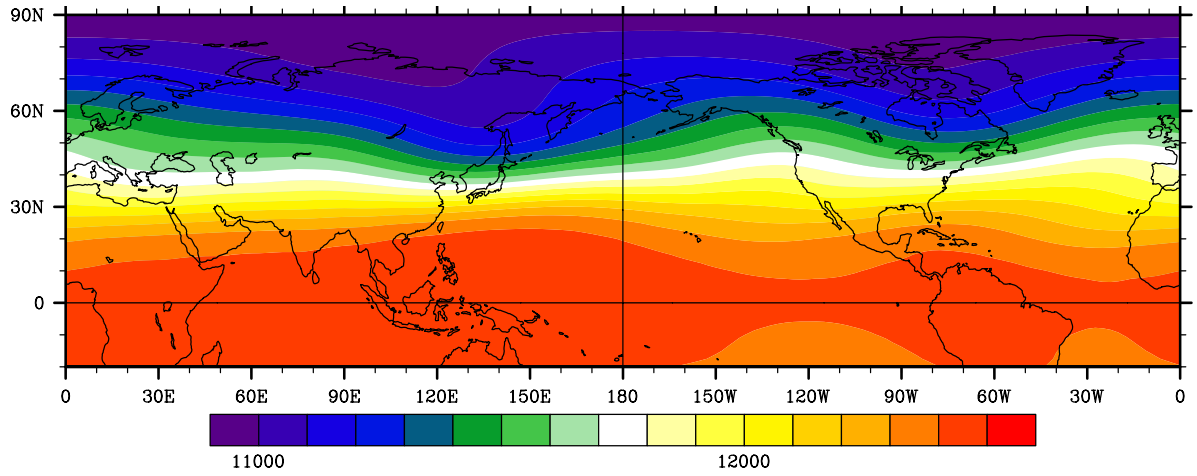

Figure 4. Long term mean 200-hPa geopotential heights from 1968-2003 for the months of October – March.

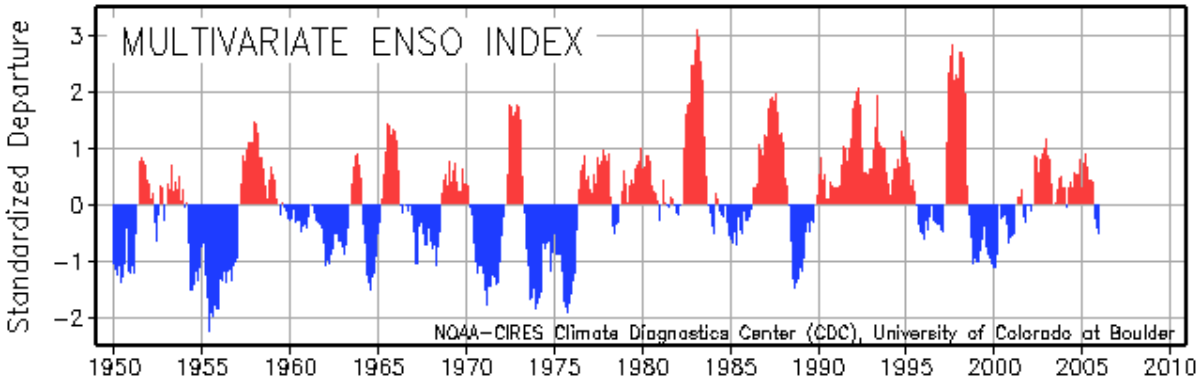

Figure 5. Index of ENLN activity from 1950 to present. Positive values (red) indicate EN regimes while negative values (blue) indicate LN events. Note the bias towards EN events from 1979 to present. From http://www.cdc.noaa.gov/people/klaus.wolter/MEI/

2. Amplitude Based Method versus Case Following Method

We compared results from the ABM to the CFM to determine how using the perhaps more realistic CFM might affect our conclusions about the relationships between the MJO and NPNA circulation and precipitation. We found that the results from the two methods (not shown) were very similar to each other, and therefore both methods appeared suitable for achieving the goals of our study. We chose to use the ABM as our standard method because it allowed us to conduct our analyses on a larger sample size (i.e., larger number of days). This is because the MJO can be difficult to identify at certain times in the evolution of an individual MJO, especially in the early and late phases when the MJO can be very weak.

3. Baseline Composites

As described in Chapter II, we constructed baseline composites using the ABM and the following criteria using the following criteria: MJO events that occurred during phase 3, all MJO amplitudes that were greater than or equal to 1.0, fall and winter months combined, and no separation based on concurrent EN, LN, or neutral conditions. Phase 3 events were used in the baseline composites since our preliminary phase 3 results showed a strong extratropical wave train from the tropical eastern Pacific into the NPNA region (Fig. 6). Also, phase 3 is when the convective component of the MJO begins to gain considerable strength in the eastern IO as it approaches the Maritime Continent from the west, and therefore has a strong potential to influence the extratropical circulation pattern.

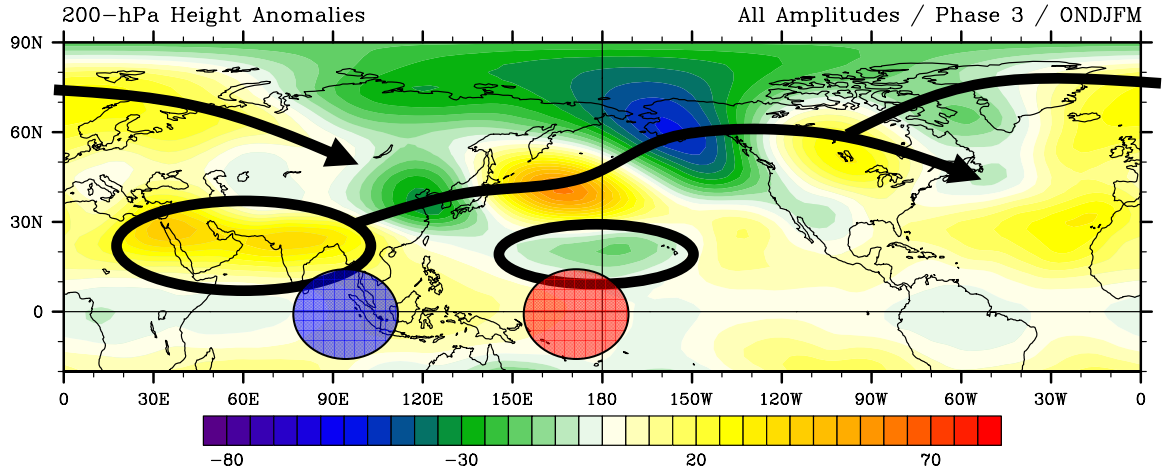

Figure 6. Baseline composite figure for 200-hPa height anomalies for phase 3 of the MJO (all amplitudes, fall and winter seasons combined, all EN / LN / neutral events included). Blue and red circles indicate centers of MJO anomalous convection and subsidence respectively. Black ovals outline the tropical Rossby wave response to the anomalous convection/subsidence. Black arrows indicate energy propagation through anomalous extratropical wave trains.

OLR anomaly patterns reveal the subsidence and convective components of the MJO (Fig. 7). Wheeler and Hendon (2004) described how in phase 3 the convective component of the MJO is typically centered in the eastern IO, while the subsidence component is near the IDL and starting to weaken. This stands out in the baseline composite OLR anomaly (Fig. 7). The anomalous convection located in the eastern IO creates an upper-level tropical Rossby wave response in the form of an upper-level anticyclone over north Africa and southern Asia (Fig. 6). This anomalous anticyclone is also the initial anomaly in an anomalous wave train extending northeastward across east Asia, the north Pacific and into North America (Fig. 6). Over Alaska, the wave train includes an anomalous cyclone and anomalously onshore flow from the southwest into British Columbia (BC) and the PNW, resulting in widespread positive precipitation anomalies over the region (Fig. 8).

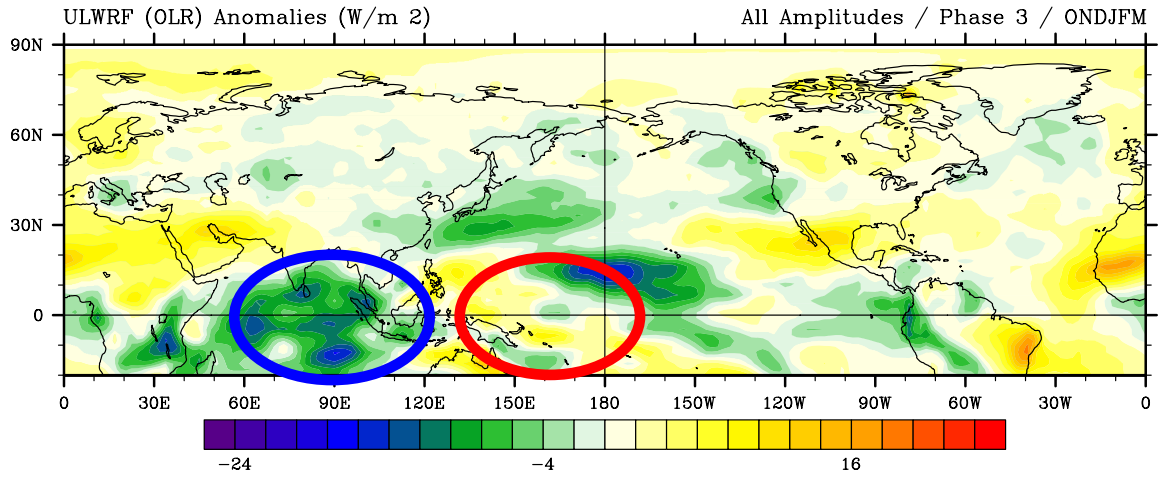

Figure 7. Baseline composite figure for OLR anomalies. Regions of anomalous convection associated with phase 3 MJO events are outlined in blue, and regions of anomalous subsidence are outlined in red

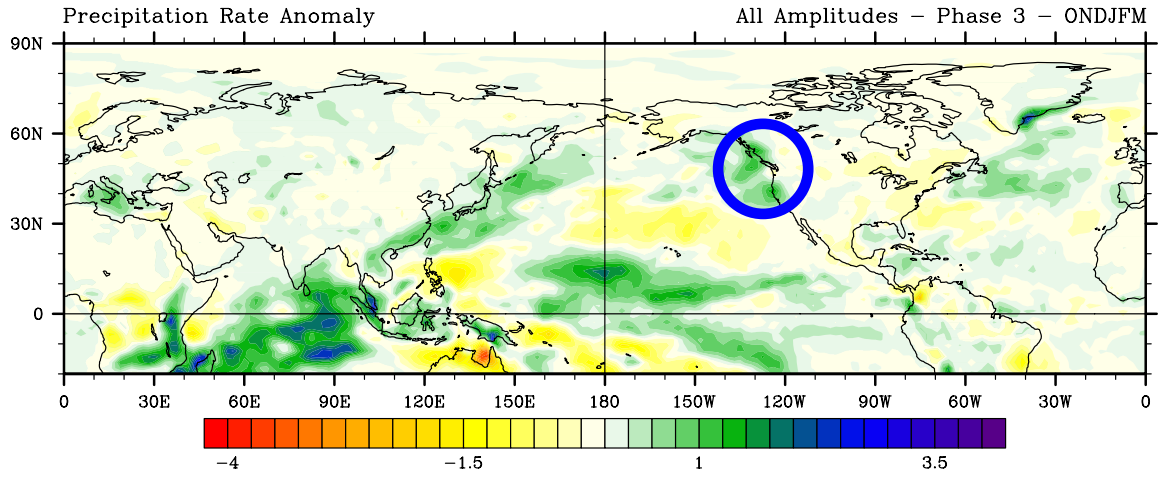

Figure 8. Baseline composite figure for precipitation rate anomalies. Blue circle highlights the anomalously high precipitation across BC and the PNW during associated with anomalously onshore flow from the southwest (cf. Fig. 7).

The 200-hPa height anomalies (Fig. 6) are very similar to those at 500 hPa and 850 hPa (Fig. 9). This indicates the extratropical height anomalies have an equivalent barotropic structure, with anomalous high (low) height patterns in

the low-levels and mid-levels (Fig. 9) being in the same approximate geographic region as anomalous high (low) height patterns in the upper-levels (Fig. 6). This equivalent barotropic structure is found in all our results and allows us to use the 200-hPa height anomalies to infer the extratropical anomalous heights and winds at mid-levels and low-levels, including anomalous onshore (offshore) flow patterns that may result in positive (negative) precipitation anomalies (Fig. 8).

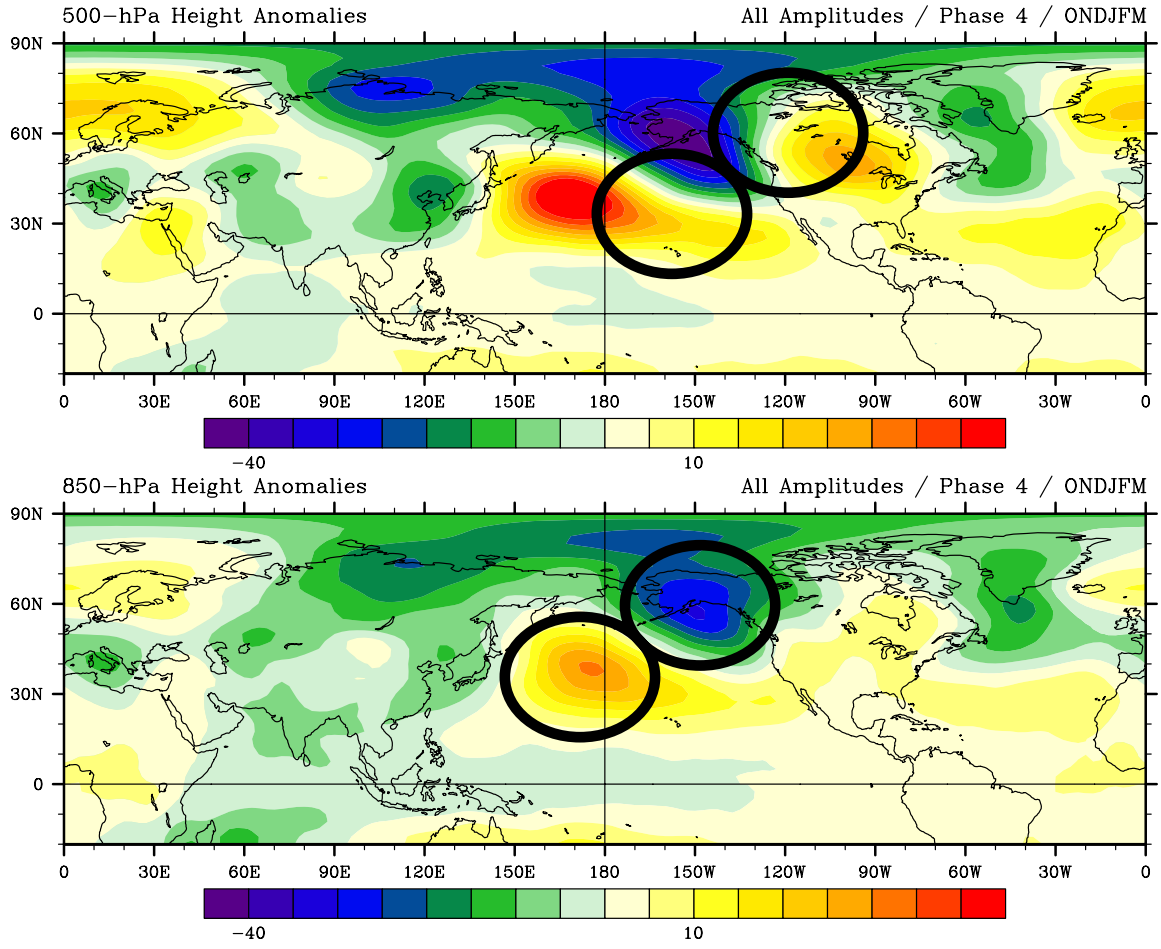

Figure 9. Illustration of the equivalent barotropic structure that occurs throughout the extratropics in terms of height anomalies in terms of 500-hPa height anomalies (top) and 850-hPa height anomalies (bottom). The ability to infer low-level height anomalies from upper-level height anomalies allows one to interpret the low-level flow characteristics from 200-hPa height anomaly charts.

For comparison purposes, actual 200-hPa height values (Fig. 10), actual OLR values (Fig. 11), and actual precipitation rate values (Fig. 12) were composited for the same periods as the anomalous charts above (Figs. 6-8). The anomalous fields are not necessarily representative of the actual weather conditions; positive precipitation anomalies do not necessarily signify that major flooding was occurring in a locale, but rather that the precipitation rate during the composite period was higher-than-average. This comparison holds true for height anomalies and OLR anomalies as well, and should be taken under consideration in the following discussions of anomaly fields.

The baseline composites of heights, OLR, and precipitation rate support the results from prior studies that indicate that the MJO can have profound effects on NPNA circulation and precipitation patterns. Anomalous onshore flow across a large portion of the west coast of North America can be associated with MJO convection and subsidence anomalies. In the following sections we analyze atmospheric variables that we have hypothesized are important in determining the NPNA circulation and precipitation response to the MJO, and that therefore must be taken into consideration when using MJO information in forecasting.

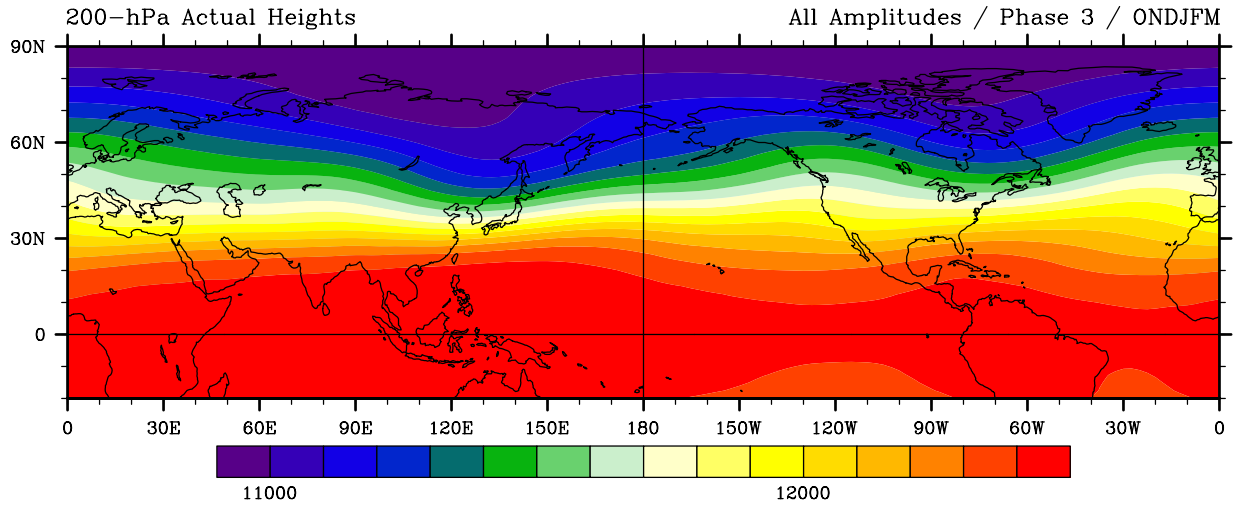

Figure 10. Actual 200-hPa height values for baseline composites (MJO: phase 3 for all amplitudes, all EN / LN / neutral regimes and for ONDJFM).

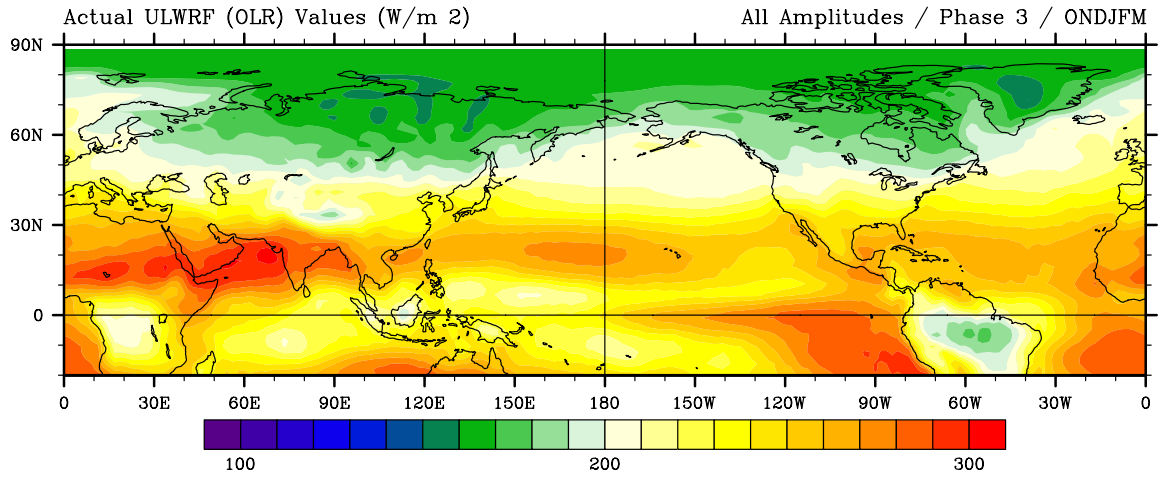

Figure 11. Actual OLR values for the baseline figures (MJO phase 3 for all amplitudes, all EN / LN / neutral regimes and for ONDJFM).

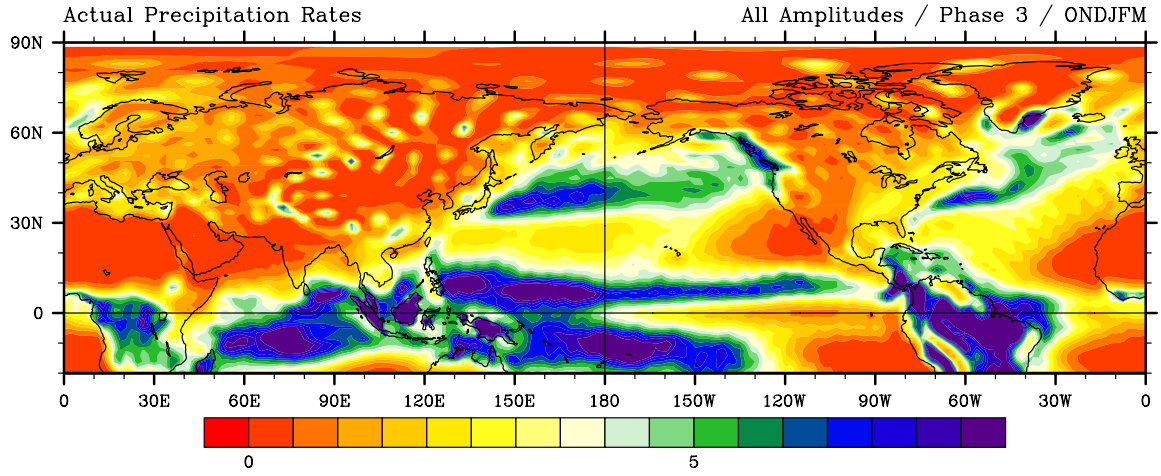

Figure 12. Actual precipitation rates for the baseline composites (MJO: phase 3 for all amplitudes, all EN / LN / neutral regimes and for ONDJFM).

4. Sensitivity of the NPNA Response to the Phase of the MJO

The first step in testing our hypotheses was to compare the phase 3 baseline composites to the corresponding composites for phases 1 through 8. Figure 13 illustrates the anomalous OLR field associated with MJO activity, from phase 1 through phase 8. Note how the convective component of the MJO emerges first near the Horn of Africa (HOA), then moves eastward across the IO

and the Maritime Continent, and weakens over the central tropical Pacific. Similarly, the subsidence component of the MJO, which is present over the western Pacific in phase 1, moves across the tropical Pacific and dissipates during phase 4 and 5, before re-emerging in the IO in phase 6.

Figure 14 depicts the 200-hPa anomalous height fields from phase 1 through phase 8 of the MJO lifecycle. Tropical Rossby wave responses to tropical convection are highlighted in this figure within the ovals, while a solid black arrow, shows the energy propagation through the anomalous extratropical

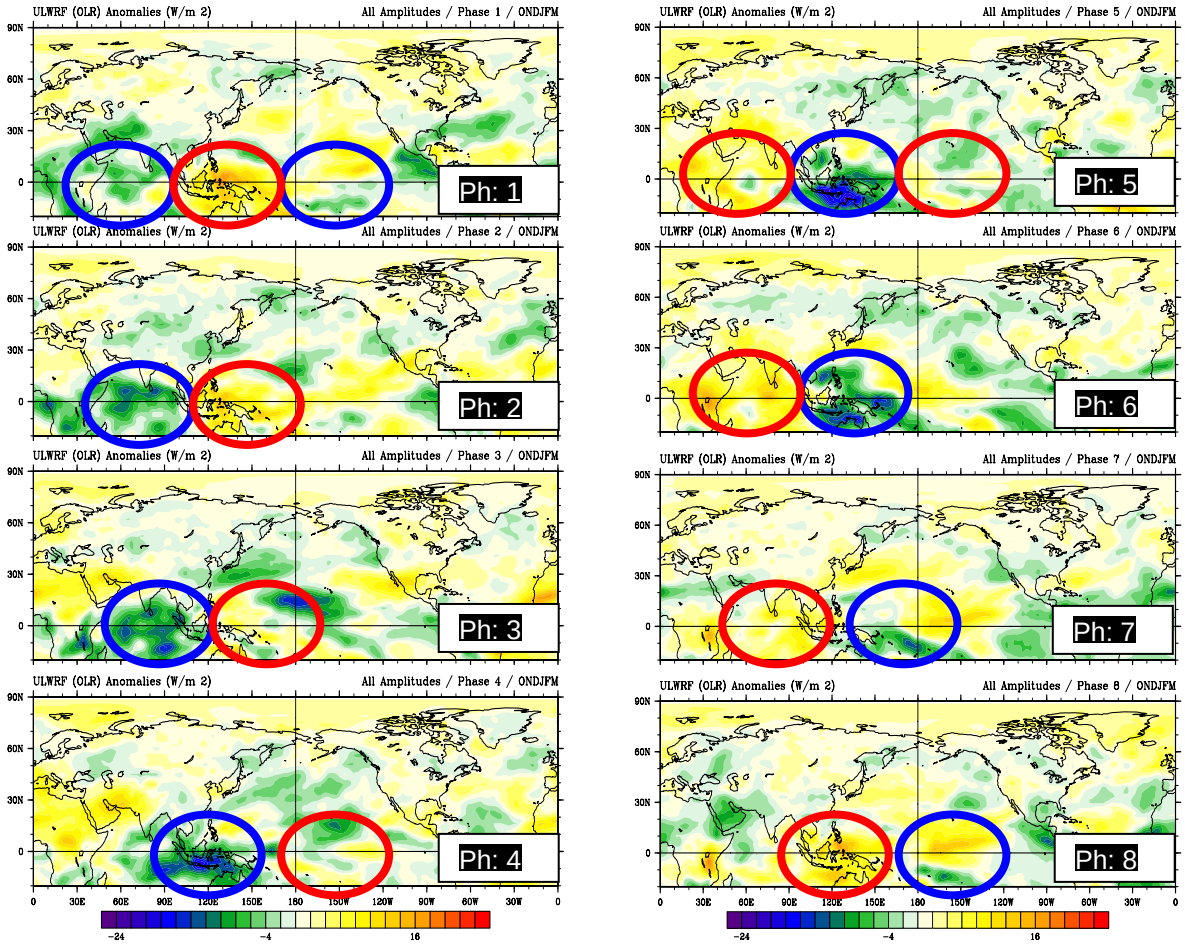

Figure 13. Evolution of baseline OLR anomalies with respect to MJO phase. Phase 1 is in the upper-left corner, with a progression to phase 8 in the lower-right corner. Red circles are indicative of the subsidence component (s) of the MJO and blue circles represent the convective component(s).

Rossby wave train. The eastward movement of the anomalous convection and subsidence associated with the MJO (Fig. 13) is associated with a similar movement of the tropical Rossby wave response centered at about 20-30°N latitude. The anticyclonic (cyclonic) part of the tropical Rossby wave response in the upper-levels is generally at about the same longitude, or slightly to the west of, the convective (subsidence) component. The tropical Rossby wave response is most obvious over southern Asia and around the IDL. These upper-level tropical Rossby wave features are related to the MJO convection and subsidence components and important in setting up extratropical wave trains (Sardeshmukh and Hoskins 1988).

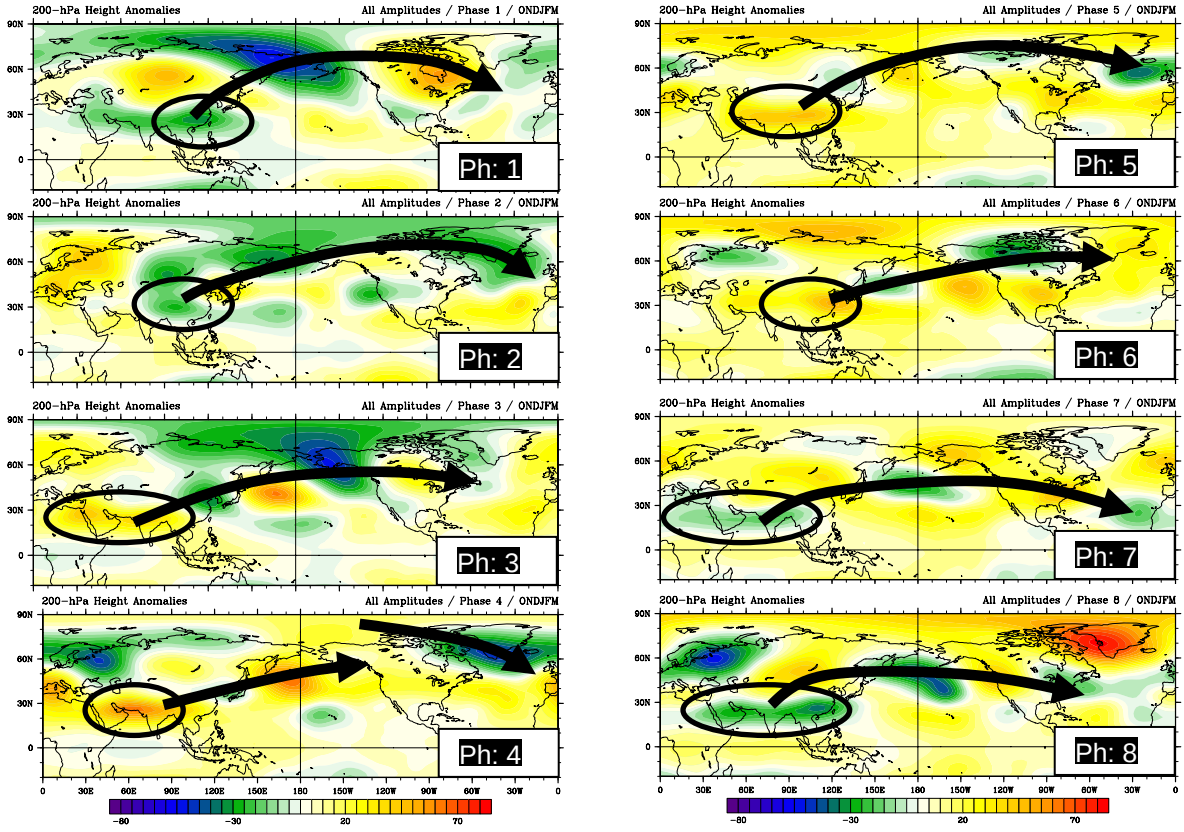

Figure 14. Evolution of baseline 200-hPa height anomalies with respect to MJO phase. Phase 1 is in the upper-left corner, with a progression to phase 8 in the lower-right corner. Black circles indicate equatorial Rossby wave responses to the anomalous tropical convection / subsidence associated with the MJO. Black arrows indicate the approximate path of energy propagation through extratropical wave trains.

Analysis of the 200-hPa height anomaly pattern as it evolves from phase 1 through phase 8 (Fig. 14) shows how the extratropical wave train evolves through time and has a strong dependence on the phase of the MJO. In some cases, the changes in the height anomalies from one phase to the next are minimal (e.g., phase 1-3, phase 6-8), but in other cases the changes are large and abrupt (e.g., phase 3 to phase 4). This may be explained in part by interactions between the MJO convective and subsidence components and the background flow (cf. Bond and Vecchi 2003). This topic is discussed further in Section D of Chapter III.

The results shown in Figures 13-14 indicate that MJO phase may have a large impact on the NPNA response to the MJO. This may be because: (a) the eastward movement of the convective and subsidence components of the MJO leads to a similar movement of the tropical Rossby wave response; and (b) this tropical wave response is involved in setting up the extratropical wave train response that extends into the NPNA region.

5. Sensitivity of the NPNA Response to MJO Amplitude

To analyze the impacts of MJO amplitude on the NPNA response, we segregated the days used to create the baseline composites according to the amplitude of the MJO during those days. We created low and high amplitude categories for all eight phases. For brevity, we only present in this chapter representative examples of the eight phases. The OLR anomalies for the low and high amplitude composites (Fig. 15) are relatively similar, although there are notable regional scale differences (e.g., in the western tropical Pacific, along the west coast of North America). Although the OLR anomalies in the low and high amplitude cases were similar, the 200-hPa height anomalies or the low and high amplitude cases (Fig. 16) were different in several respects. Across the north Pacific (NPAC) region, a strong dipole of anomalous height features stands out in both the high and low amplitude cases, but the position and orientation of the dipole is notably different and would be expected to lead to differences in anomalous winds and precipitation over much of western North America. The most obvious difference between the low and high amplitude anomalous height

composites for phase 3 occurs over the north Atlantic (NATL) region, where the low amplitude case has an anomalous high feature, and the high amplitude case has an anomalous low feature. These results indicate that the NPNA response to variations in MJO amplitude may be small from a large scale perspective but may be large from a regional scale perspective.

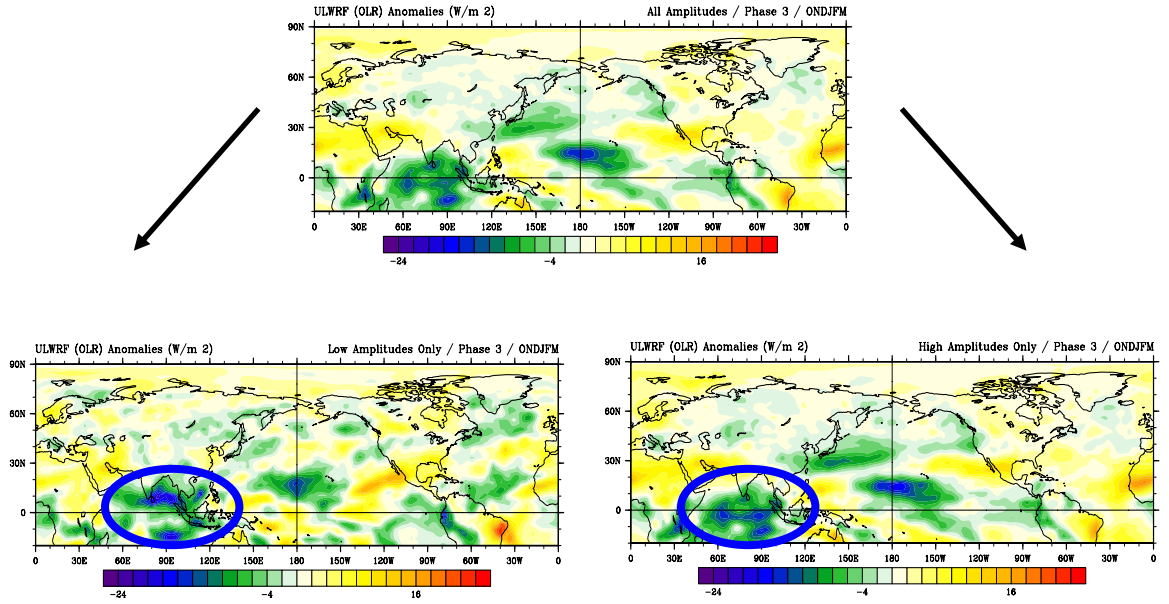

Figure 15. Composite OLR anomalies for low (left figure) and high (right figure) amplitude phase 3 MJO events with respect to the baseline OLR anomalies (top figure). These composites illustrate how the OLR anomalies are stronger during high amplitude MJO events when separated from the low amplitude events, albeit slightly in some phases, including phase 3.

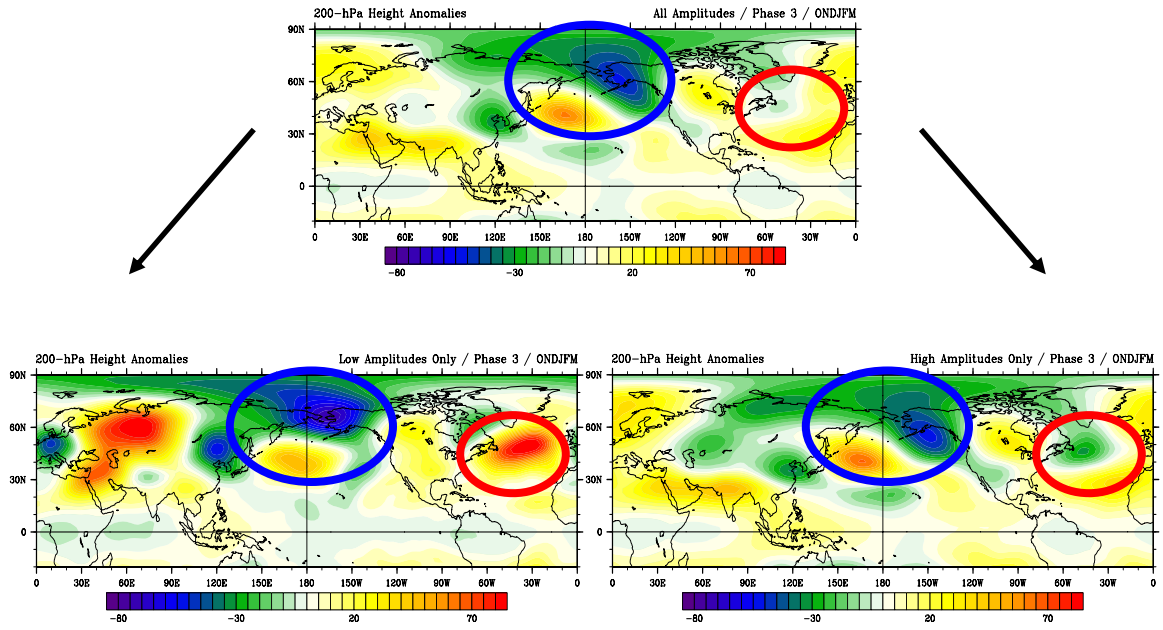

Figure 16. 200-hPa anomalies for low (left figure) and high (right figure) amplitude phase 3 MJO events with respect to the corresponding baseline figure (top figure). Blue and red circles highlight features discussed in the text.

Figures 17-20 are similar to Figures 15-16, but for phase 1 and phase 8. These figures indicate that the tropical OLR and the extratropical height anomalies tend to be somewhat larger in the high amplitude composites. The extratropical height anomalies tend to have similar overall patterns, but somewhat different positions, shapes, and orientations. Although these differences are relatively small at basin and global scales, they may be very important at regional scales (e.g., the scale of the North American west coast).

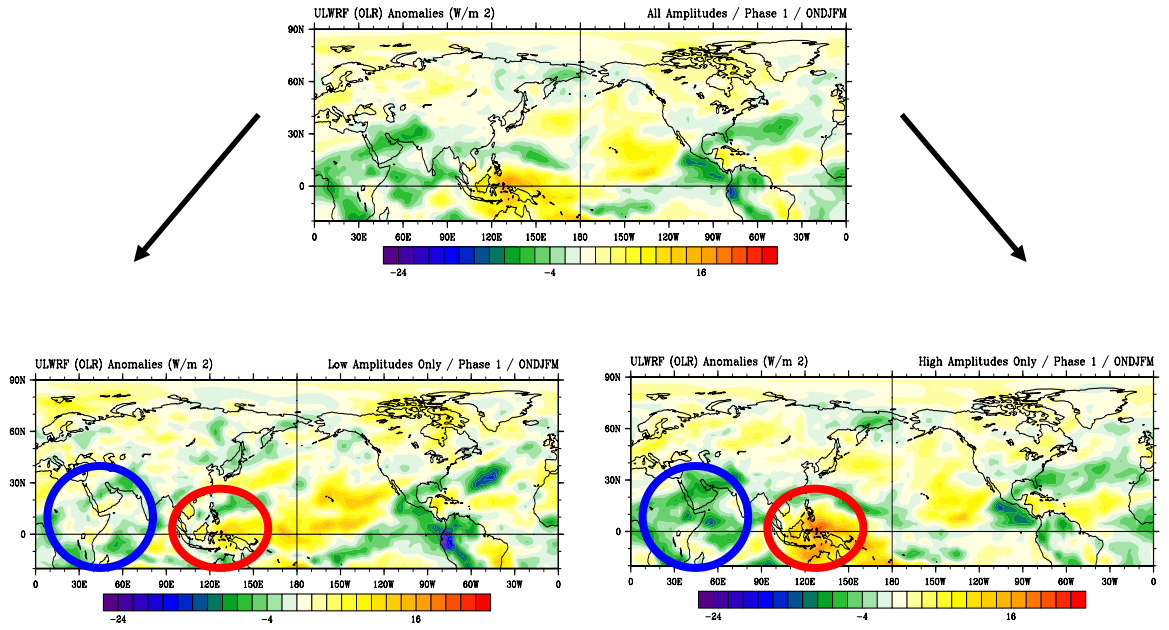

Figure 17. Same as Fig. 15, but for phase 1 composites. Note the stronger anomalous convection (subsidence) over the western IO (Maritime Continent) in the high amplitude case composite than in the low amplitude composite.

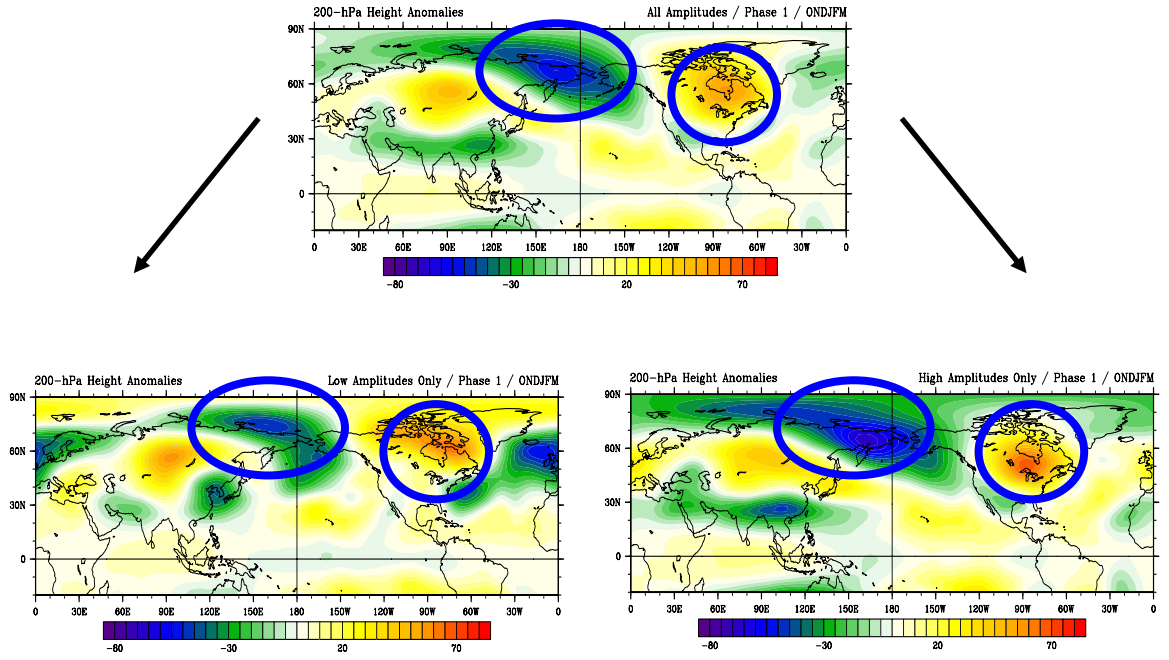

Figure 18. Same as Fig. 16, but for phase 1 composites. The height anomalies in the low and high amplitude composites have roughly similar overall patterns but different positions, shapes, and orientations.

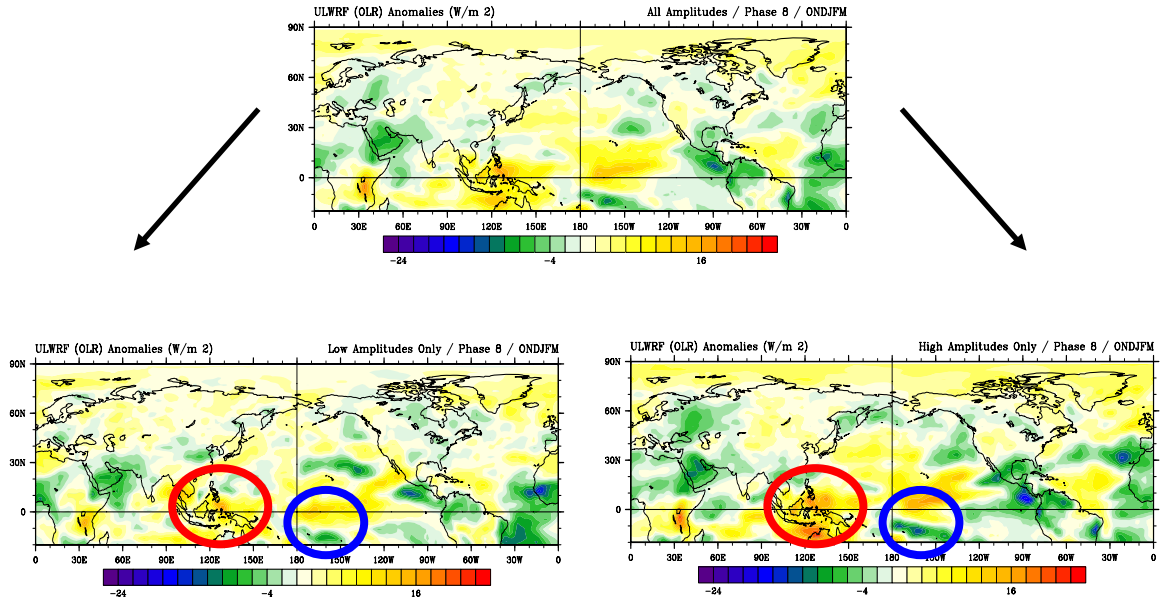

Figure 19. Same as Figs. 15 and 17, but for phase 8 composites. A stronger subsidence component of the MJO is evident in the high amplitude composite.

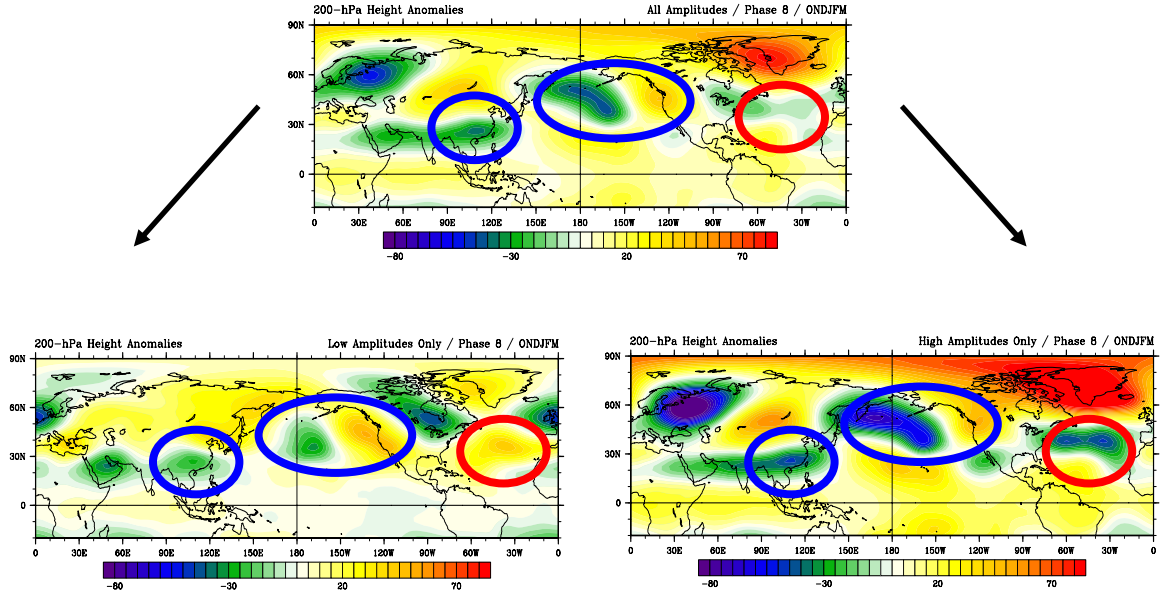

Figure 20. Same as Figs. 16 and 18, but for phase 8 composites. The height anomalies in the low and high amplitude composites have similar overall patterns but different positions, shapes, and orientations.

6. Sensitivity of the NPNA Response to the Season of MJO Occurrence

Figures 21-25 show the differences — for phases, 3, 4, 5, and 8 — between the three seasonal groupings we analyzed: October-March, OND, and JFM. For phase 3, the OLR anomalies are similar for fall and winter, although the winter anomalies are located further south, consistent with the southward seasonal migration of tropical from fall to winter (Fig. 21). This southward shift suggests that the extratropical response to the convective and subsidence components might also shift southward. However, Figures 22-25 provide no clear evidence to support this suggestion.

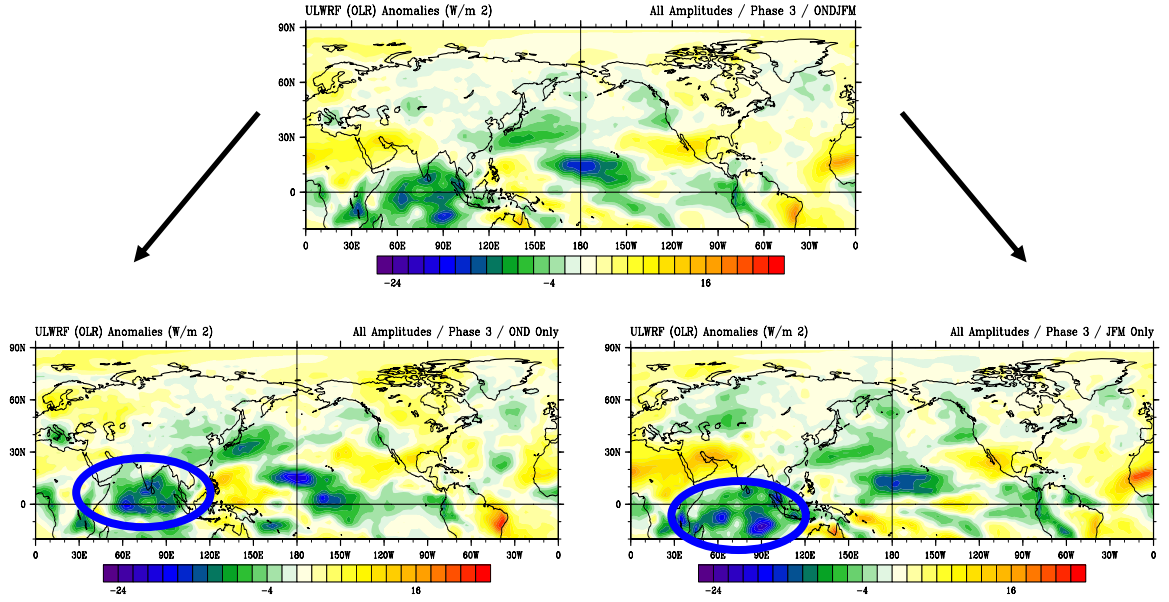

Figure 21. Phase 3 MJO baseline figure (top) for OLR anomalies separated into OND (left) and JFM (right) composites for the purposes of testing the sensitivity of the NPNA response to the season of MJO occurrence. Note the southward shift from fall to winter in the anomalous tropical convection and subsidence components of the MJO.

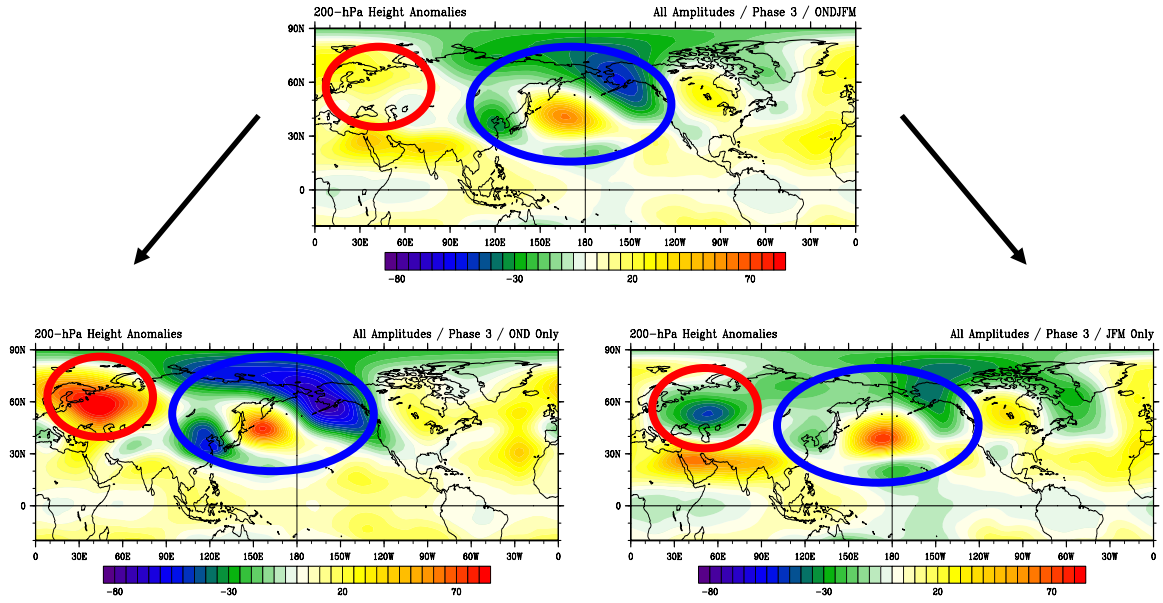

Figure 22. Phase 3 MJO baseline figure (top) for OLR anomalies separated into OND (bottom left) and JFM (bottom right) composites for the purposes of testing the sensitivity of the NPNA response to the season of MJO occurrence. Strong differences in anomaly intensities are evident between the seasons, but the overall anomalous wave train patterns are roughly similar.

The comparisons of the fall and winter 200-hPa height anomalies for phases 4, 5, and 8 are shown in Figures 23-25. In these cases, the fall-winter differences are much larger than for phase 3. In particular, the NPNA anomalies in fall can be opposite in sign to those in winter. This indicates that the NPNA response to the MJO is strongly affected by the season in which the MJO is occurring. This, of course, is important in determining what factors need to be considered when forecasting the impacts of the MJO on the NPNA region.

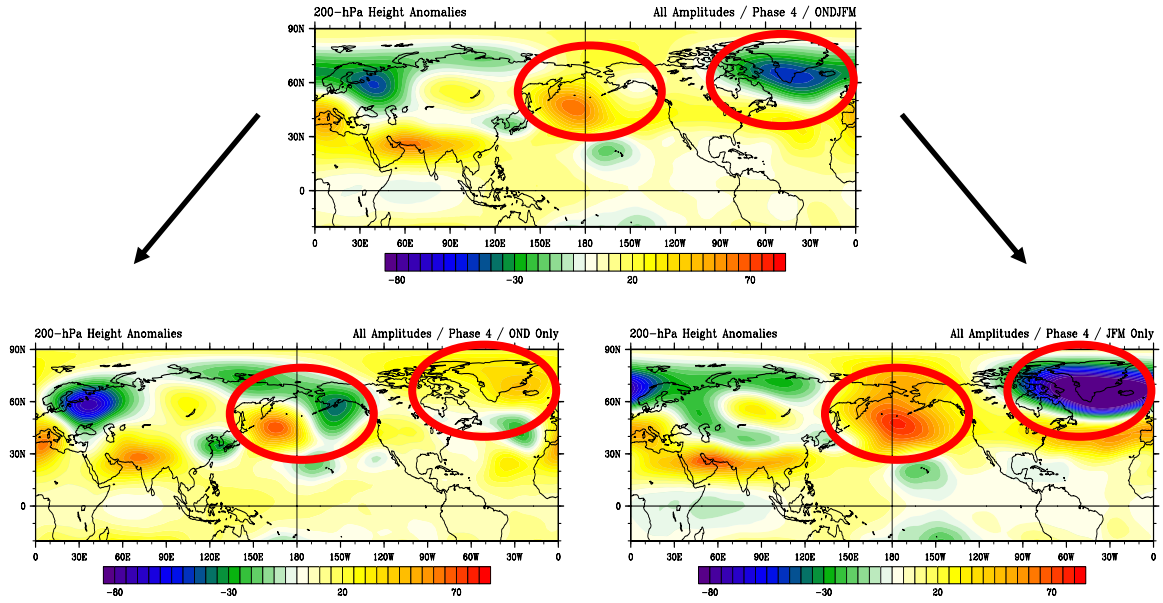

Figure 23. Same as Fig. 23, but for phase 4. Note the major differences circled in red across the NPAC and NATL regions between the OND and JFM composites.

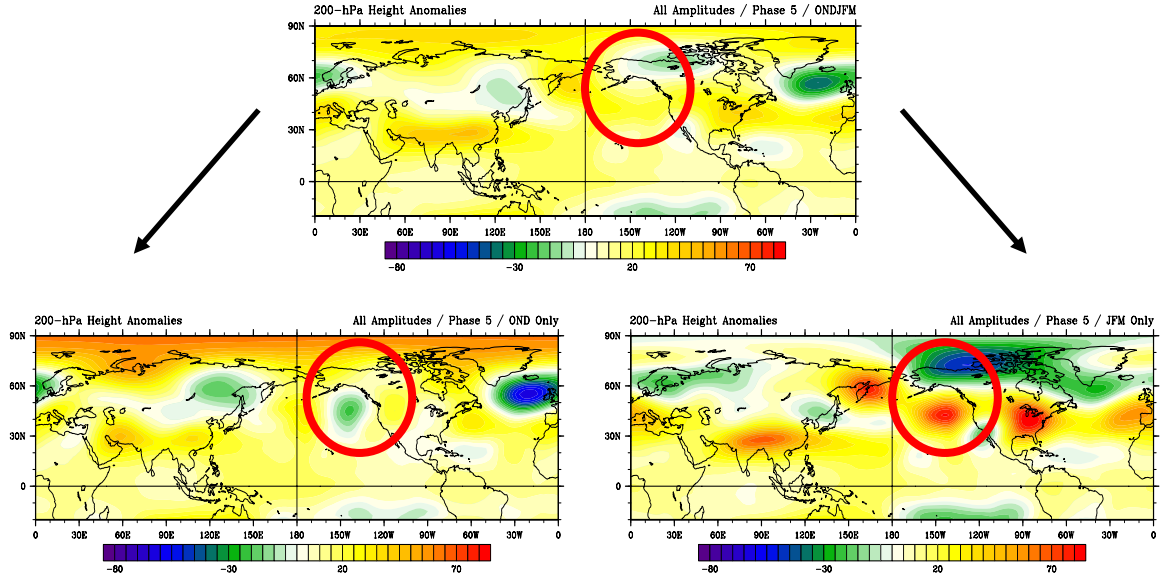

Figure 24. Same as Figs. 23 and 24, but for phase 5. Implications in separating the OND composites from the JFM composites are significant over the western CONUS for this phase by the anomalous flow that would result from the anomalous offshore height patterns.

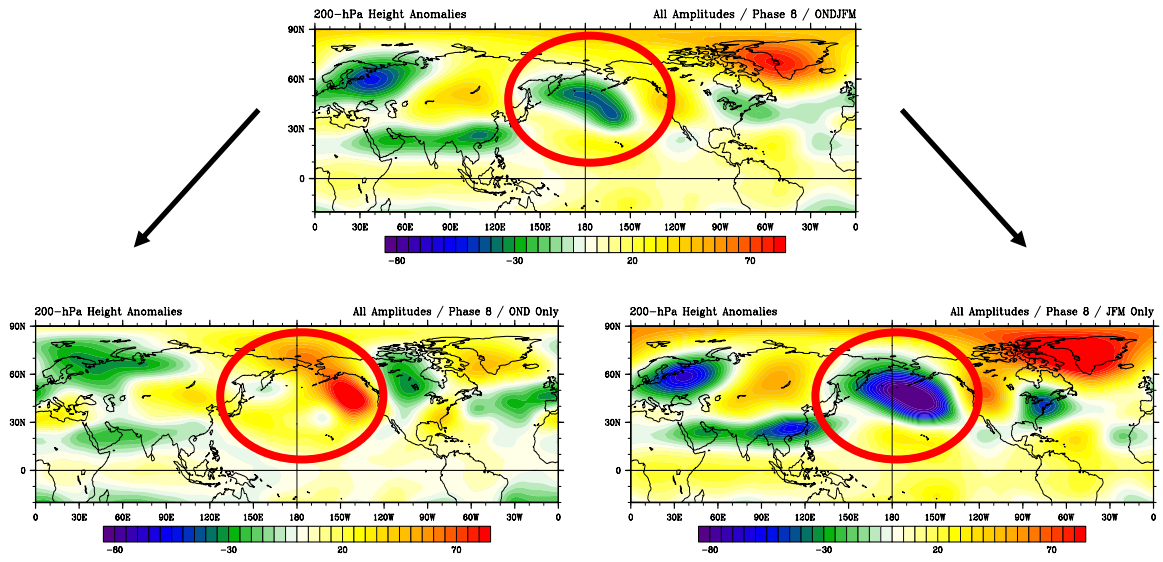

Figure 25. Same as Figs. 23 – 25, but for Phase 8. This phase exhibited the most significant differences from OND to JFM, which is evidenced by a strong anomalous high over the NPAC in fall transitioning to a strong anomalous low in winter.

7. Sensitivity of the NPNA Response to Concurrent El Niño / La Niña / Neutral Conditions

Figure 26 shows the phase 3 OLR anomalies for the baseline, EN, LN, and neutral composites. Note the large differences in the locations and magnitudes of the implied convective and subsidence regions (highlighted by red and blue ovals). This is due to constructive and destructive interference between the convection and subsidence anomalies associated with the MJO, EN, and LN (Fig. 27). This indicates that the MJO tropical forcing that helps initiate the extratropical wave train responses to MJO can be substantially changed by the co-occurrence of an EN or LN event. This we would expect large differences in the extratropical (e.g., NPNA) response to the MJO depending on the state of the ENLN climate variation.

Figure 27 confirms this expectation. This figure shows the height anomalies for the baseline, EN, LN, and neutral composites. In each of these four cases, the tropical Rossby wave response lies over southern Asia and is located to the north and northwest of the anomalous convection (see Fig. 26). However, because the anomalous convection is altered by the EN, LN, and

neutral background conditions, the tropical Rossby wave response is also altered. These differences in the tropical Rossby wave response contribute to marked differences in the extratropical wave train and lead to very large differences in the NPNA response to the MJO. Table 6 shows the relationships between the convective and subsidence components of MJO, EN, and LN by the phase of the MJO. Because concurrent EN and LN events can strongly alter MJO induced anomalies in the NPNA region, it is imperative for forecasters to account for the background climate state (with respect to EN, LN, or neutral conditions) when attempting to forecast the impacts of the MJO on the NPNA region.

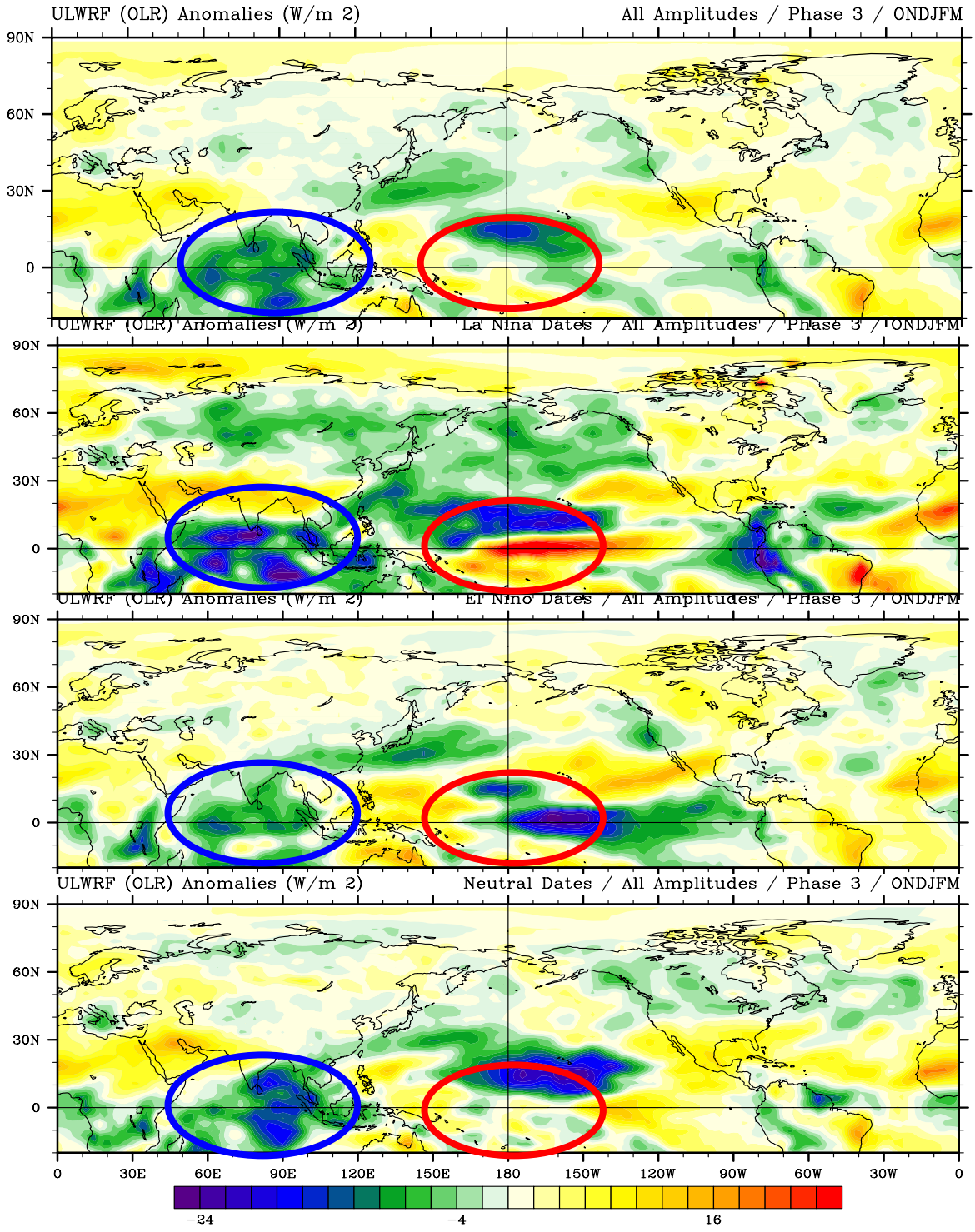

Figure 26. Breakdown of phase 3 MJO events in terms of ENLN background regime. OLR anomalies for: baseline composite (top) LN composite (2nd from top) and EN composite (3rd from top) and neutral composite (neither EN nor LN, bottom). Differences in tropical OLR anomalies are consistent with constructive and destructive interference between convective and subsidence components of the MJO, EN, and LN. Ovals highlight features discussed in text.

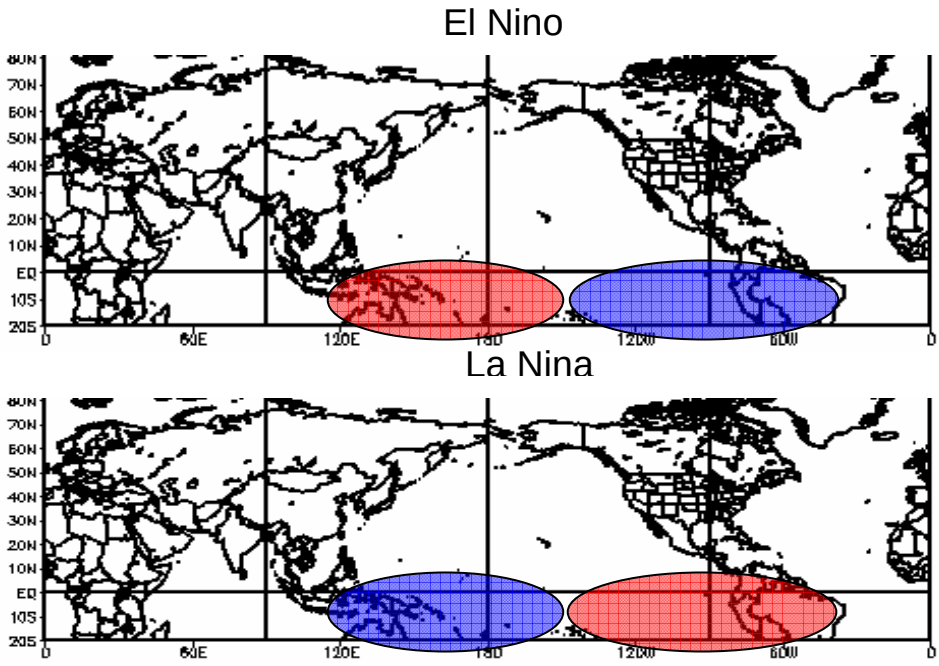

Figure 27. Schematic of EN (top) and LN (bottom) convective and subsidence components. Blue (red) ovals are indicative of anomalous convection (subsidence) due to ENLN.

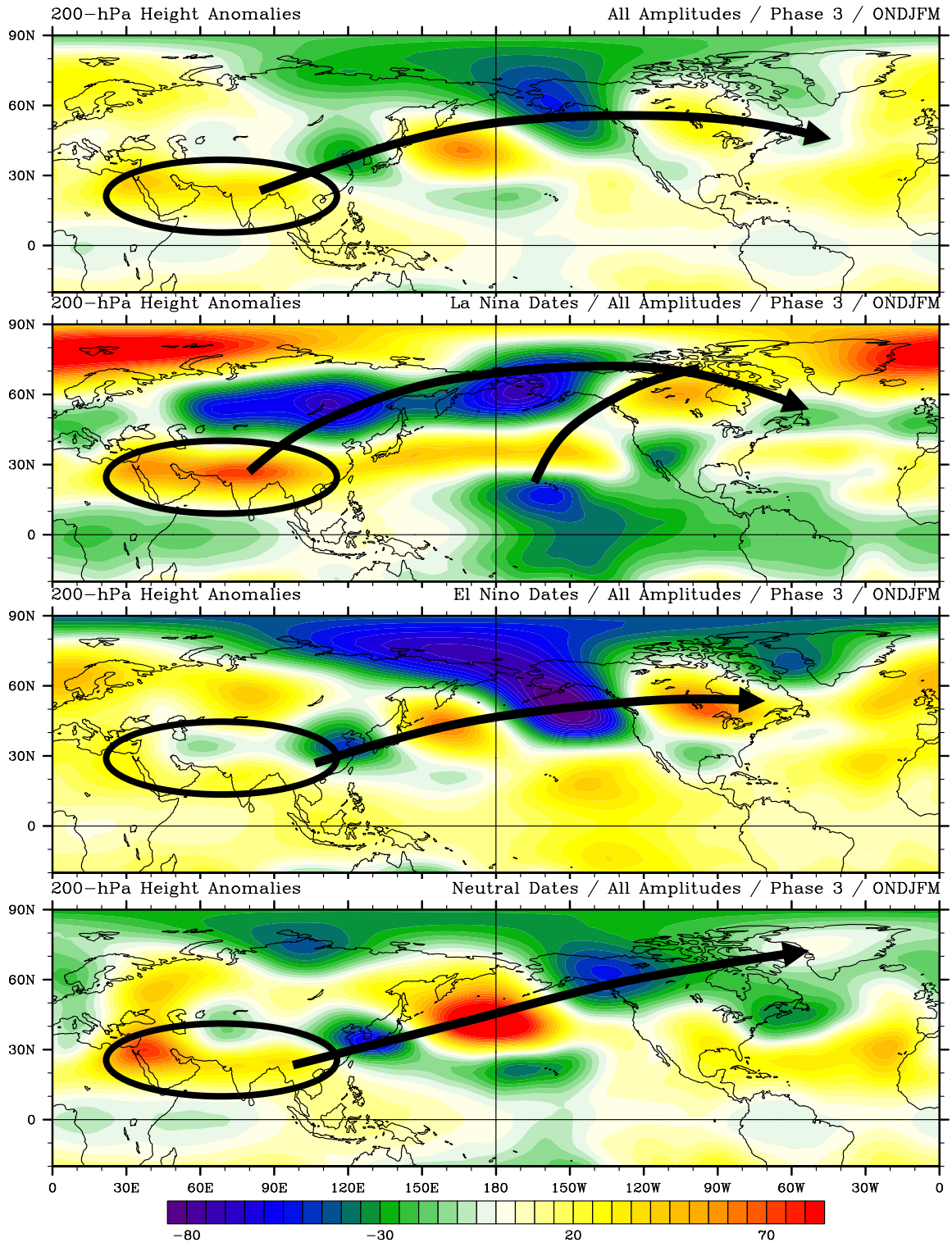

Figure 28. Same as Figure 28, but for 200-hPa height anomalies. Note the large differences in the strength of the tropical Rossby wave response over southern Asia (black ovals).

MJO Phase	With Concurrent El Niño	With Concurrent La Niña
1	Constructive Interference	Destructive Interference
2	Minor Constructive Interference	Minor Destructive Interference
3	Minor Destructive Interference	Minor Constructive Interference
4	Destructive Interference	Constructive Interference
5	Destructive Interference	Constructive Interference
6	Minor Destructive Interference	Minor Constructive Interference
7	Minor Constructive Interference	Minor Destructive Interference
8	Constructive Interference	Destructive Interference

Table 6. Relationships between convective and subsidence components of MJO, EN, and LN by the phase of the MJO. Constructive interference means that the convective and subsidence components of the MJO are reinforced by co-located convective and subsidence components of EN or LN. Destructive interference means that the MJO convective and subsidence components are weakened by co-located subsidence and convective components of EN or LN.

8. Impacts of Applying a Lag to MJO Event Composites

Dynamical reasoning indicates that the NPNA response to the MJO develops over a week or more (see chapters I-II) before reaching its maximum intensity. Thus we experimented with lags of 7, 10, and 12 days between the occurrence of a given MJO condition in the tropics (e.g., phase 4 conditions) and the occurrence of the extratropical response to that MJO condition. Our results (not shown) showed notable differences between the baseline results and those using a 7 day lag. But the differences were small between the 7 and 10 day lag results, and moderate between the 10 and 12 day lag results. We chose to use a 7-day lag in constructing composites we used to analyze the details of the NPNA response (see following section). The use of lagged gives a more realistic

depiction of the relationships between the MJO and the NPNA response, and a depiction that is more suited than one based on non-lagged composites for developing forecasting guidance.

Additional research into how long it takes the MJO to manifest itself in the form of teleconnections across the NPNA region would be beneficial. We have hypothesized that the amount of time differs from phase to phase due to different levels of interaction with the east Asian – north Pacific jet.

B. AN ANALYSIS OF MJO IMPACTS ON PRECIPITATION IN WESTERN NORTH AMERICA

1. Three Critical Factors and 48 Composites Approach

Based on the results discussed in the prior sections of this chapter indicate, we concluded that teleconnections between the MJO and NPNA circulation and precipitation exhibit the greatest sensitivity three critical factors:

1. the phase of the MJO
2. the season of MJO occurrence
3. concurrent EN, LN, or neutral background conditions

We also concluded that the NPNA response to the MJO is less sensitive to MJO amplitude. And we concluded that a lag of one week provided a more realistic depiction than no lag of the relationship between the MJO and NPNA circulation and precipitation.

We used these conclusions in developing our approach for analyzing the western North American precipitation response to the MJO. In particular, we constructed lagged composites based on the three critical factors listed above. These lagged composites were intended to identify how the critical factors impacted NPNA circulation and precipitation. To do so, we needed to construct composites representing all possible combinations of the three factors. The three factors represent eight phases of the MJO, two seasons (fall and winter), and three background states (EN, LN, and neutral). That meant we needed to

construct 48 composites, so that we could isolate the NPNA anomalies associated with each factor while holding all the other factors constant. Most of the composites consisted of approximately 50 to 75 MJO event days. Any composite containing less than 25 event days was not considered for analysis as the results were considered unreliable. However, only five of the 48 composites, or ten percent of them, did not meet this criterion.

We analyzed the 48 composites to identify the conditions that were associated with positive and negative precipitation anomalies along the west coast. By comparing the composites, we identified four regions along the coast within which the precipitation rate anomalies tended to be uniform for any given composite. These regions were southern AK, BC, PNW, and CA-DSW (Fig. 3).

For each of the four regions, we identified the five composites for which the PRA was most positive and the five composites for which the PRA was most negative. We termed these the five wettest and five driest composites for each region. We analyzed these composites to identify the combinations of critical factors, and the corresponding patterns and processes, which contributed to anomalous wetness and dryness in the four regions.

2. Analysis of Wet and Dry Regimes for Regions Along the Pacific Coast of North America

The following sections describe the sets of conditions under which anomalous wetness and dryness tended to occur during MJO events in each of the four regions, as determined from our analyses of the 48 composites described in the preceding section.

a. California and Desert Southwest

Table 7 lists the critical factor conditions for the five composites in which the CA-DSW region had the most positive PRA composites and the five composites in which the CA-DSW region had the most negative PRA. This table indicates some of the conditions that may be favorable for anomalous wetness associated with the MJO, including early phases of the MJO under neutral conditions in the fall, and early phases of the MJO under EN conditions in the

winter. Conditions that may be favorable for anomalous dryness associated with the MJO include: middle or late phases of the MJO under LN conditions in the winter.

Figure 29 shows the PRAs for each of the five positive PRA composites, and Figure 30 shows the PRAs for the five negative PRA composites. Note that when anomalously wet (dry) conditions occurred over CA-DSW, anomalously dry (wet) conditions tended to occur over BC. As will be shown in the corresponding figures for the other west coast regions, this PRA dipole is a common occurrence in conjunction with MJO influenced precipitation anomalies.

5 Wettest Composites for CA-DSW	5 Driest Composites for CA-DSW
Phase 2 / El Niño / OND	Phase 7 / La Niña / OND
Phase 2 / Neutral / OND	Phase 3 / La Niña / JFM
Phase 6 / Neutral / OND	Phase 4 / Neutral / JFM
Phase 1 / El Niño / JFM	Phase 7 / La Niña / JFM
Phase 7 / El Niño / JFM	Phase 8 / Neutral / JFM

Table 7. Critical factor conditions for the five wettest and five driest composites for the CA-DSW region.

Figure 31 shows the 200-hPa height anomalies for the five wettest composites shown in Figure 29. This figure indicates that during periods in which CA-DSW is anomalously wet, there tends to be an anomalous low positioned to the north and west of CA, with an anomalous high positioned south and west of CA. This sets up a strong anomalous onshore flow into CA between the anomalous low and high. In addition, the anomalous offshore low has a northeast to southwest orientation. With this orientation, the anomalous onshore flow originates in tropical locations, causing warm, moist advection anomalies in

the region. Conversely, in anomalously dry conditions, an anomalous upper-level high is positioned to the north and west of CA, and an anomalous low sits to the south of west (Fig. 32). Flow in between these features is anomalously offshore, leading to cool, dry advection anomalies over CA-DSW. The opposite

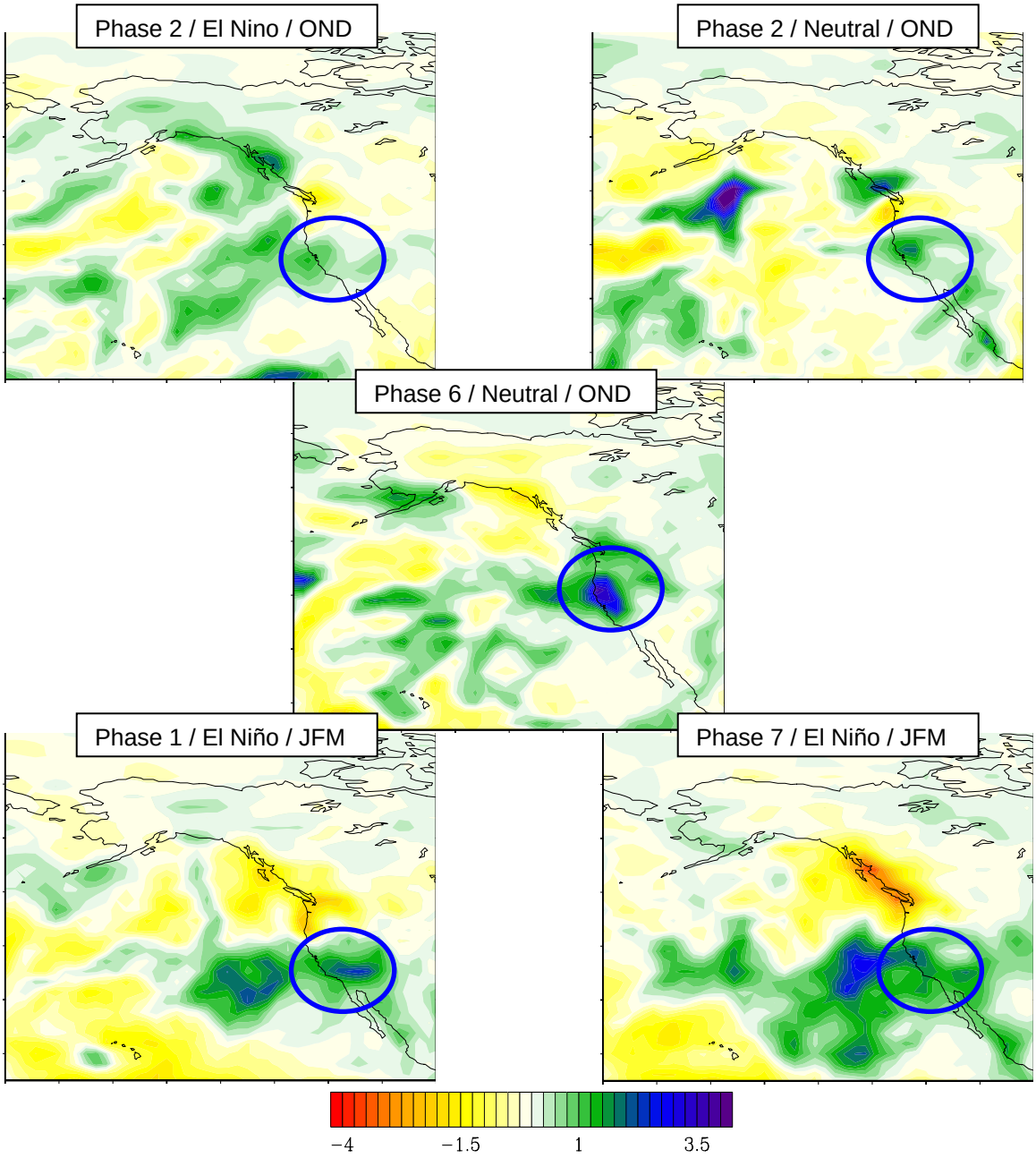

Figure 29. Precipitation rate anomalies for the five composites with the most positive precipitation rate anomalies for the CA-DSW region. The critical factor conditions for these five composites are shown in Table

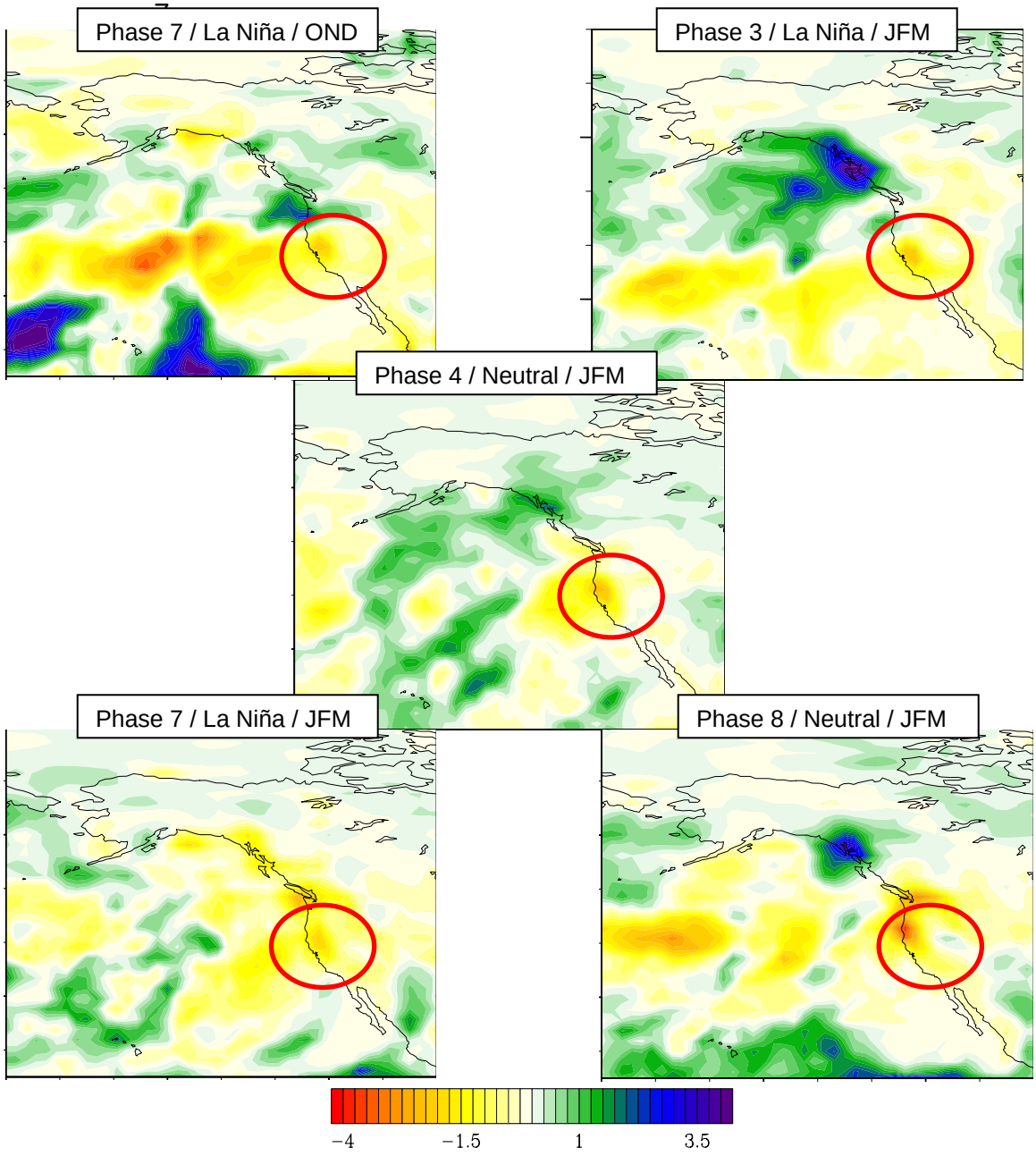

Figure 30. Precipitation rate anomalies for the five composites with the most negative precipitation rate anomalies for the CA-DSW region. The critical factor conditions for these five composites are shown in Table 7.

nature of the circulation anomalies that create the opposite precipitation anomalies suggests that two different phases of the same mechanism might be causing both the wet and dry anomalies.

Figure 33 shows the 200-hPa height anomalies and precipitation rate anomalies derived from compositing all the days in the five wettest composites. This grouping of days characterizes the large-scale patterns that are responsible for anomalously high precipitation rates over the CA-DSW region. The most striking feature is strong anomalous onshore flow between anomalous low positioned north and west of the CA-DSW region over the extratropical northeast Pacific, and an anomalous high positioned southwest of the CA-DSW region over the tropical northeast Pacific. The anomalous low seems to be part of an anomalous wave train extending from southeast Asia across the NPNA region and into Europe. The anomalous high is part of a twin anticyclone anomaly straddling the equator and clearly indicative of EN conditions. So it appears that the circulation anomalies over the northeast Pacific are the result of: (1) anomalous tropical forcing in the western tropical Pacific that generates a wave train into the NPNA region; and (2) EN forcing of the northern half of an anticyclone pair in the eastern tropical Pacific.

Figure 34 shows the 200-hPa height anomalies and precipitation rate anomalies derived from compositing all the days in the five driest composites. Over the northeast Pacific, the patterns are roughly opposite to those in the wettest composite (Figure 33). In addition, there are indications that an oppositely signed wave train emanating form southeast Asia may have contributed to the anomalous high over the extratropical northeast Pacific, and that LN forcing led to the anomalous low over the tropical northeast Pacific.

These results strongly indicate that major precipitation anomalies in the CA-DSW region are driven in large part by an anomalous circulation dipole over the northeast Pacific. This dipole is composed of an anomalous cyclone (anticyclone) over the extratropical northeast Pacific and anticyclone (cyclone) over the tropical northeast Pacific during EN (LN). The results also suggest that:

(1) the MJO contributes to the northern portion of this dipole by setting up a wave train from southeast Asia into the northeast Pacific; and (2) EN and LN contribute to the southern part of the dipole by creating a Rossby-Kelvin wave response in the eastern tropical Pacific.

Table 8 summarizes, for periods of MJO activity, the favorable and unfavorable conditions for positive and negative precipitation anomalies in the CA-DSW region. Of particular note is the tendency for anomalously wet (dry) conditions to be associated with EN (LN) conditions in the winter. These favorable and unfavorable conditions may be viewed as preliminary or hypothesized guidelines for accounting for the MJO when developing extended range forecasts for the CA-DSW region in fall and winter.

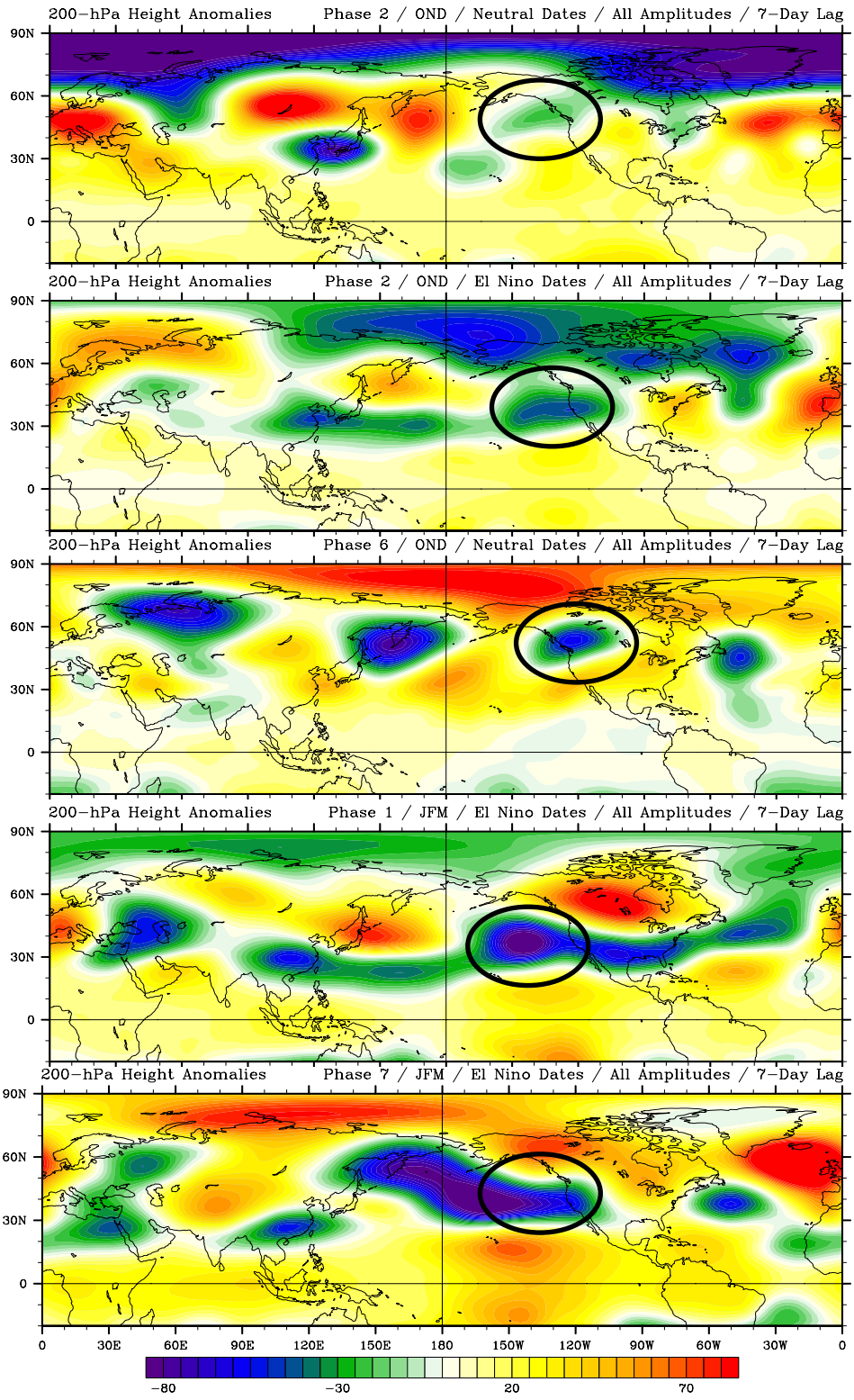

Figure 31. 200-hPa height anomalies for the five composites with the most positive precipitation rate anomalies for the CA-DSW region. The critical factor conditions for these five composites are shown in Table 7.

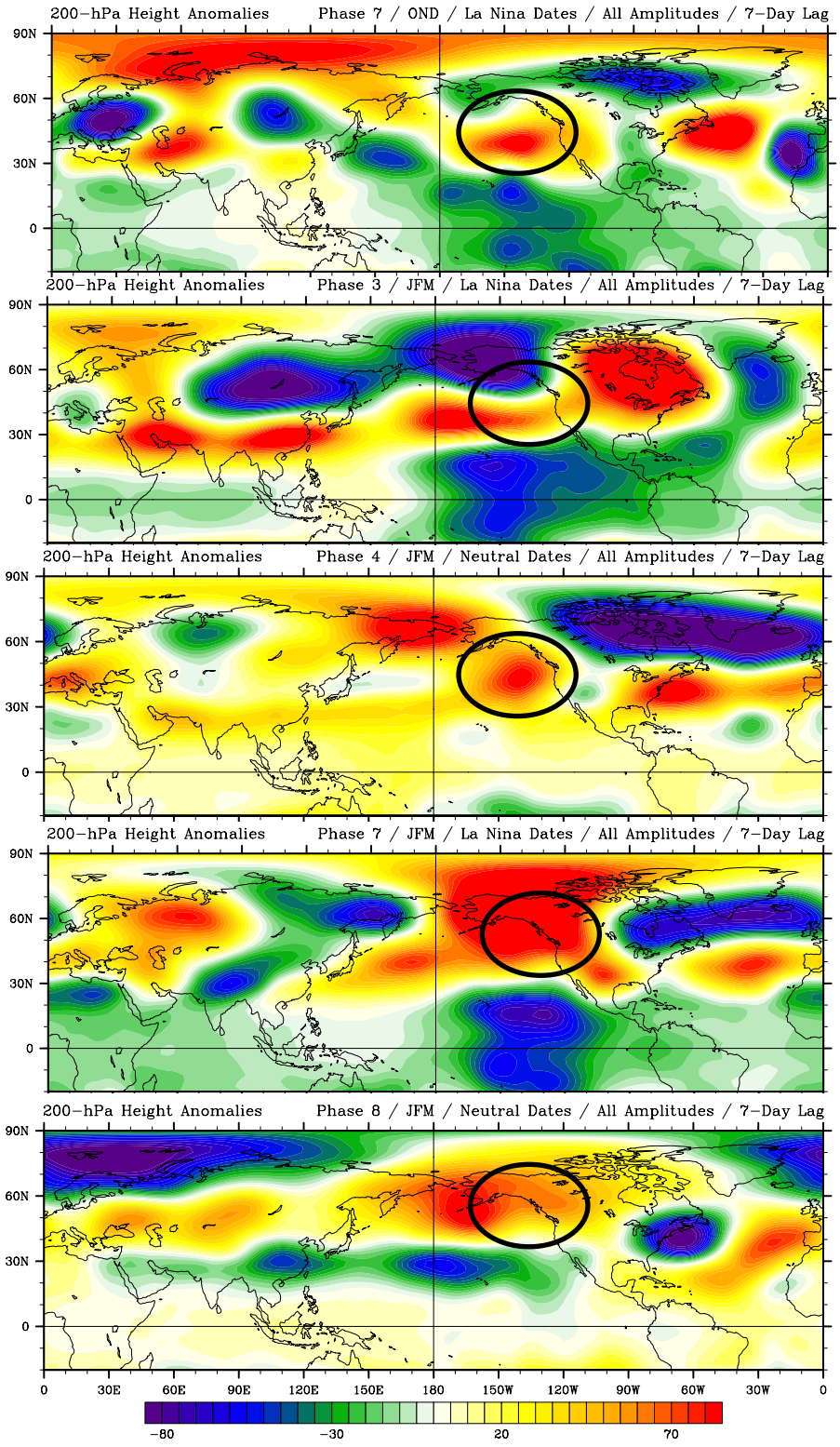

Figure 32. 200-hPa height anomalies for the five composites with the most negative precipitation rate anomalies for the CA-DSW region. The critical factor conditions for these five composites are shown in Table 7.

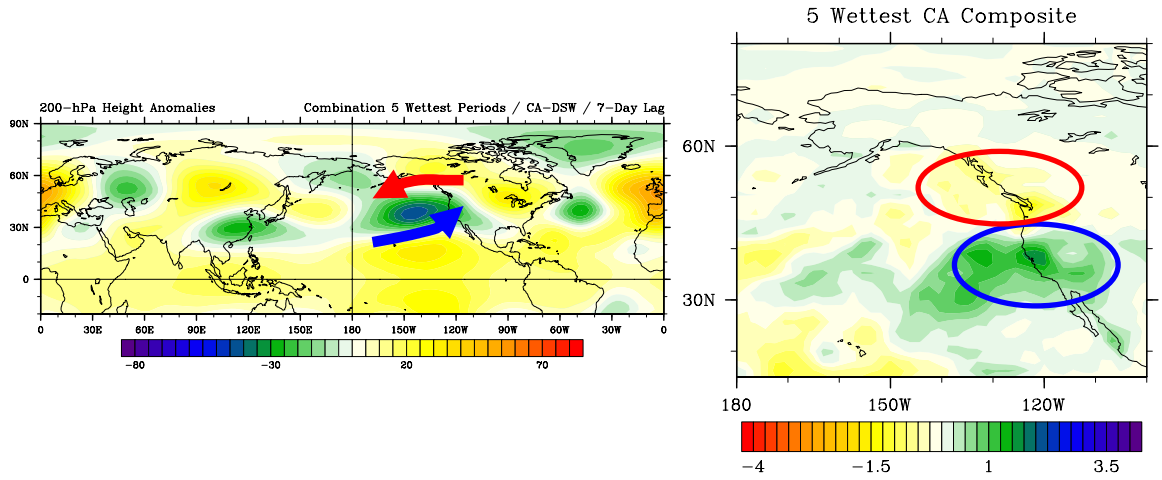

Figure 33. Composites of all days in the five composites with the most positive precipitation rate anomalies for the CA-DSW region (Fig. 29) for 200-hPa height anomalies (left) and precipitation rate anomalies (right). Blue arrows and ovals highlight regions of anomalously onshore flow and positive precipitation rates, and red ovals and arrows indicate anomalously offshore flow and negative precipitation rates.

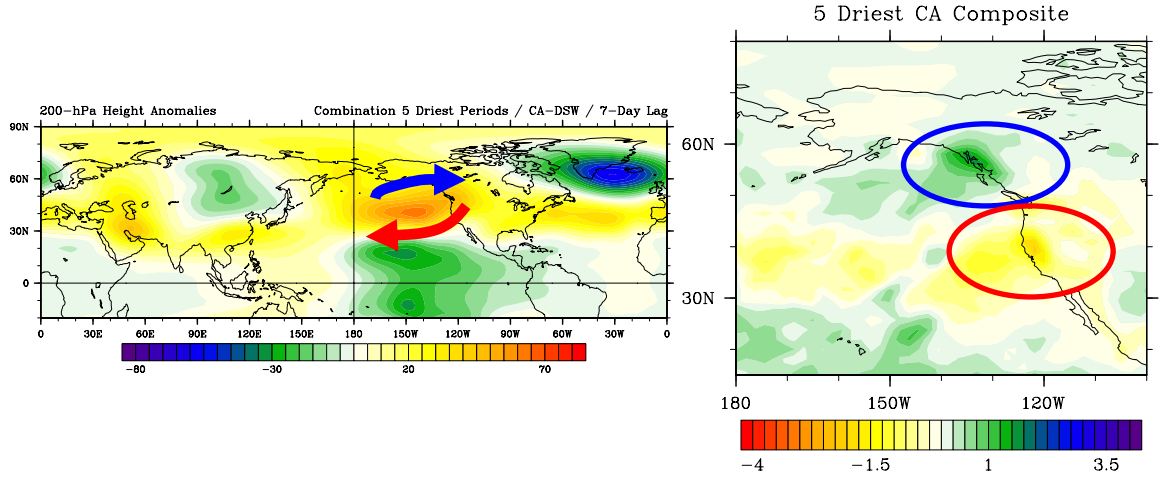

Figure 34. Composites of all days in the five composites with the most negative precipitation rate anomalies for the CA-DSW region (Fig. 30) for 200-hPa height anomalies (left) and precipitation rate anomalies (right). Blue arrows and ovals highlight regions of anomalously onshore flow and positive precipitation rates, and red ovals and arrows indicate anomalously offshore flow and negative precipitation rates.

Favorable / Unfavorable Conditions for MJO-Associated Anomalously Wet Conditions in CA-DSW	
Favorable	**Unfavorable**
1. Early or late phases of the MJO 2. OND or JFM 3. El Niño or neutral background state 4. Anomalous wave train emanating from Asia with an anomalous low north and west of CA 5. Southwest to northeast tilt to the anomalous low off CA	1. La Niña background state 2. Middle phases of the MJO
Favorable / Unfavorable Conditions for MJO-Associated Anomalously Dry Conditions in CA-DSW	
Favorable	**Unfavorable**
1. Middle or late phases of the MJO 2. JFM 3. La Niña background state 4. Anomalous high over northeastern Pacific	1. Early phases of the MJO 2. El Nino background state

Table 8. Favorable and unfavorable conditions during MJO activity for anomalously wet and dry periods in the CA-DSW region.

b. Pacific Northwest

Table 9 lists the critical factor conditions for the five composites in which the PNW region had the most positive PRA composites and the five composites in which the PNW region had the most negative PRA. This table indicates some of the conditions that may be favorable for anomalous wetness associated with the MJO, including late phases of the MJO during a La Niña background regime. Conditions that may be favorable for anomalous dryness associated with the MJO include the early and late phases of the MJO.

Figure 35 shows the PRAs for each of the five positive PRA composites, and Figure 36 shows the PRAs for the five negative PRA

composites. A dipole effect is again evident, with anomalously dry (wet) conditions to the north of the PNW region when anomalously high (low) precipitation is occurring over the PNW.

5 Wettest Composites for the PNW	5 Driest Composites for the PNW
Phase 5 / La Niña / OND	Phase 1 / El Niño / OND
Phase 6 / Neutral / OND	Phase 2 / La Niña / OND
Phase 7 / La Niña / OND	Phase 1 / Neutral / JFM
Phase 6 / Neutral / JFM	Phase 7 / El Niño / JFM
Phase 8 / La Niña / JFM	Phase 8 / Neutral / JFM

Table 9. Critical factor conditions for the five wettest and five driest composites for the PNW region.

Figure 37 shows the 200-hPa height anomalies for the five wettest composites shown in Figure 35. This figure indicates that during periods in which the PNW is anomalously wet, there tends to be an anomalous low situated either to the north or west of the PNW, with an anomalously high feature to the south and west. This sets up a strong anomalous onshore flow into the PNW between the anomalous low and high. This anomalous onshore flow has origins in the tropical locations, similar to that seen for the CA-DSW periods (Figs. 31-32). Conversely, in anomalously dry conditions, an anomalous upper-level high is positioned to the north and west of the PNW, and an anomalous low is situated to the south. Flow in between these features is anomalously offshore, leading to cool, dry advection anomalies over the PNW. The opposite nature of the circulation anomalies, which is again similar to the circulation anomalies noted for CA-DSW, but located further to the north, suggests that two different phases of the same mechanism might be causing both the wet and dry anomalies.

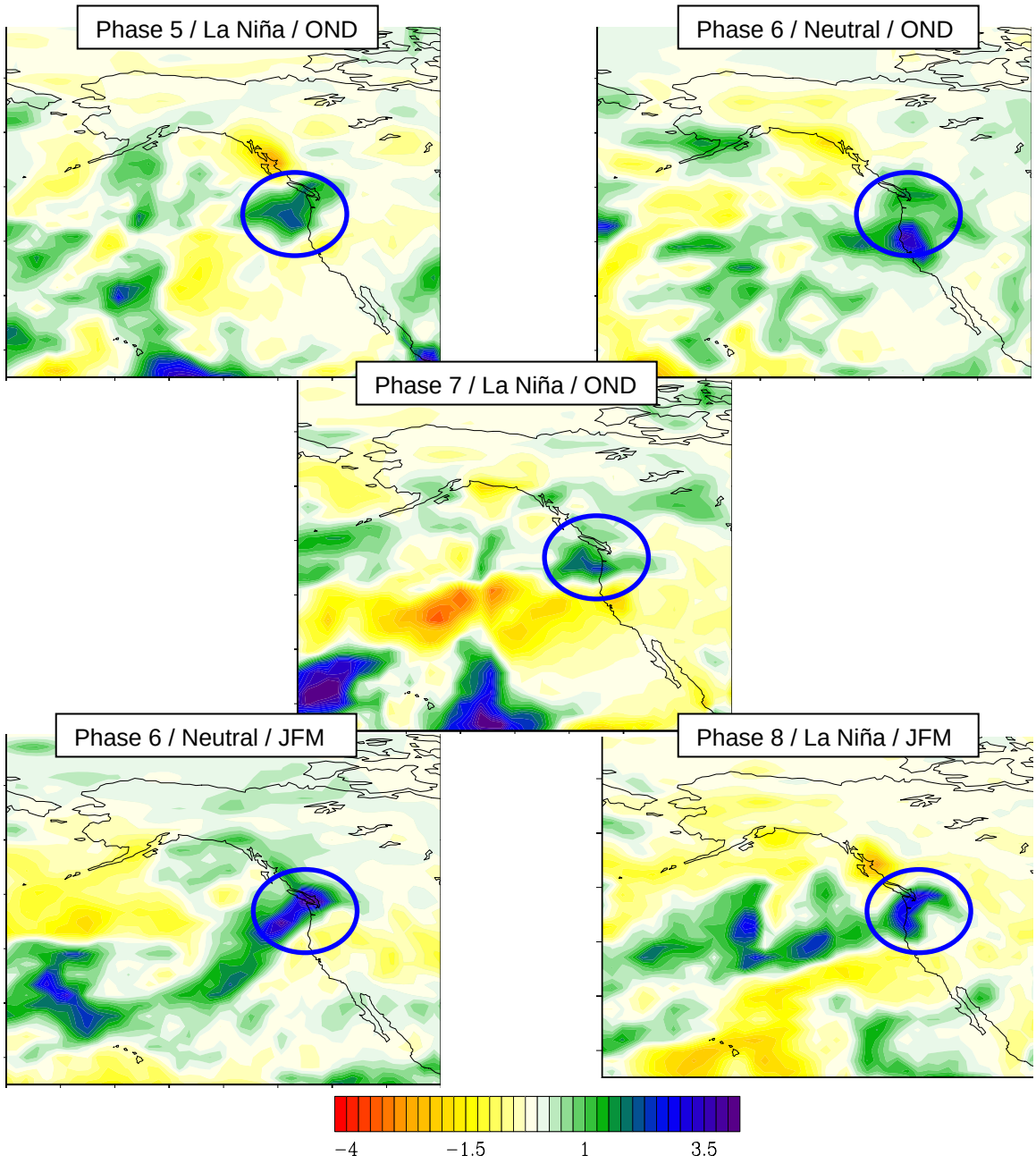

Figure 35. Precipitation rate anomalies for the five composites with the most positive precipitation rate anomalies for the PNW region. The critical factor conditions for these five composites are shown in Table 9.

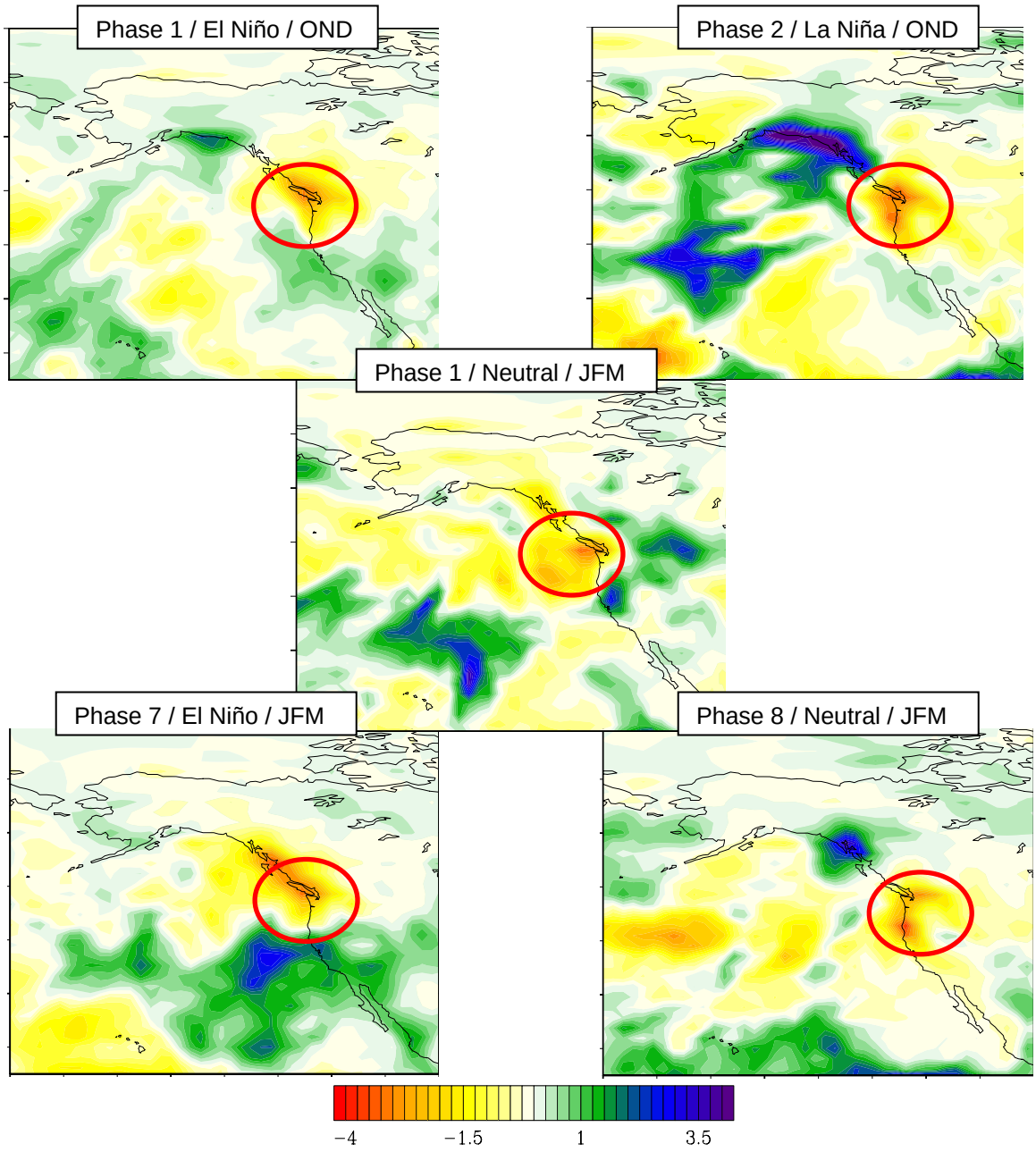

Figure 36. Precipitation rate anomalies for the five composites with the most negative precipitation rate anomalies for the PNW region. The critical factor conditions for these five composites are shown in Table 9.

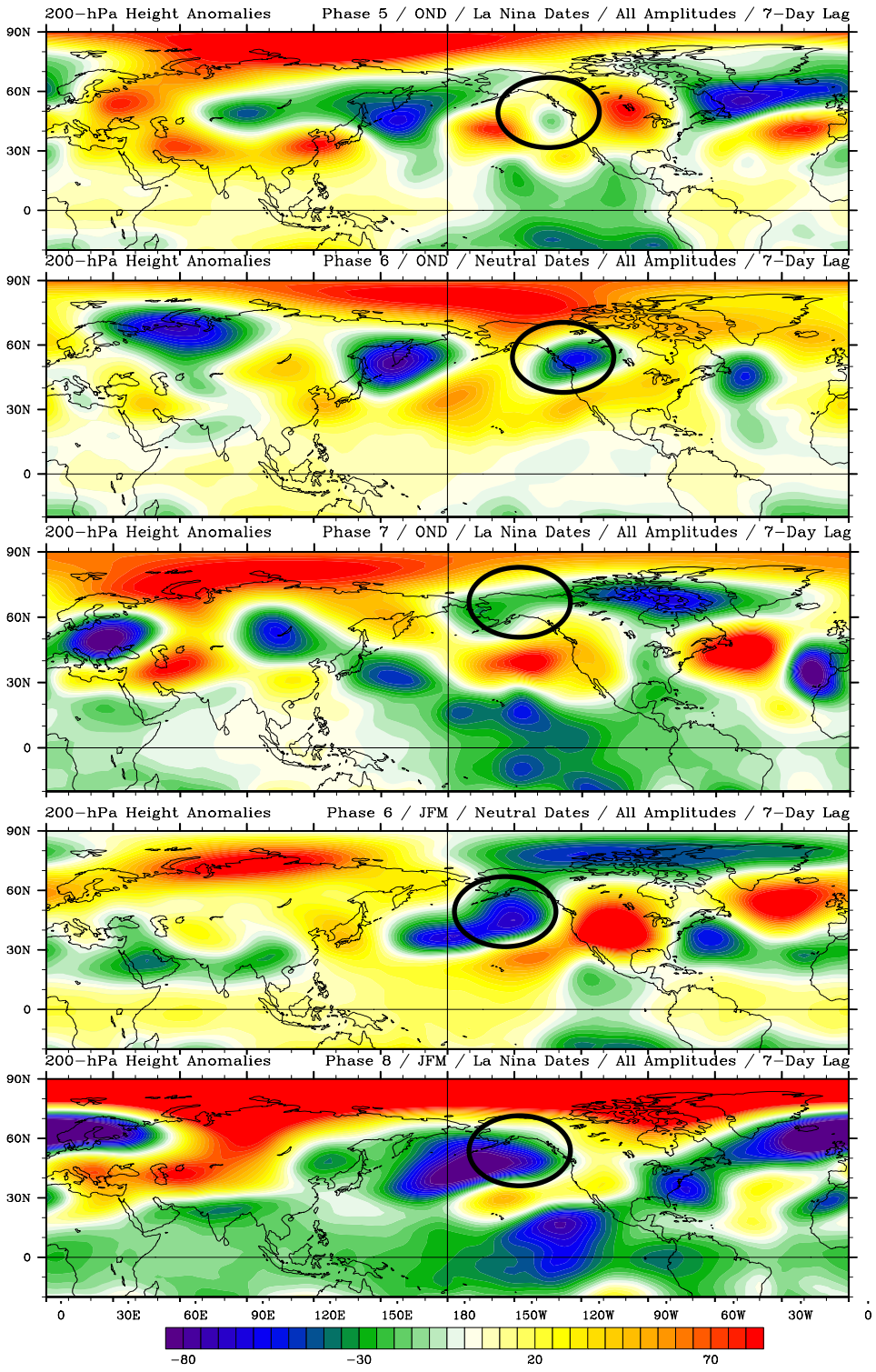

Figure 37. 200-hPa height anomalies for the five composites with the most positive precipitation rate anomalies for the PNW region. The critical factor conditions for these five composites are shown in Table 9.

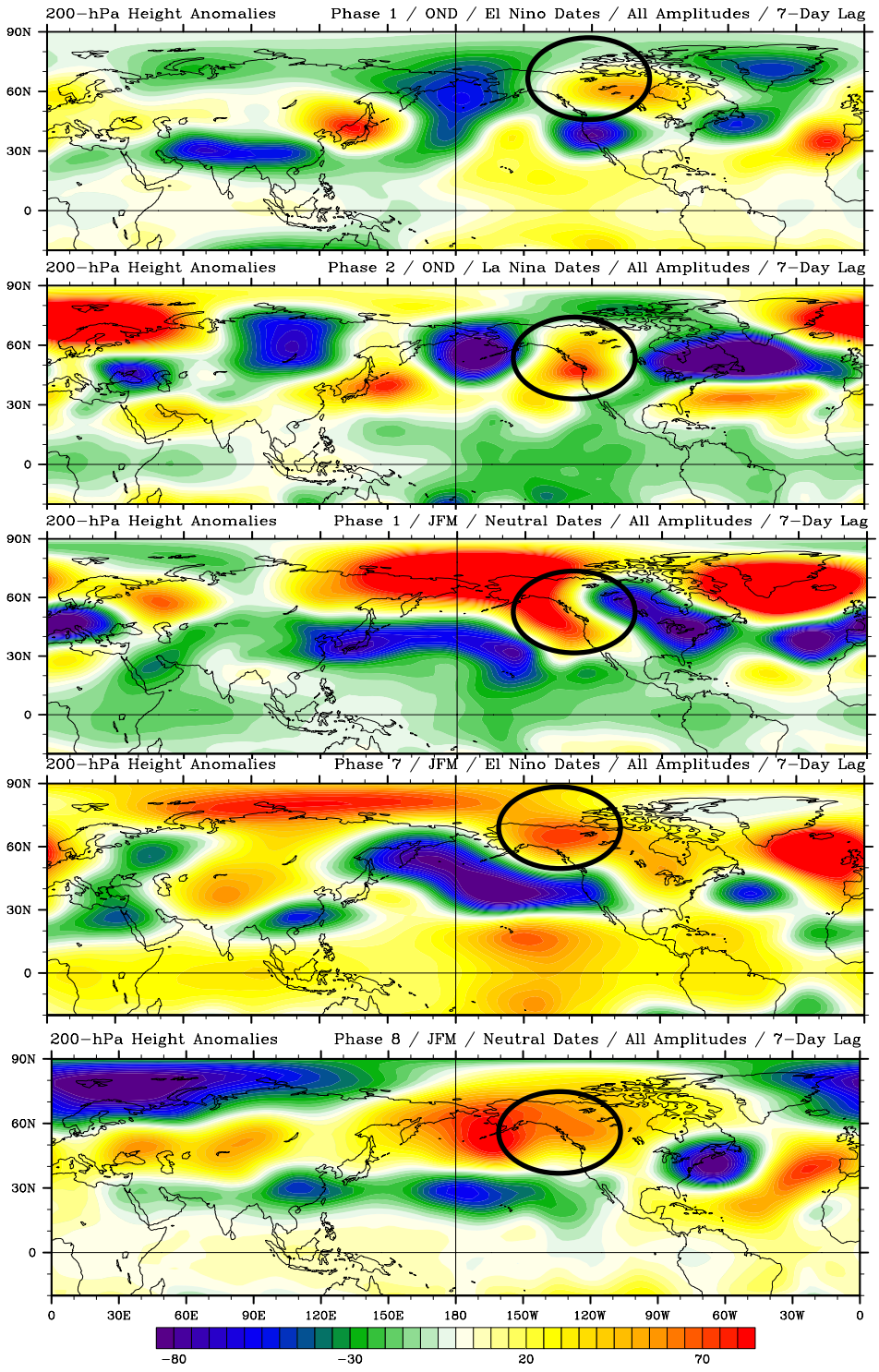

Figure 38. 200-hPa height anomalies for the five composites with the most negative precipitation rate anomalies for the PNW region. The critical factor conditions for these five composites are shown in Table 9.

Figure 39 shows the 200-hPa height anomalies and precipitation rate anomalies derived from compositing all the days in the five wettest composites. This grouping of days characterizes the large-scale patterns that are responsible for anomalously high precipitation rates over the PNW region. The most striking feature is an anomalous upper-level high over the interior of the western United States and an anomalous upper-level low over the Gulf of Alaska. This sets up a strong anomalous onshore flow into the PNW region. There appears to be a connection to an anomalous wave train extending from southeast Asia across the NPNA region, but it is not as developed as the anomalous wave train noted in the anomalous precipitation cases for CA-DSW. The anomalous high over the interior of the United States appears to stem from a twin cyclone anomaly straddling the equator and clearly indicative of LN conditions. Therefore, it appears that the circulation anomalies over the northeast Pacific are the result of: (1) anomalous tropical forcing in the western tropical Pacific that generates a weak wave train into the NPNA region; and (2) LN forcing of the northern half of a cyclonic pair in the eastern tropical Pacific.

Figure 40 shows the 200-hPa height anomalies and precipitation rate anomalies derived from compositing all the days in the five driest composites. Over the northeast Pacific, the patterns are approximately opposite of those seen in the wettest composite (Fig. 39). There are indications that an anomalous wave train again extends from southern Asia, and that weak LN conditions in the tropical eastern Pacific are contributing to an anomalous low over CA-DSW.

Similar to the CA-DSW region, these results indicate that major precipitation anomalies in the PNW region are driven by a dipole of anomalous circulation in the northeast Pacific. This dipole is composited of an anomalous cyclone (anticyclone) over the extratropical northeast Pacific and a cyclone (anticyclone) over the tropical northeast Pacific during EN (LN). The results suggest that: (1) the MJO contributes to the northern portion of this dipole by setting up a wave train from southern Asia into the NPNA region; and (2) EN and

LN contribute to the southern part of the dipole by creating a Rossby-Kelvin wave response in the eastern tropical Pacific.

Table 10 summarizes the favorable and unfavorable conditions for positive and negative precipitation anomalies in the PNW region concurrent with periods of MJO activity. Of particular note is the tendency for anomalously wet conditions to be associated with LN conditions. These favorable and unfavorable conditions may be viewed as preliminary or hypothesized guidelines for accounting for the MJO when developing extended-range forecasts for the PNW region in fall and winter.

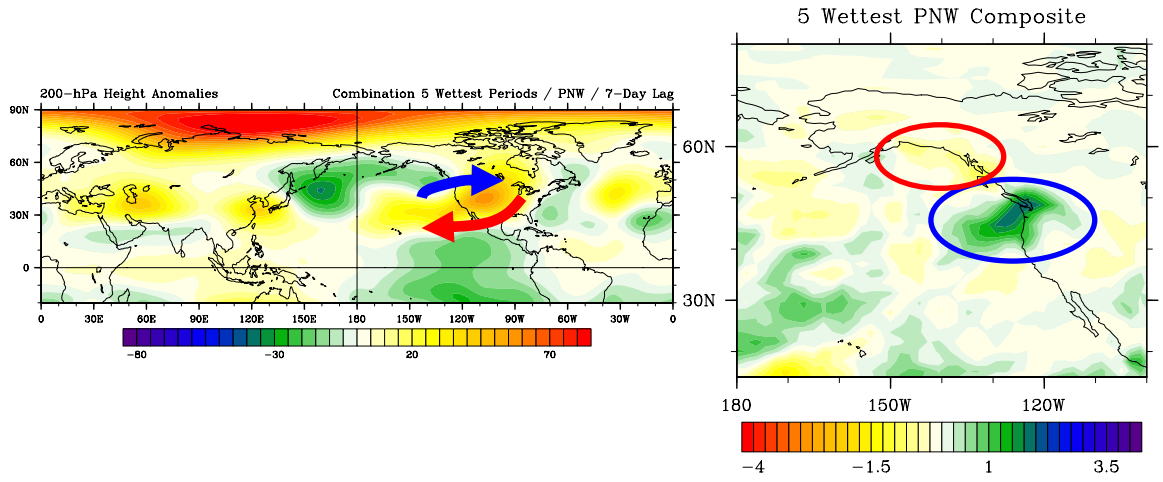

Figure 39. Composites of all days in the five composites with the most positive precipitation rate anomalies for the PNW region (Fig. 35) for 200-hPa height anomalies (left) and precipitation rate anomalies (right). Blue arrows and ovals highlight regions of anomalously onshore flow and positive precipitation rates, and red ovals and arrows indicate anomalously offshore flow and negative precipitation rates.

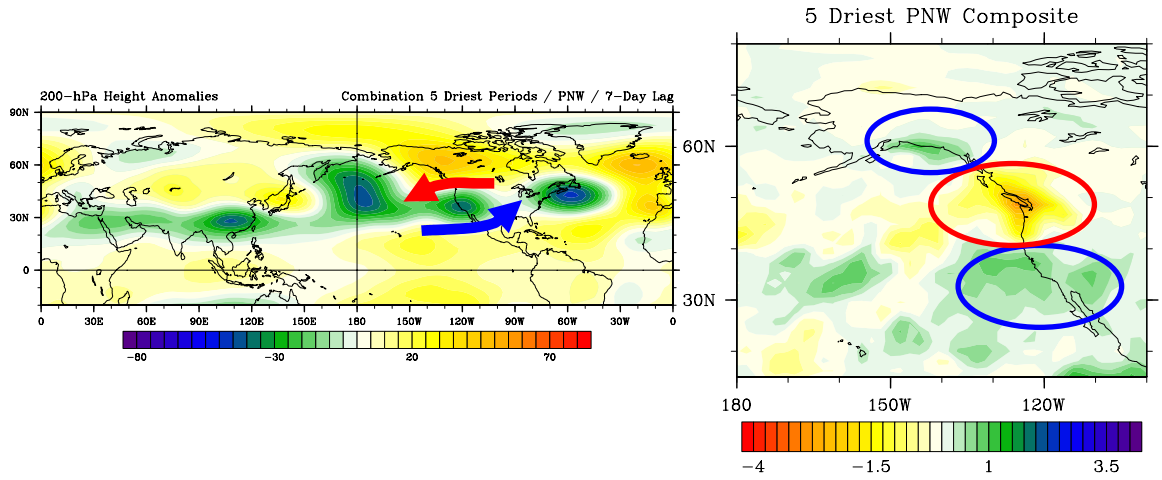

Figure 40. Composites of all days in the five composites with the most negative precipitation rate anomalies for the PNW region (Fig. 36) for 200-hPa height anomalies (left) and precipitation rate anomalies (right). Blue arrows and ovals highlight regions of anomalously onshore flow and positive precipitation rates, and red ovals and arrows indicate anomalously offshore flow and negative precipitation rates.

Favorable / Unfavorable Conditions for MJO-Associated Anomalously Wet Conditions in the PNW	
Favorable	**Unfavorable**
1. Middle or late phases of the MJO 2. OND or JFM 3. La Niña or neutral background state 4. Elongated anomalous low north and west of the PNW	1. Early phases of the MJO 2. El Niño background state
Favorable / Unfavorable Conditions for MJO-Associated Anomalously Dry Conditions in the PNW	
Favorable	**Unfavorable**
1. Early or late phases of the MJO 2. OND or JFM 3. Elongated anomalous low south of the PNW and an anomalous high to the north of the PNW over AK and Canada	1. Middle phases of the MJO 2. La Niña background state

Table 10. Favorable and unfavorable conditions during MJO activity for anomalously wet and dry periods in the PNW region.

c. British Columbia

Table 11 lists the critical factor conditions for the five composites in which the BC region had the most positive PRA composites and the five composites in which the BC region had the most negative PRA. This table indicates some of the conditions that may be favorable for anomalous wetness associated with the MJO, including early to middle phases of the MJO under EN conditions. Conditions that may be favorable for anomalous dryness associated with the MJO include very early or late phases of the MJO under EN conditions.

Figure 41 shows the PRAs for each of the five positive PRA composite, and Figure 42 shows the PRAs for the five negative PRA composites. A dipole relationship with anomalous wetness (dryness) over BC being associated with anomalous dryness (wetness) over CA-DSW is still notable, but much weaker than the dipole noted in both the CA-DSW and PNW composites.

5 Wettest Composites for BC	5 Driest Composites for BC
Phase 3 / Neutral / OND	Phase 1 / El Niño / OND
Phase 4 / El Niño / OND	Phase 8 / Neutral / OND
Phase 2 / El Niño / JFM	Phase 1 / El Niño / JFM
Phase 3 / La Niña / JFM	Phase 7 / El Niño / JFM
Phase 5 / El Niño / JFM	Phase 8 / La Niña / JFM

Table 11. Critical factor conditions for the five wettest and five driest composites for the BC region.

Figure 43 shows the 200-hPa height anomalies for the five wettest composites shown in Figure 41. This figure indicates that during periods in which BC is anomalously wet, there tends to be an anomalous low situated west of BC, with an anomalously high feature over the interior of Canada. This sets up a strong anomalous onshore flow into BC between the anomalous low and high from the southwest. Conversely, in anomalously dry conditions, an anomalous upper-level low is positioned south of BC, with an anomalous upper-level high over

Canada into AK. Flow in between these features is anomalously offshore, leading to cool, dry advection anomalies over BC. Although the circulation anomalies are not truly opposite in nature, the different positioning of the anomalous low in particular is critical to the orientation of the anomalous flow across the BC region.

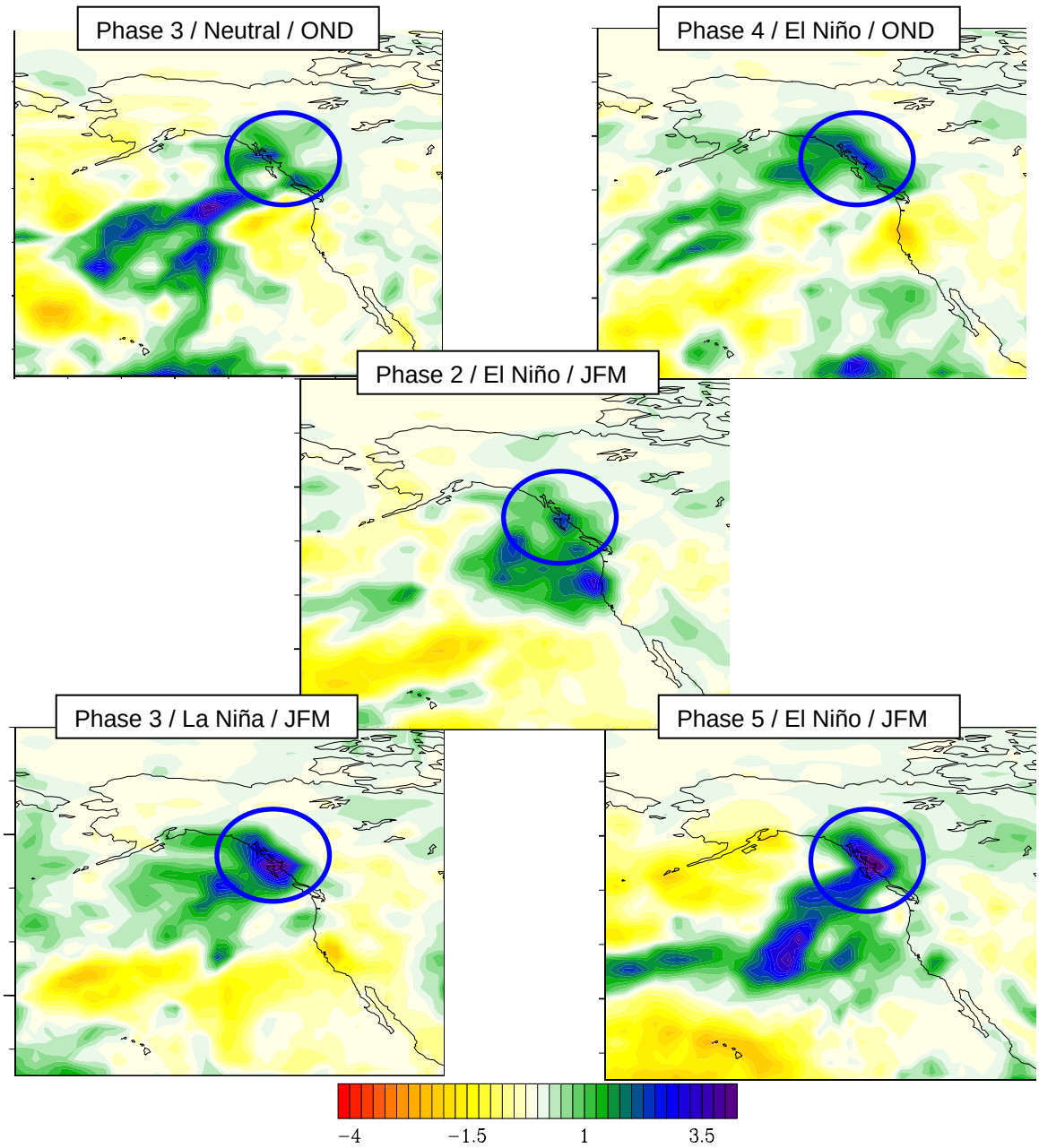

Figure 41. Precipitation rate anomalies for the five composites with the most positive precipitation rate anomalies for the BC region. The critical factor conditions for these five composites are shown in Table 11.

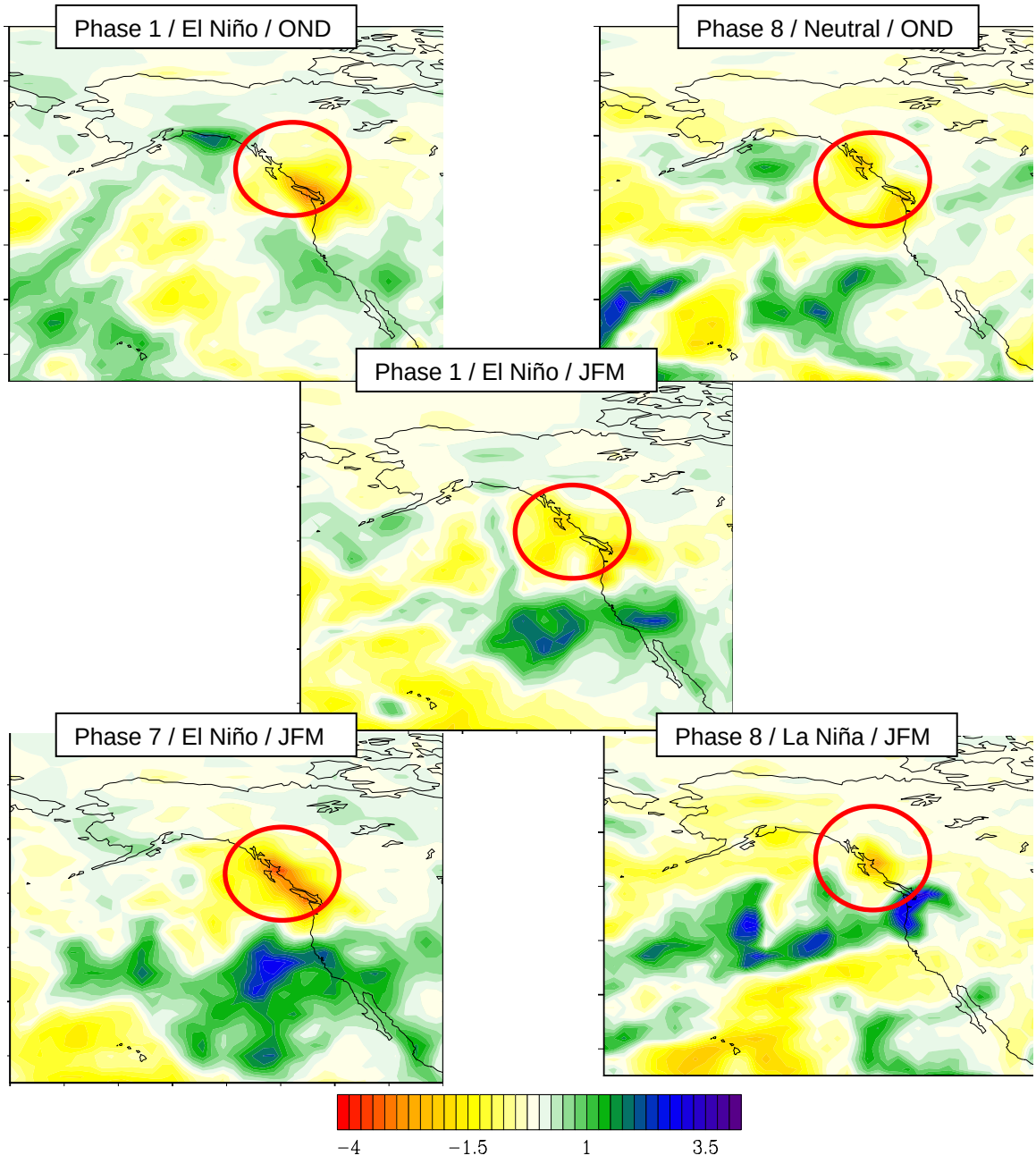

Figure 42. Precipitation rate anomalies for the five composites with the most negative precipitation rate anomalies for the BC region. The critical factor conditions for these five composites are shown in Table 11.

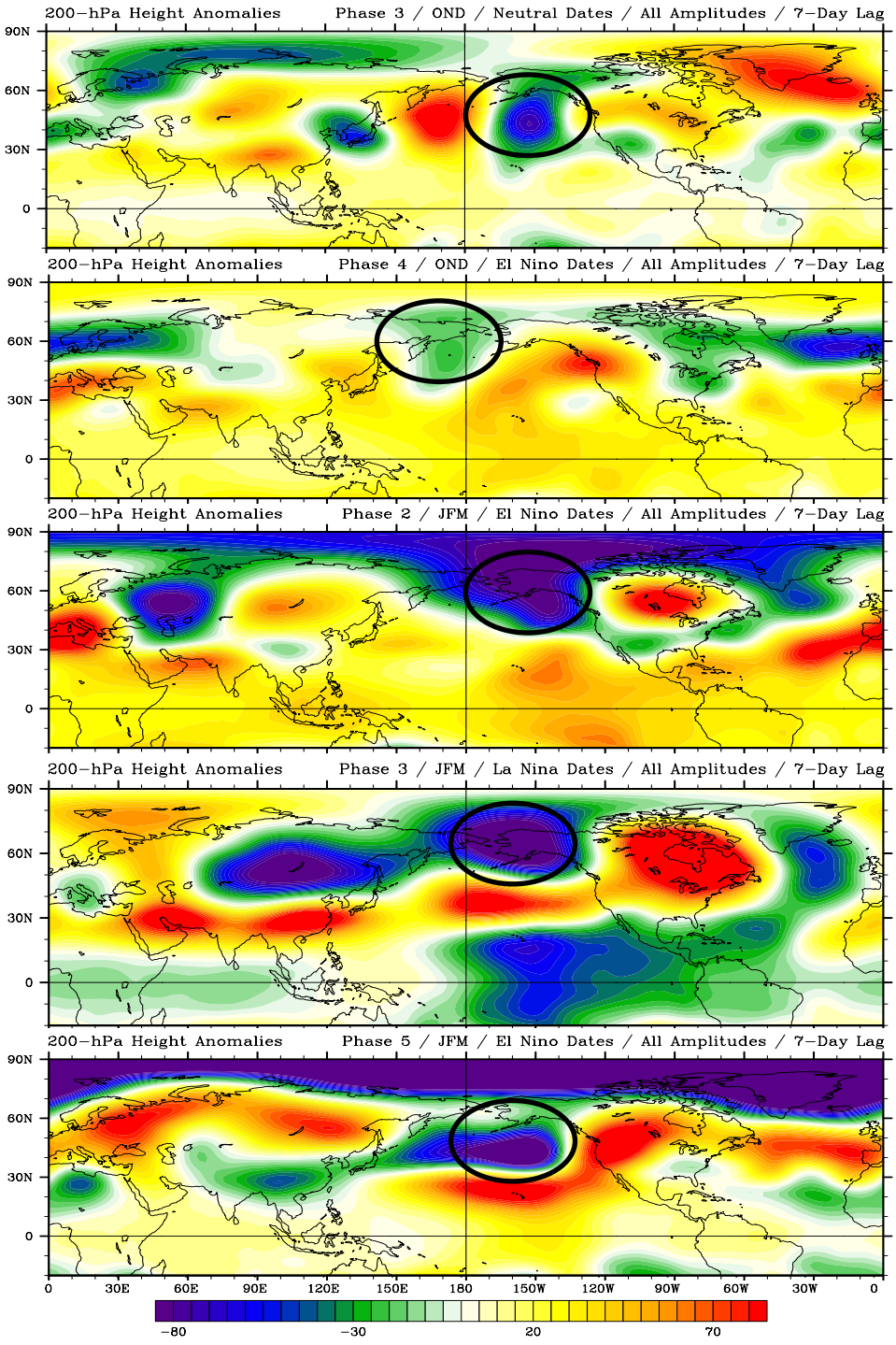

Figure 43. 200-hPa height anomalies for the five composites with the most positive precipitation rate anomalies for the BC region. The critical factor conditions for these five composites are shown in Table 11.

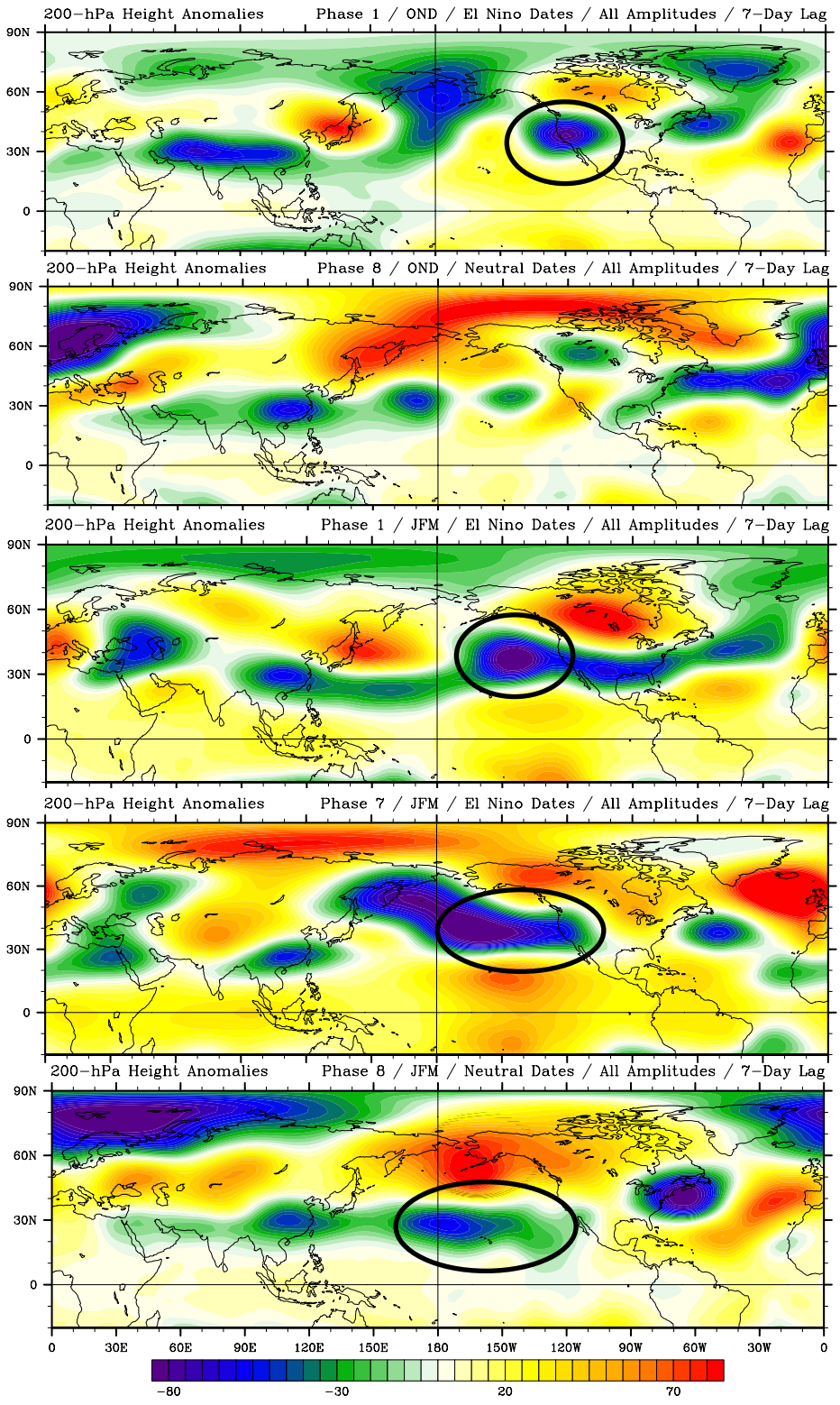

Figure 44. 200-hPa height anomalies for the five composites with the most negative precipitation rate anomalies for the BC region. The critical factor conditions for these five composites are shown in Table 11.

Figure 45 shows the 200-hPa height anomalies and precipitation rate anomalies derived from compositing all the days in the five wettest composites. This grouping of days characterizes the large-scale patterns that are responsible for anomalously high precipitation rates over the BC region. An intense anomalous upper level low over AK and an anomalous upper-level high over Canada help set up a strong anomalous onshore flow into BC. A weak shallow arching wave train from southwest Asia appears to be contributing to these features; this wave train stems from an upper-level anticyclone which is a product of the tropical Rossby wave response to anomalous convection in the IO in the early phases of the MJO.

Figure 46 shows the 200-hPa height anomalies and precipitation rate anomalies derived from compositing all the days in the five driest composites. Over the northeast Pacific, an elongated low stretches from the western United States out into the CPAC. There are indications that an anomalous wave train again extends from southern Asia, and that weak EN conditions in the tropical eastern Pacific are contributing to the upper-level anomalous low.

These results indicate that major precipitation anomalies in the BC region are driven by a dipole of anomalous circulation, with the anomalous high over the interior of Canada, and the anomalous upper-level low transitioning from north and west of BC in positive PRA periods to south of BC in negative PRA periods. In contrast to previous regions, it appears that the conditions that contribute to the anomalous positive PRAs are largely contributable to MJO activity, with little additional contribution from ENLN (Fig. 45). Conversely, the negative PRA periods have EN conditions that enhance the anomalous upper-level low that is part of an extratropical wave train (Fig. 46).

Table 12 summarizes the favorable and unfavorable conditions for positive and negative precipitation anomalies across BC concurrent with periods of MJO activity. There is a tendency for anomalously wet conditions to be associated with EN conditions in early and middle phases of the MJO. Similarly, EN conditions are also associated with anomalously dry conditions, but in the

very early or late phases of the MJO. Thus, one must be careful in associating MJO activity during EN events with PRA over BC. In addition, MJO activity concurrent with LN conditions is not favorable to either positive or negative PRAs over BC. These favorable and unfavorable conditions may be viewed as preliminary or hypothesized guidelines for accounting guidelines for accounting for the MJO when developing extended-range forecasts for the BC region in fall and winter.

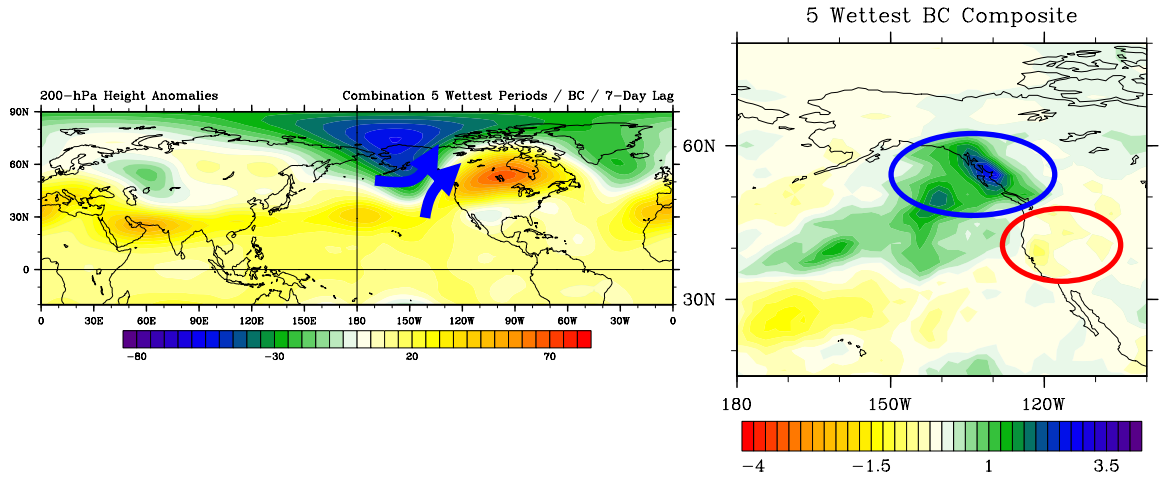

Figure 45. Composites of all days in the five composites with the most positive precipitation rate anomalies for the BC region (Fig. 41) for 200-hPa height anomalies (left) and precipitation rate anomalies (right). Blue arrows and ovals highlight regions of anomalously onshore flow and positive precipitation rates, and red ovals and arrows indicate anomalously offshore flow and negative precipitation rates.

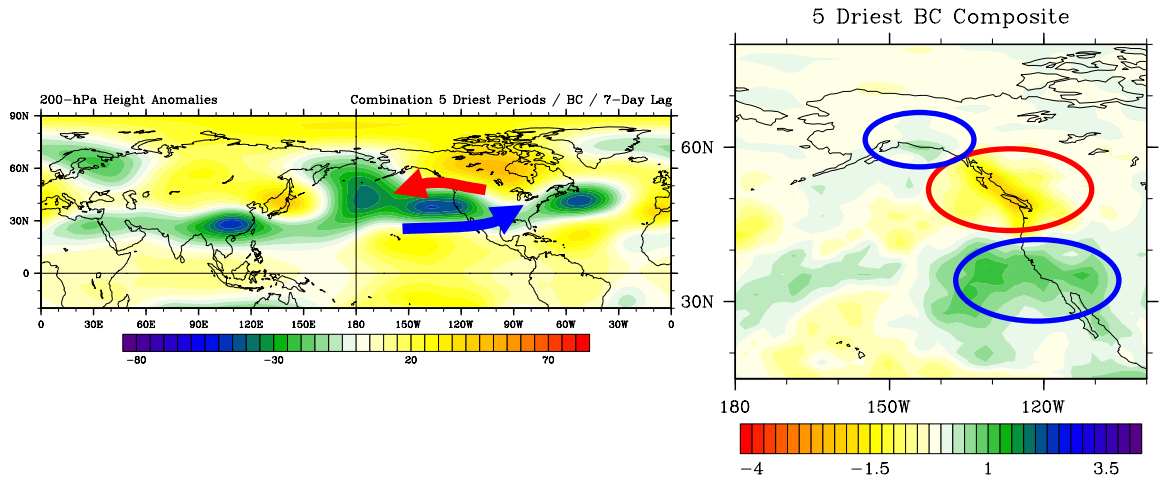

Figure 46. Composites of all days in the five composites with the most negative precipitation rate anomalies for the BC region (Fig. 42) for 200-hPa height anomalies (left) and precipitation rate anomalies (right). Blue arrows and ovals highlight regions of anomalously onshore flow and positive precipitation rates, and red ovals and arrows indicate anomalously offshore flow and negative precipitation rates.

Favorable / Unfavorable Conditions for MJO-Associated Anomalously Wet Conditions in BC	
Favorable	**Unfavorable**
1. Early or middle phases of the MJO 2. OND or JFM 3. El Niño background state 4. Presence of a strong anomalous low over Alaska and a strong anomalous high over the interior of Canada	1. Late phases of the MJO 2. La Niña background state
Favorable / Unfavorable Conditions for MJO-Associated Anomalously Dry Conditions in BC	
Favorable	**Unfavorable**
1. Very early or late phases of the MJO 2. OND or JFM 3. El Niño background state 4. Elongated anomalous low stretching from NPAC into western United States	1. Middle phases of the MJO 2. La Niña background state

Table 12. Favorable and unfavorable conditions during MJO activity for anomalously wet and dry periods in the BC region.

d. Alaska

Table 13 lists the critical factor conditions for the five composites in which the southern AK region had the most positive PRA composites and the five composites in which the southern AK region had the most negative PRA. This table indicates some of the conditions that may be favorable for anomalous wetness associated with the MJO, including the early or middle phases of the MJO during the fall months in conjunction with EN conditions. Conditions favorable for anomalous dryness associated with the MJO are less uniform and do not indicate any clearly patterns.

Figure 47 shows the PRAs for each of the five positive PRA composites, and Figure 48 shows the PRAs for the five negative composites. Similar to the BC cases, a weak dipole exists to the southeast of AK, with anomalously wet (dry) conditions over southern AK occurring simultaneously with anomalously dry (wet) conditions over the PNW region. This relationship is much weaker than in the CA-PNW and PNW region examples, but still shows how PRA relationships exist throughout western North America.

Figure 49 shows the 200-hPa height anomalies for the five wettest composites shown in Figure 47. This figure indicates that during periods that southern AK is wet, a strong anomalous low lies to the west and south of AK and an anomalous upper-level high is located over Canada. This sets up an anomalous onshore flow from the south with the longest fetch over the open waters of the Pacific. Conversely, in anomalously dry conditions, either an anomalous upper-level high sets up over and to the west of AK, or an anomalous low sets up over and to the east over Canada (Fig 50). There is no strong agreement between the five most negative PRAs over southern AK, with a variety of patterns resulting in the anomalously low precipitation.

5 Wettest Composites for AK	5 Driest Composites for AK
Phase 1 / El Niño / OND	Phase 1 / Neutral / OND
Phase 2 / La Niña / OND	Phase 3 / La Niña / OND
Phase 3 / El Niño / OND	Phase 6 / El Niño / OND
Phase 5 / El Niño / OND	Phase 2 / Neutral / JFM
Phase 6 / El Niño / JFM	Phase 8 / La Niña / JFM

Table 13. Critical factor conditions for the five wettest and five driest composites for the AK region.

Figure 51 shows the 200-hPa height anomalies and precipitation rate anomalies derived from compositing all the days in the five wettest composites for southern AK. This grouping of days includes the feature of a strong anomalous low centered over the Aleutian Islands with an anomalous high over west-central Canada, with anomalous onshore flow from the CPAC. An arching wave train originating in southeast Asia is easily identifiable, and appears to have connections to the subsidence component of the MJO around the Maritime Continent region. Considering that the early to middle phases of the MJO are conducive to anomalously high PRAs over southern AK, the subsidence component of the MJO is approaching and moving over the Maritime Continent, and the tropical Rossby wave response to this feature is an anomalous upper-level cyclone over southeast Asia. Although an EN pattern is evident by a twin anticyclone anomaly straddling the equator in response to the anomalous convection in the tropical eastern Pacific, this does not contribute heavily to the anomalous height patterns affecting the southern AK region.

Figure 52 shows the 200-hPa height anomalies and precipitation rate anomalies derived from compositing all the days in the five driest composites. The most striking feature is an elongated low over Canada, with a northwest to southeast orientation on the western fringes near AK. No other

strong signals are apparent, with any anomalous wave trains too weak to determine their relationship to the MJO.

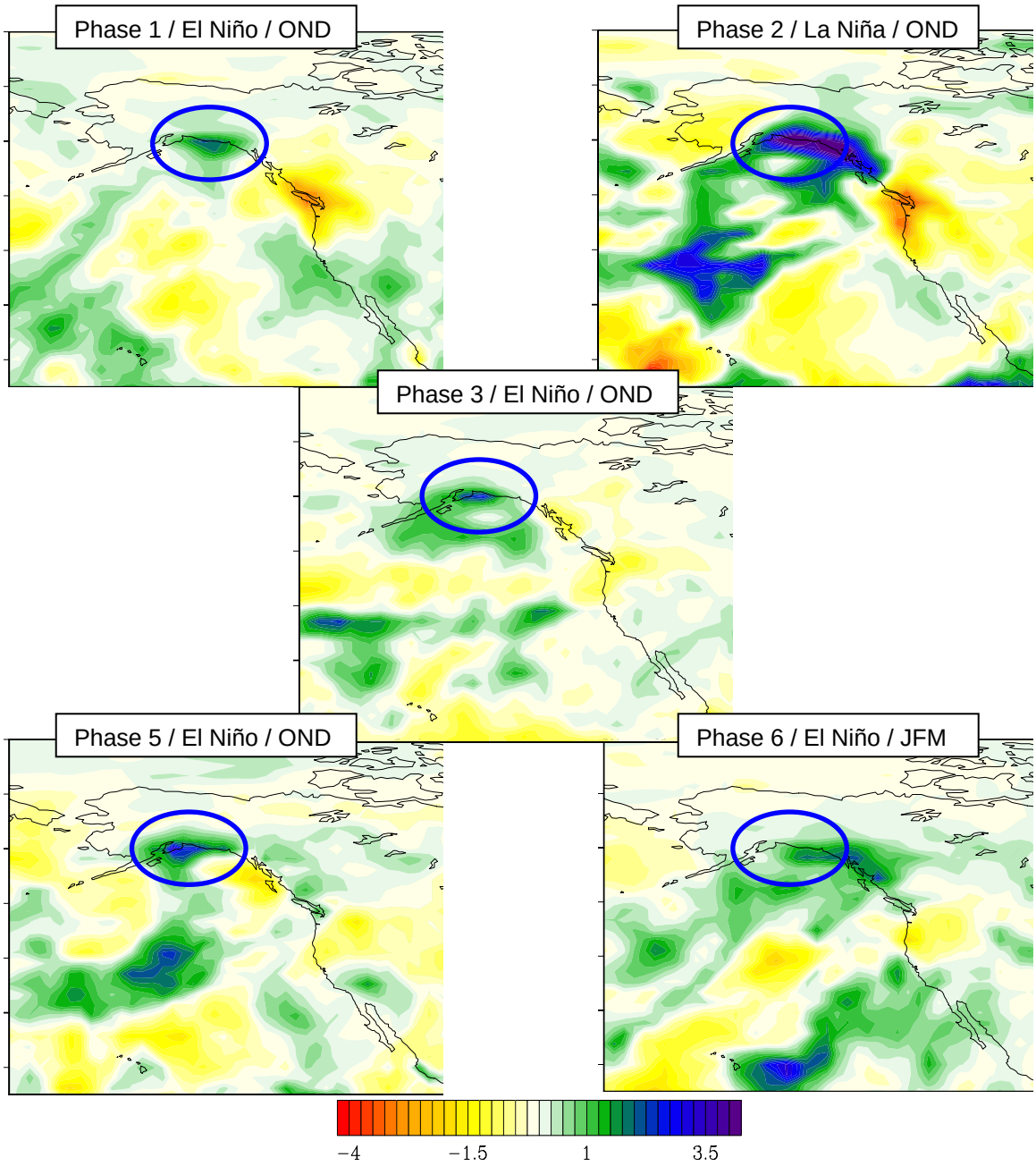

Figure 47. Precipitation rate anomalies for the five composites with the most positive precipitation rate anomalies for the southern AK region. The critical factor conditions for these five composites are shown in Table 13.

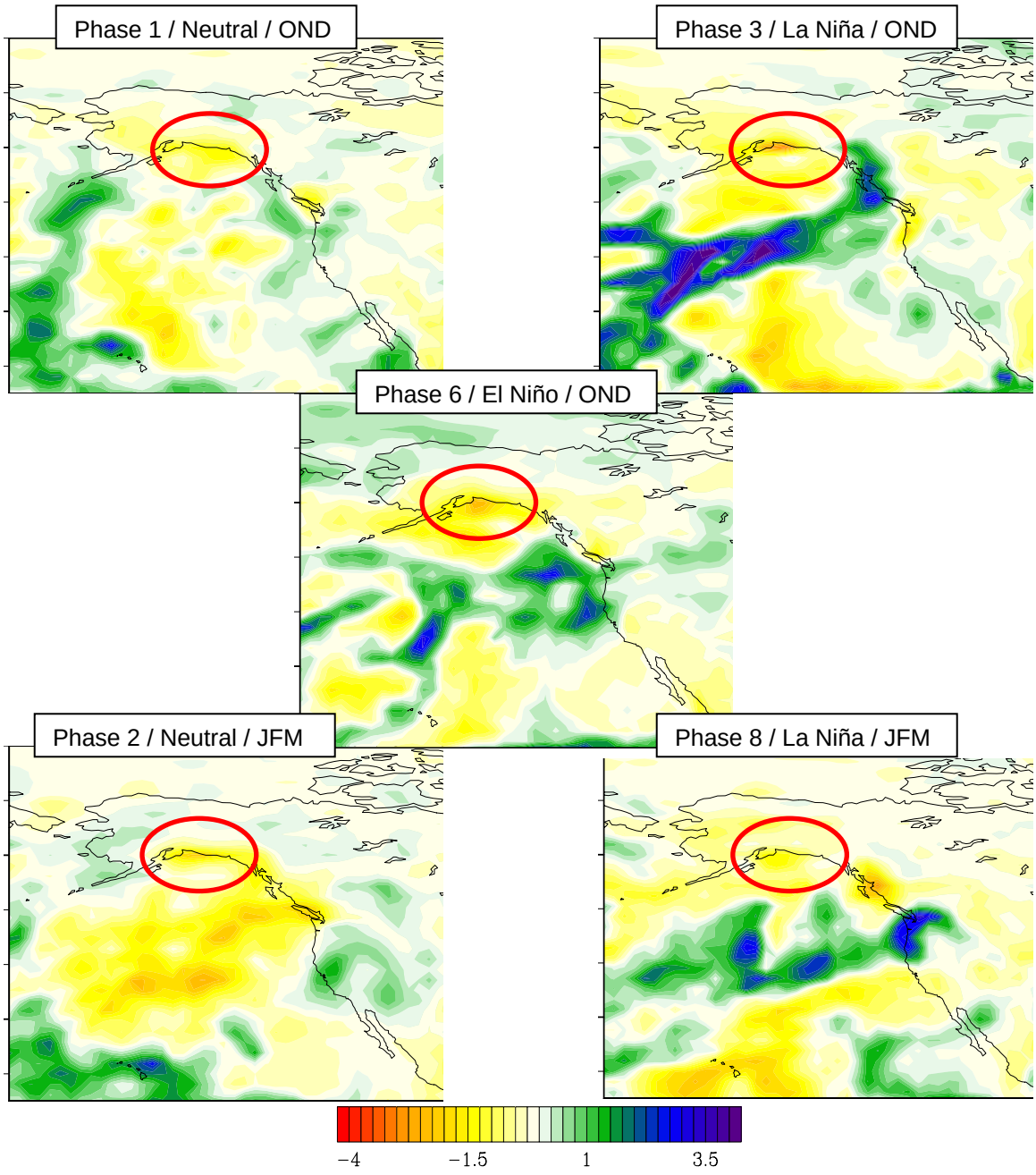

Figure 48. Precipitation rate anomalies for the five composites with the most negative precipitation rate anomalies for the southern AK region. The critical factor conditions for these five composites are shown in Table 13.

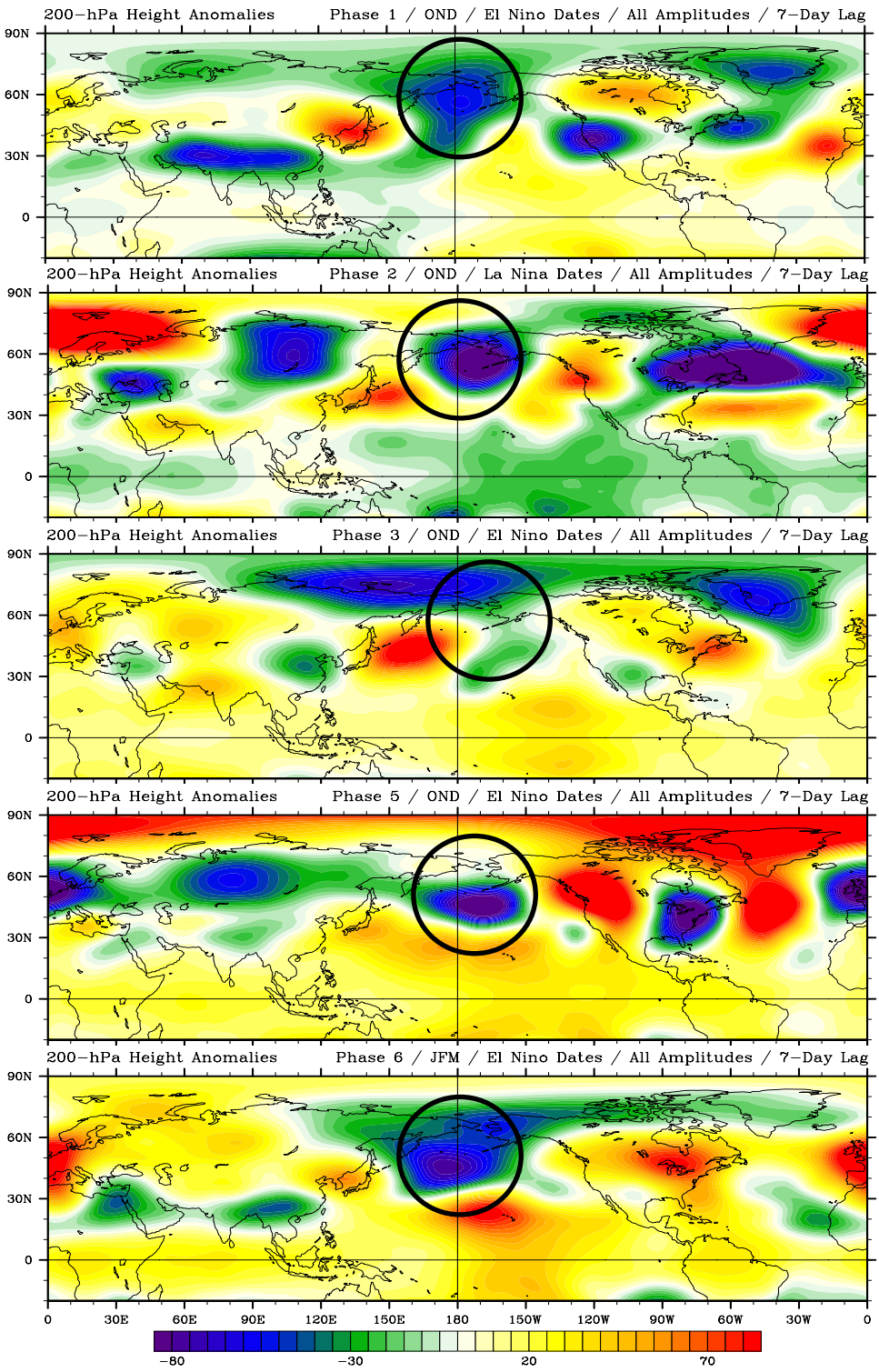

Figure 49. 200-hPa height anomalies for the five composites with the most positive precipitation rate anomalies for the southern AK region. The critical factor conditions for these composites are shown in Table 13.

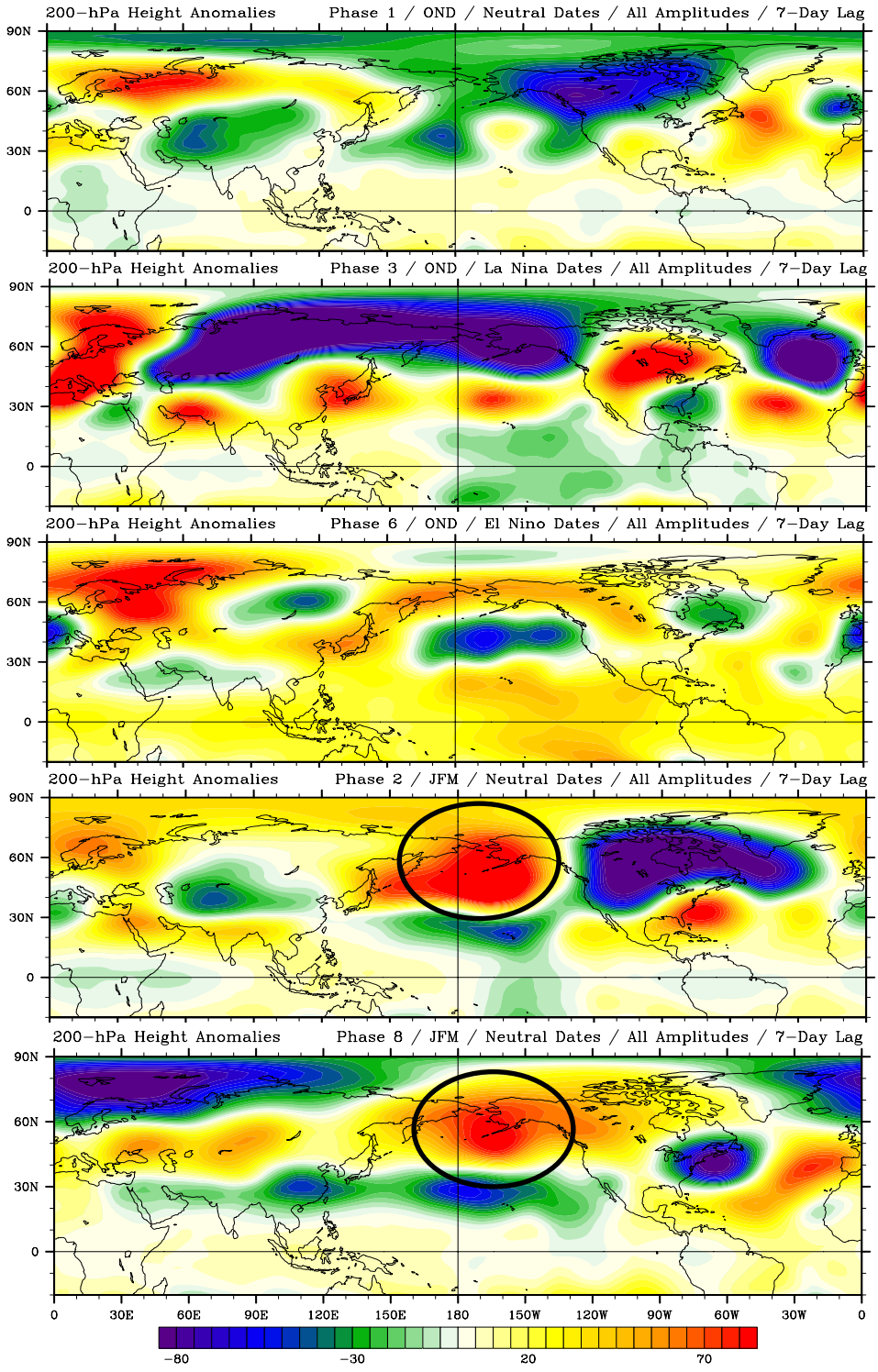

Figure 50. 200-hPa height anomalies for the five composites with the most negative PRAs for the southern AK region. The critical factor conditions for these composites are shown in Table 13.

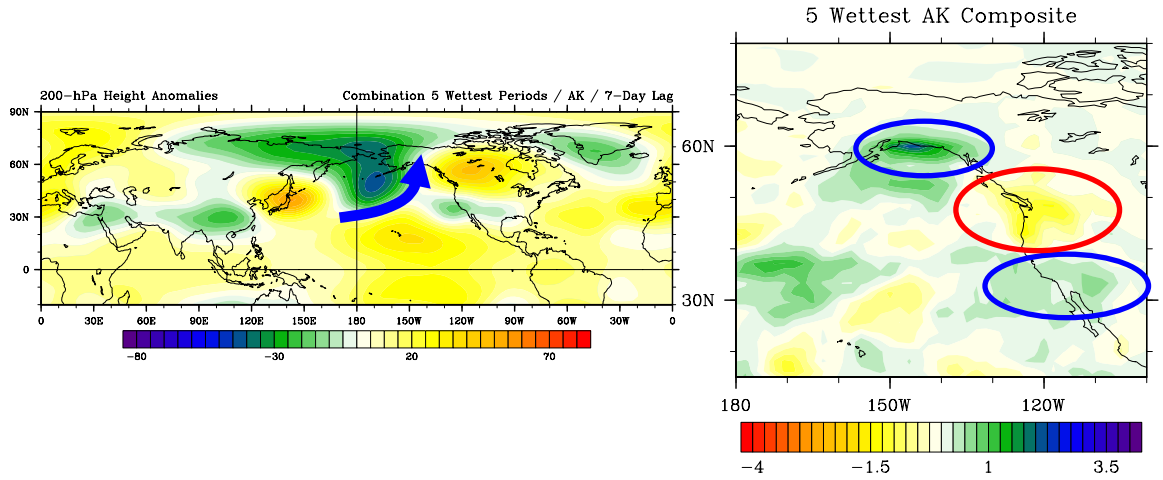

Figure 51. Composites of all days in the five composites with the most positive precipitation rate anomalies for the southern AK region (Fig. 47) for 200-hPa height anomalies (left) and precipitation rate anomalies (right). Blue arrows and ovals highlight regions of anomalously onshore flow and positive precipitation rates, and red ovals and arrows indicate anomalously offshore flow and negative precipitation rates.

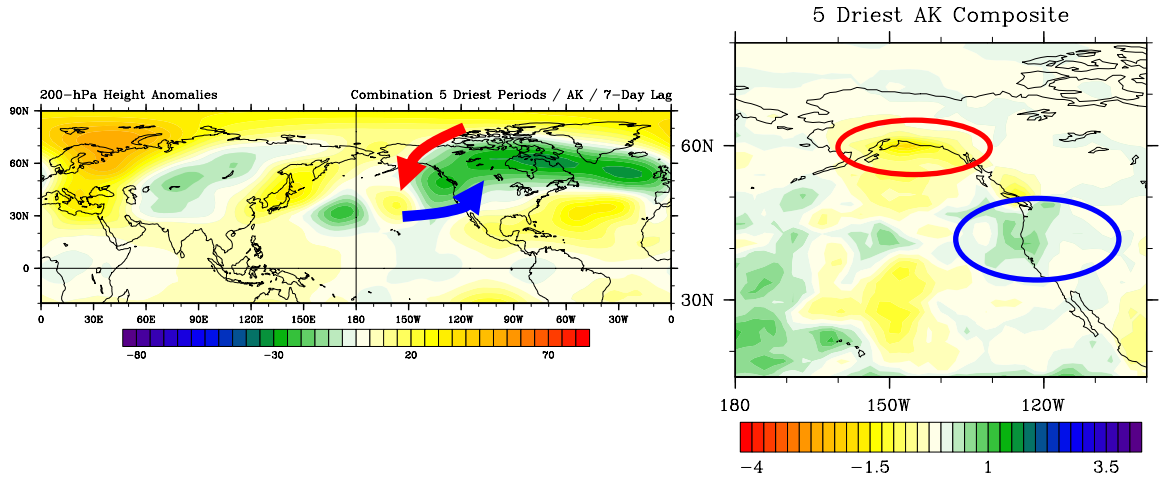

Figure 52. Composites of all days in the five composites with the most negative precipitation rate anomalies for the southern AK region (Fig. 48) for 200-hPa height anomalies (left) and precipitation rate anomalies (right). Blue arrows and ovals highlight regions of anomalously onshore flow and positive precipitation rates, and red ovals and arrows indicate anomalously offshore flow and negative precipitation rates.

Table 14 summarizes, for periods of MJO activity, the favorable and unfavorable conditions for positive and negative precipitation anomalies over southern AK. In particular, the early and middle phases of the MJO, in conjunction with EN conditions during the fall months are conducive to positive PRAs over AK. However, no clear patterns related to the MJO have been identified for anomalously low PRAs over southern AK. The favorable conditions may be viewed as preliminary or hypothesized guidelines for accounting for the MJO when developing extended-range forecasts for southern AK.

Favorable / Unfavorable Conditions for MJO-Associated Anomalously Wet Conditions in southern AK	
Favorable	**Unfavorable**
1. Early or middle phases of the MJO 2. OND 3. El Niño background state	1. Late phases of the MJO 2. JFM 3. Neutral or La Niña background state
Favorable / Unfavorable Conditions for MJO-Associated Anomalously Dry Conditions in southern AK	
Favorable	**Unfavorable**
1. OND or JFM 2. Presence of a strong anomalous low to the south and east of AK	1. No clear unfavorable conditions

Table 14. Favorable and unfavorable conditions during MJO activity for anomalously wet and dry periods in the AK region.

3. Relationships to Prior Studies

The findings of our research are both similar to and different from those of prior studies. We compared our results for the CA-DSW region to those from Jones (2000) and Mo and Higgins (1998), and for the PNW to those from Bond and Vecchi (2003) and Mo and Higgins (1998). We were unable to compare our results for BC and AK since no comparable studies exist for those regions.

Our results for CA-DSW were in strong contrast to prior results. In particular, we found anomalously wet conditions for the MJO phases which prior studies had associated with dry conditions, and vice versa (see Table 15). However, for the PNW, our study agreed closely with prior studies in finding that anomalously high precipitation was more common in the middle to late phases of the MJO, and anomalously low precipitation values was more common in the early phases of the MJO. Of course, many of the differences are probably attributable to different methods we used for identifying the NPNA response to the MJO. Our methods were unique in many ways (e.g., no filtering, segregating by MJO phase, season, and EN/LN/neutral background conditions). Table 15 summarizes our comparison of our results to prior studies.

Region & Prior Studies	Results from Prior Study	Our Results
CA & the DSW Mo and Higgins (1998) Jones (2000)	*Mo and Higgins:* Anomalously Wet Conditions: Phase 7 & 8 Anomalously Dry Conditions: Phase 4 & 5 (Jones results similar to those from Mo and Higgins)	Anomalously Wet Conditions: - Early Phases (1 & 2) - El Niño Conditions Anomalously Dry Conditions: - Late Phases (7 & 8) - La Niña Conditions
PNW Bond and Vecchi (2003) Mo and Higgins (1998)	*Bond and Vecchi:* OND: Anomalously Wet Conditions: Phase 7 & 8 Anomalously Dry Conditions: Phase 1, 2 & 4 JFM: Anomalously Wet Conditions: Phase 5 Anomalously Dry Conditions: Phase 2 & 7 *Mo and Higgins:* Anomalously Wet Conditions: Phase 4 & 5 Anomalously Dry Conditions: Phase 6, 7 & 8	Anomalously Wet Conditions: - Middle to Late Phases (5 – 8) - La Niña Conditions Anomalously Dry Conditions: - Early and Late Phases (1, 2, 7 & 8)

Table 15. Overview comparison of our result with those from prior studies.

C. CASE STUDIES OF INDIVIDUAL EVENTS

We analyzed several cases in which anomalously high precipitation occurred in CA in association with MJO activity. Our objective was to determine if and how our CA-DSW results applied to individual events. (see the patterns, processes, relationships, favorable/unfavorable conditions identified in the prior CA-DSW section). The following cases were analyzed from a backwards perspective in which we first identified anomalously positive precipitation events were identified, and then related them back to the MJO, especially the three critical factors: (1) phase of the MJO, (2) season of MJO occurrence; and (3) EN / LN/ neutral background state.

1. December 2004 – January 2005

Late December of 2004 into early January 2005 was a period of highly anomalous heavy rainfall across southern California. Considerable flooding occurred throughout much of the region, and copious amounts of rainfall were received at numerous DoD installations, including Edwards AFB. During this anomalously high precipitation event, there was a moderate MJO that was in phases 1-4, with weak amplitudes in phases 1-3, and moderate amplitudes in phase 4 (Fig. 53). Background conditions in the tropical Pacific were neutral (i.e., no concurrent EN or LN event), so there was no interference occurring between the MJO and a coexisting EN or LN event.

The 200-hPa height anomaly for this event (Fig. 54) shows an anomalous shallow arching wave train extending from southeast Asia into the NPNA region. One feature of this wave train is an anomalous cyclone to the north and west of CA, tilted so that there is anomalously onshore flow from the tropics into southern CA.

The favorable conditions for anomalously high precipitation in the CA-DSW region are (see Table 8):

1. Early or late phases of the MJO
2. OND or JFM
3. El Niño or neutral background state
4. Anomalous wave train emanating from Asia with an anomalous low north and west of CA
5. Southwest to northeast tilt to the anomalous low off CA

Figures 53-54 show that the conditions during the late December 2004 – early January 2005 event were:

1. Early phases of the MJO
2. Late OND and early JFM
3. Neutral background state
4. Anomalous wave train emanating from Asia with an anomalous low north and west of CA
5. Southwest to northeast tilt to the anomalous low off CA

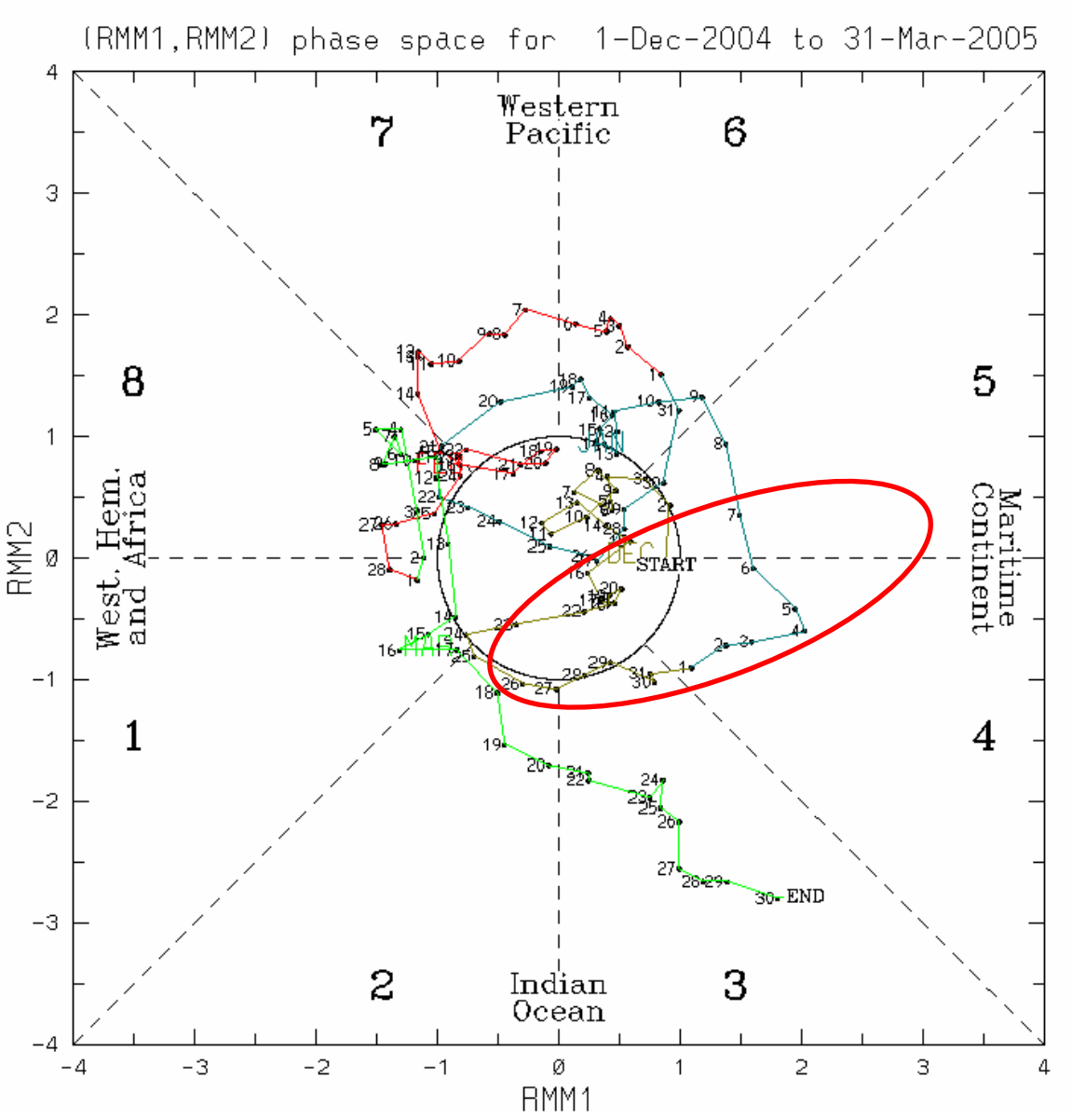

Figure 53. Wheeler phase-space diagram for 1 Dec 2004 to 31 Mar 2005 (Dec in brown, Jan in blue). The late December – early January period in which anomalously heavy precipitation occurred in southern CA is highlighted by the red oval. Accounting for a lag of about one week between the development of MJO conditions in the tropics and the development of an NPNA response to those conditions, indicates that the MJO conditions most closely associated with the southern CA precipitation anomaly were: phases 1-4, with low amplitudes in phases 1-3 and moderate amplitudes in phase 4.

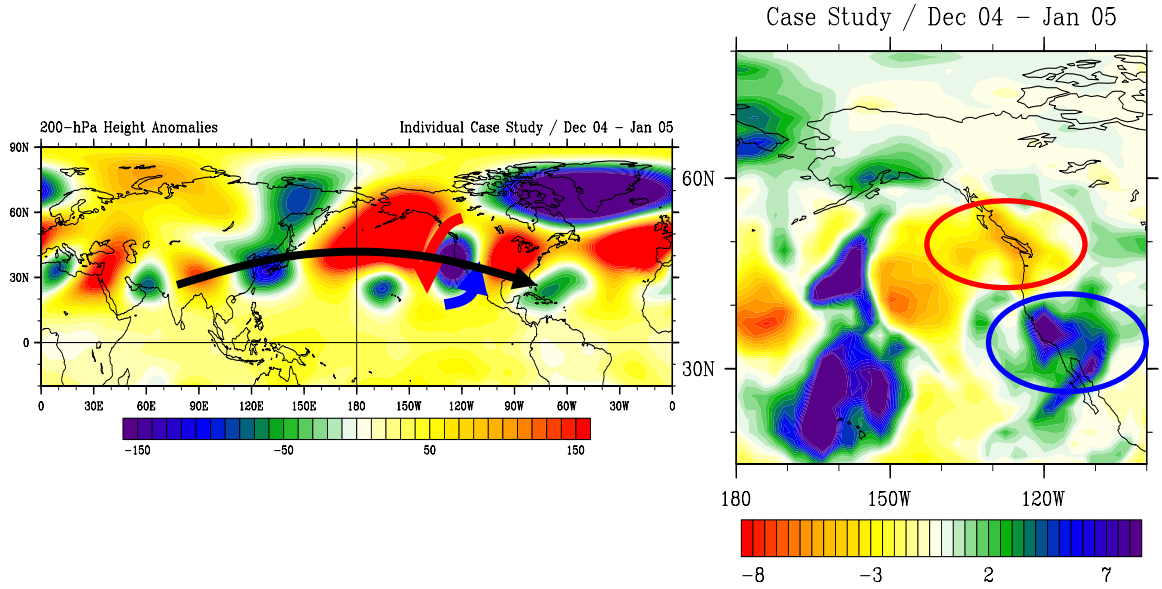

Figure 54. 200-hPa height anomalies (left) and precipitation rate anomalies (right) for a strong precipitation event over southern California during late December 2004 - early January 2005. Anomalously onshore (offshore) flow and positive (negative) precipitation anomalies are marked by blue (red) arrows (left panel) and ovals (right panel). Black arrows designate the energy propagation through an anomalous extratropical wave train extending from southeast Asia into the NPNA region.

Thus, all five favorable conditions were met for this individual event. Our analysis of this individual case suggests that the guidance provided by the CA-DSW table of favorable / unfavorable conditions (Table 8) may be useful in preparing MJO-based extended range forecasts for the CA-DSW region.

2. December 1996 – January 1997

One of the most significant flooding events in CA history occurred during the months of December 1996 and January 1997. Catastrophic rainfall occurred through much of the central and northern part of the state, and record rainfall amounts occurred in and around the Sierra Nevada mountain range. Civilians who were evacuated from areas affected by some of the worst flooding were sheltered on Beale AFB, resulting in an extensive humanitarian effort conducted by USAF and other DoD personnel.

An intense MJO was ongoing throughout this period of extreme positive PRAs, stretching from phase 3 to 8 (Fig. 55). The 200-hPa height anomaly for this event (Fig 56) shows a significant anomalous wave train and intense anomalous onshore flow around the base of an anomalous low to the north and west of CA. This anomalous flow helped usher in an extended period of anomalous precipitation across a broad region of the western CONUS (Fig. 56).

The favorable conditions for anomalously high precipitation in the CA-DSW region are (see Table 8):

1. Early or late phases of the MJO
2. OND or JFM
3. El Niño or neutral background state
4. Anomalous wave train emanating from Asia with an anomalous low north and west of CA
5. Southwest to northeast tilt to the anomalous low off CA

Figures 55-56 show that the conditions during the December 1996 – January 1997 event were:

1. All phases of the MJO (especially middle to late)
2. Late OND and early JFM
3. Neutral background state
4. Anomalous wave train emanating from Asia with an anomalous low north and west of CA
5. Southwest to northeast tilt to the anomalous low off CA

All five favorable conditions were met for this individual event, although anomalously high rainfall did occur throughout the middle phases of the MJO as well. Our analysis of this individual case suggests that the guidance provided by the CA-DSW table of favorable / unfavorable conditions (Table 8) may be useful in preparing MJO-based extended range forecasts for the CA-DSW region.

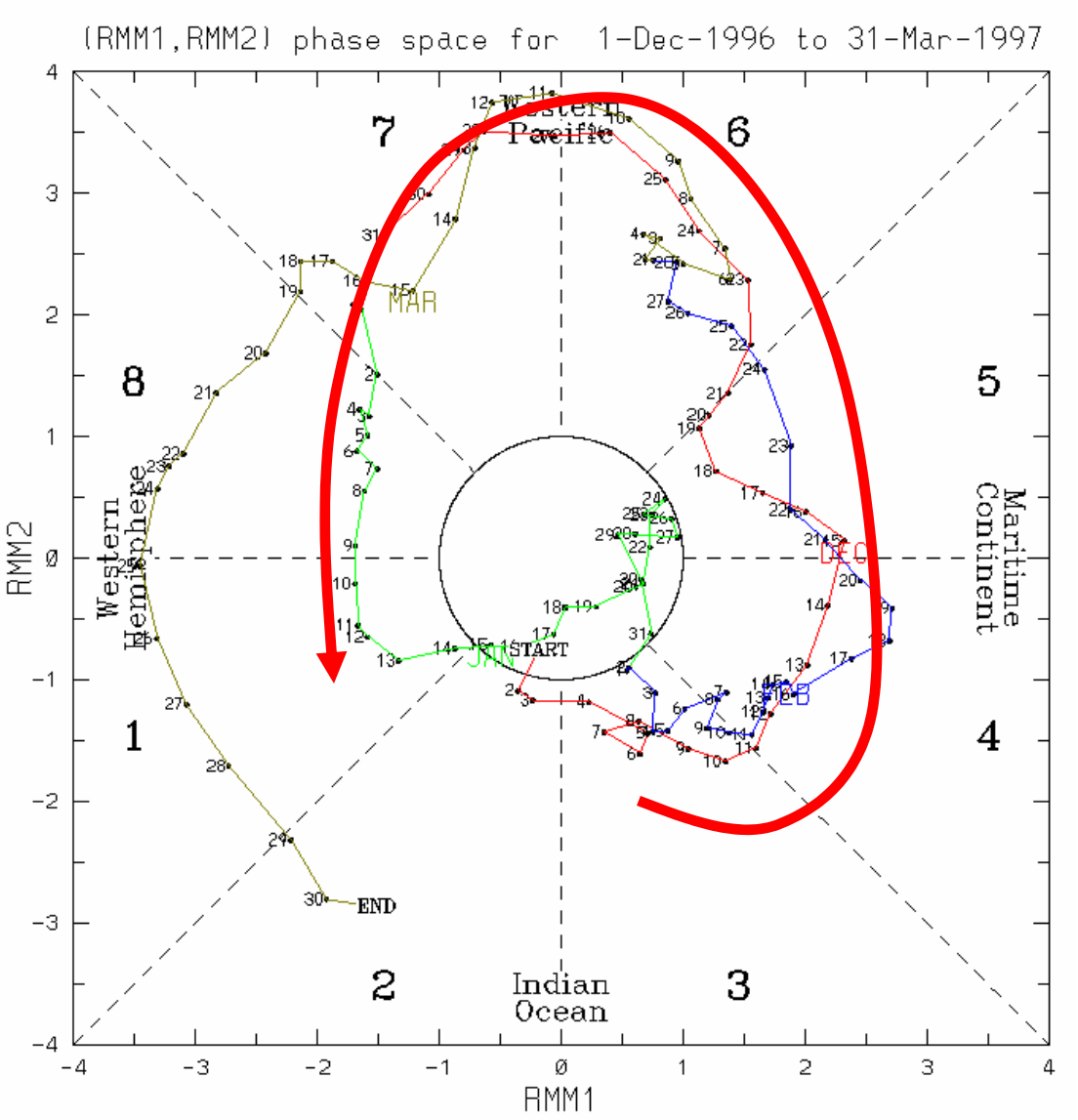

Figure 55. Wheeler phase-space diagram for 1 Dec 1996 to 31 Mar 1997 (Dec in red, Jan in green). The December – January period in which anomalously heavy precipitation occurred across central and northern CA is outlined by the red arrow. Accounting for a lag of about one week between the development of MJO conditions in the tropics and the development of an NPNA response to those conditions indicate that intense rainfall periods occurred in the middle to late phases of the MJO.

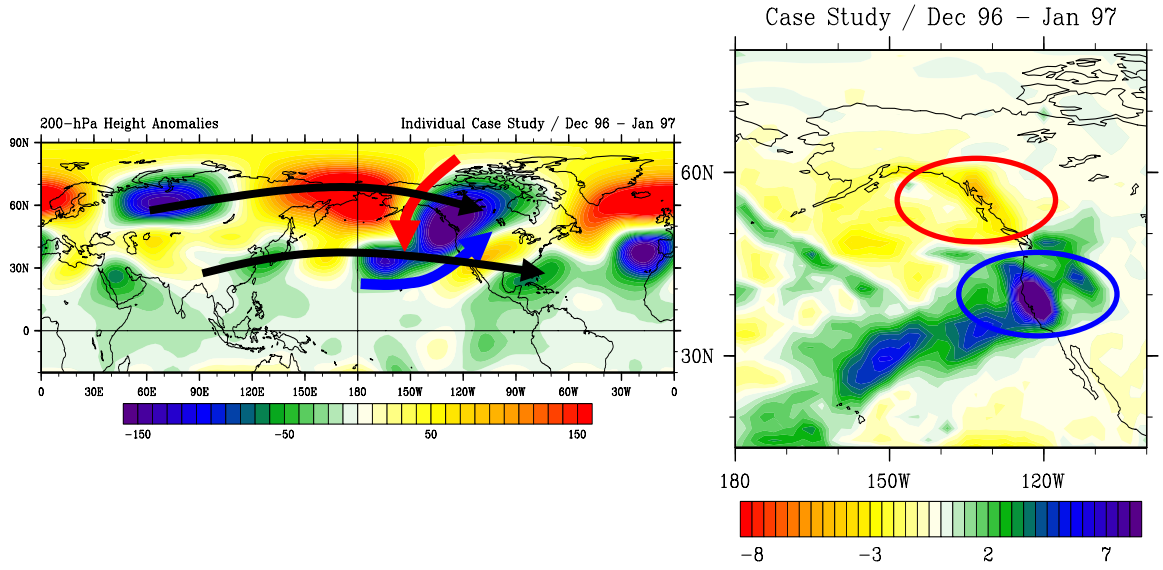

Figure 56. 200-hPa height anomalies (left) and precipitation rate anomalies (right) for a strong precipitation event over central and northern California during late December 1996 – March 1997. Anomalously onshore (offshore) flow and positive (negative) precipitation anomalies are marked by blue (red) arrows (left panel) and ovals (right panel). Black arrows designate the energy propagation through anomalous extratropical wave trains extending from Asia into the NPNA region.

3. January 1995

January 1995 was a period of highly anomalous heavy rainfall across much of CA. During this event, a weak to moderate MJO was located in phases 3 and 4 (Fig. 57). Background conditions in the tropical Pacific were characterized by a strong El Niño. While in phases 3 and 4, the convective component of the MJO is approaching the Maritime Continent, and the subsidence component of the MJO is near the IDL over the tropical CPAC, so at least some destructive interference would have been occurring between the convective and subsidence components of the MJO and EN event (Table 6).

The 200-hPa height anomaly for this event (Fig. 58) shows an anomalous wave train through the NPNA region. One feature of this wave train appears to be interference between a wave train originating across Asia and another wave train originating from the tropical Rossby wave response to anomalous El Niño

convection over the tropical eastern Pacific. This sets up an anomalous cyclone to the west of CA, with anomalous moist onshore flow from the oceanic regions.

The favorable conditions for anomalously high precipitation in the CA-DSW region are (see Table 8):

1. Early or late phases of the MJO
2. OND or JFM
3. El Niño or neutral background state
4. Anomalous wave train emanating from Asia with an anomalous low north and west of CA
5. Southwest to northeast tilt to the anomalous low off CA

Figures 57-58 show that the conditions during the January 1995 event were:

1. Early to middle phases of the MJO
2. Early JFM
3. El Niño background state
4. Anomalous wave train emanating from Asia with an anomalous low north and west of CA
5. West to east tilt of the anomalous low off CA

The majority of the favorable conditions listed above were met for the January 1995 event, including the EN background state. Our analysis of this individual case suggests that the guidance provided by the CA-DSW table of favorable / unfavorable conditions (Table 8) may be useful in preparing MJO-based extended-range forecasts for the CA-DSW region

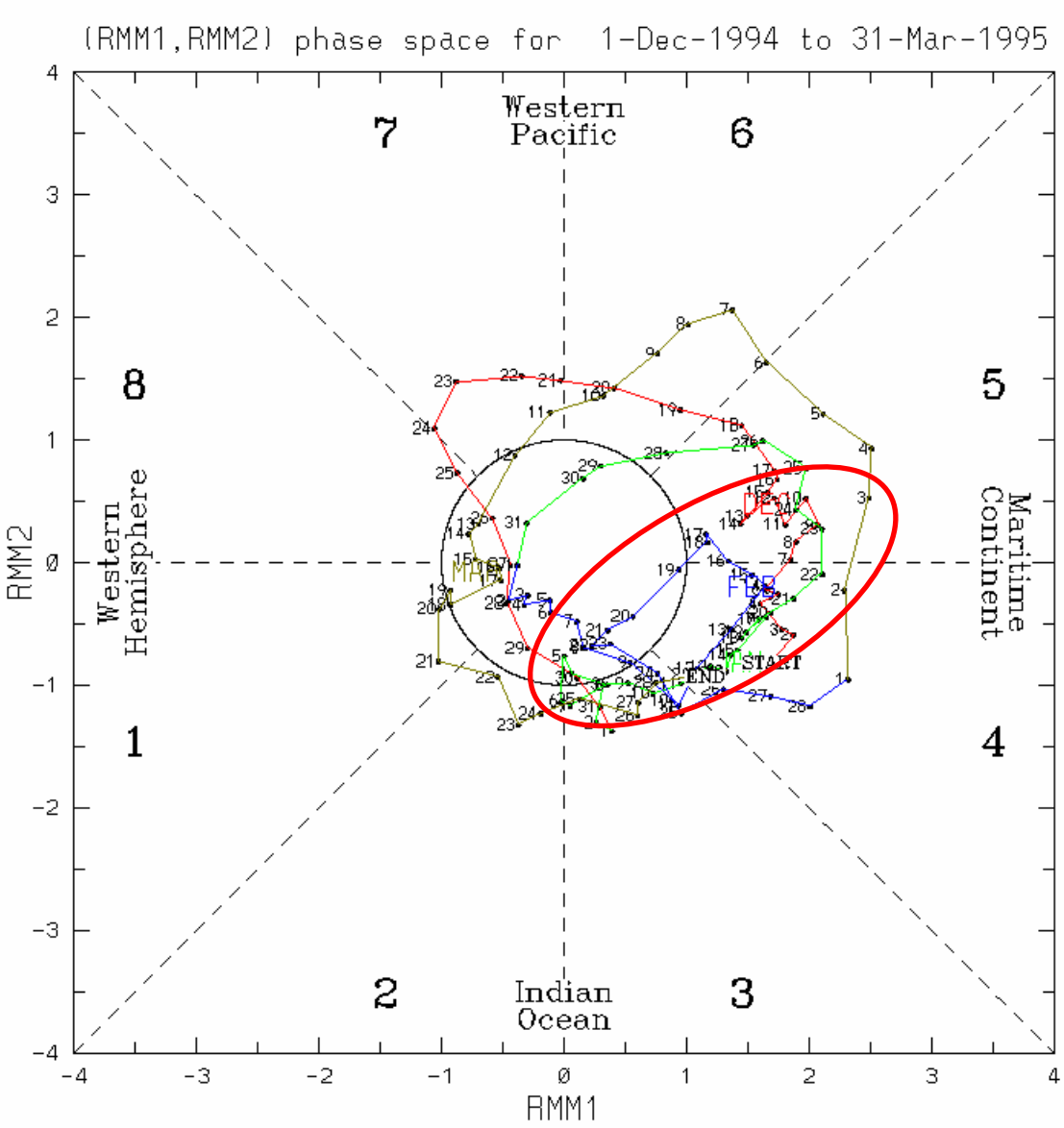

Figure 57. Wheeler phase-space diagram for 1 Dec 1994 to 31 Mar 1995 (Jan in green). The January period in which anomalously heavy precipitation occurred in CA is highlighted by the red oval. Accounting for a lag of about one week between the development of MJO conditions in the tropics and the development of an NPNA response to those conditions, indicates that the MJO conditions most closely associated with the positive precipitation anomalies in CA were phases 2-5, with low amplitudes in phases 2-3 and moderate amplitudes in phases 4-5.

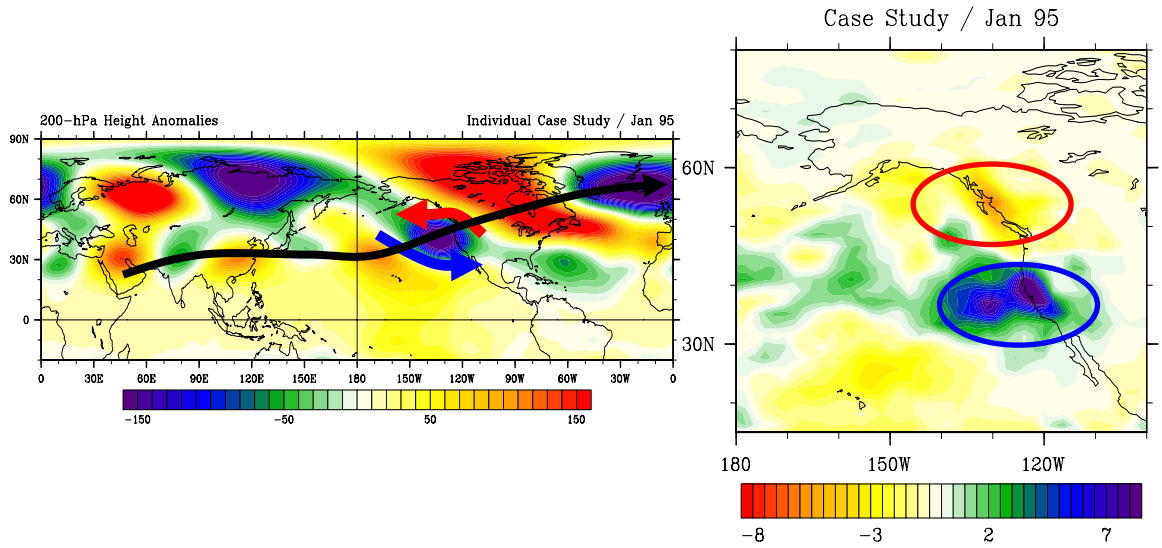

Figure 58. 200-hPa height anomalies (left) and precipitation rate anomalies (right) for a strong precipitation event over California during January 1995. Anomalously onshore (offshore) flow and positive (negative) precipitation anomalies are marked by blue (red) arrows (left panel) and ovals (right panel). Black arrows designate the energy propagation through an anomalous extratropical wave train extending from southeast Asia into the NPNA region.

4. Summary of Individual Case Studies

Through our investigation of three anomalously high precipitation events in the CA-DSW region, we found that our preliminary guidelines for forecasting the impacts of the MJO on CA-DSW were consistent with the conditions that occurred during the individual cases. Thus, it appears that these guidelines may be useful as a basis for developing extended range forecasts of MJO impacts n precipitation in CA-DSW during fall and winter. One additional indication that the preliminary guidelines may be useful is that they were developed using a forward approach but confirmed using a different approach, the forward approach. That is, we developed them by identifying and compositing according to the anomalies associated with the different critical factors that precede the precipitation anomalies in the CA-DSW region and that occur in locations that are far from the CA-DSW region. But we tested them by identifying and compositing according to the positive precipitation anomalies in the CA-DWS region that follow the

development of the remote critical factors. This of course increases our confidence in the usefulness of the guidelines.

However, we have only examined three cases corresponding to anomalously high precipitation events across CA-DSW, so similar examinations are needed of anomalously low precipitation events, and of anomalously high and low precipitation events in the other regions of western North America.

D. ADDITIONAL RESULTS WITH NPNA FORECAST IMPLICATIONS

1. Role of the Subsidence Component of the MJO

We noted throughout our examination of the MJO composites that the subsidence component of the MJO was associated with a tropical Rossby wave response, similar to the association of a tropical Rossby wave response to the convective component. For the subsidence (convective) component, there was an upper tropospheric Rossby wave cyclonic (anticyclonic) anomaly situated poleward and westward of the subsidence (convective) component. Thes relationships between the subsidence and convective components are expected from basic tropical dynamics theory (Matsuno 1966, Gill 1980).

Our composite analyses often showed that the upper-level off-equatorial cyclone associated with the subsidence component was the initial anomaly in an anomalous wave train extending from southeast Asia into the NPNA region. The same was true for the upper-level off-equatorial anticyclone associated with the convective component, but with the anomalous wave train in that case being oppositely signed than to the wave train associated with the subsidence component.

Figure 59 shows the 200-hPa height anomaly for a composite of all MJO events with an amplitude of 1.0 or greater, in phase 1, during October-March, and during EN, LN, or neutral conditions. The position of the subsidence component during phase 1 is over the Maritime Continent. The cyclonic anomaly over southern Asia and centered over eastern China, represents the tropical Rossby wave response to the subsidence component. Note that this cyclonic

anomaly is the initial anomaly in an anomalous wave train arching into the NPNA region. This indicates that the subsidence component of the MJO must be accounted for in extended range forecasting for the NPNA region, along with the convective component. The results in Figure 59 are representative of the many composites we constructed and analyzed.

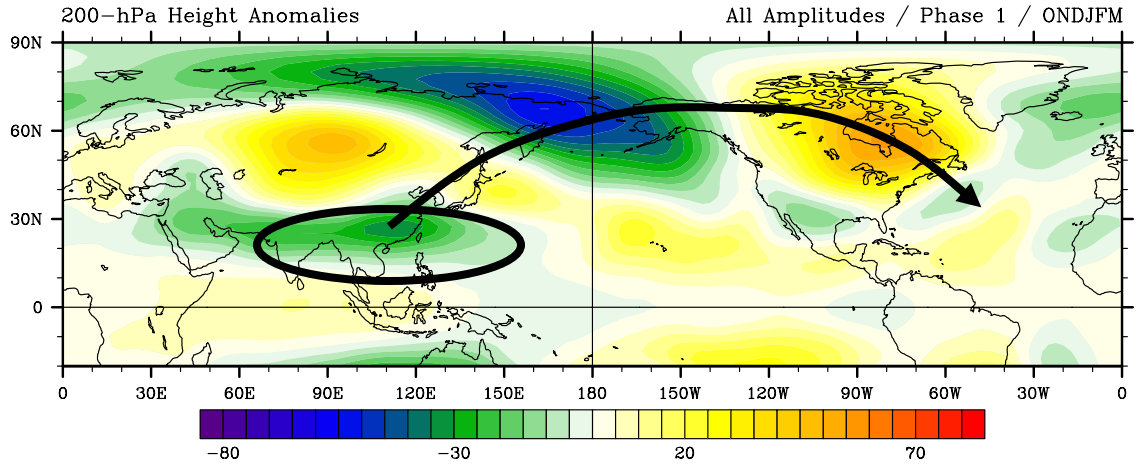

Figure 59. 200-hPa height anomaly for a composite of all MJO events with an amplitude of 1.0 or greater, in phase 1, during October-March, and during EN, LN, or neutral conditions. Black oval indicates tropical Rossby wave response to MJO subsidence over the Maritime Continent. Black arrow indicates the propagation of energy through the anomalous extratropical wave train.

Prior studies of the extratropical impacts of tropical climate variations in general, and the MJO in particular, have focused on the convective component of the climate variation. For example, Mo and Higgins (1998) based their results solely on the convective component in their effort to determine the relationships between intraseasonal oscillation and western CONUS precipitation. Recognition that the subsidence component can excite an extratropical wave train in a similar fashion to its convective counterpart should be useful in guiding future research. Additionally, future research needs to account for the high potential for interference between the anomalous wave trains excited by different components, or by different tropical climate variations. This includes constructive

and destructive interference between the anomalous wave trains excited by the subsidence and convective components of the MJO, or the anomalous wave trains excited by the MJO and a concurrent EN or LN event.

2. Rapid and Smooth Transitions in MJO Phase

As discussed earlier, analyses of numerous MJO composites indicates that there are periods in which the changes in the anomalous extratropical wave train as the MJO changes phase are small, and other periods in which the changes are relatively large and abrupt. In particular, the anomalous extratropical wave train tends to: (1) evolve gradually as the MJO transitions from phase 1 to phase 3; (2) evolve rapidly as the MJO transitions into phases 4 and 5; and (3) evolves gradually between phases 6 and 8. These differences in the evolution of the anomalous wave train may be related to interactions of the MJO convective and subsidence components with the east Asian – north Pacific jet (cf. Sardeshmukh and Hoskins 1988), and/or interference between the wave trains excited by the MJO convective and subsidence components. Of course, understanding of these tendencies in the evolution of the anomalous wave train could be very useful in extended range forecasting, for example in estimating: (1) the predictability of the NPNA response to the MJO; and (2) the uncertainty associated with extended range forecasts.

3. Relationships between MJO Amplitude and MJO Event Days

We also identified an inverse relationship between the amplitude of the MJO and its propagation speed. We found that the number of days it takes the MJO to move through a single phase of the MJO, which we have termed *event days*, tends to increase as the amplitude increases Figure 60 shows this relationship for high, medium, and low amplitude cases, and for OND, JFM, and October-March.

We have hypothesized that this relationship represents variations in the degree of atmosphere-ocean coupling, with: (1) stronger events being stronger because they involve stronger coupling; and (2) stronger events being slower

because stronger coupling reduces the propagation speed to more closely match the speeds of internal oceanic waves which are inherently slower internal atmospheric waves.

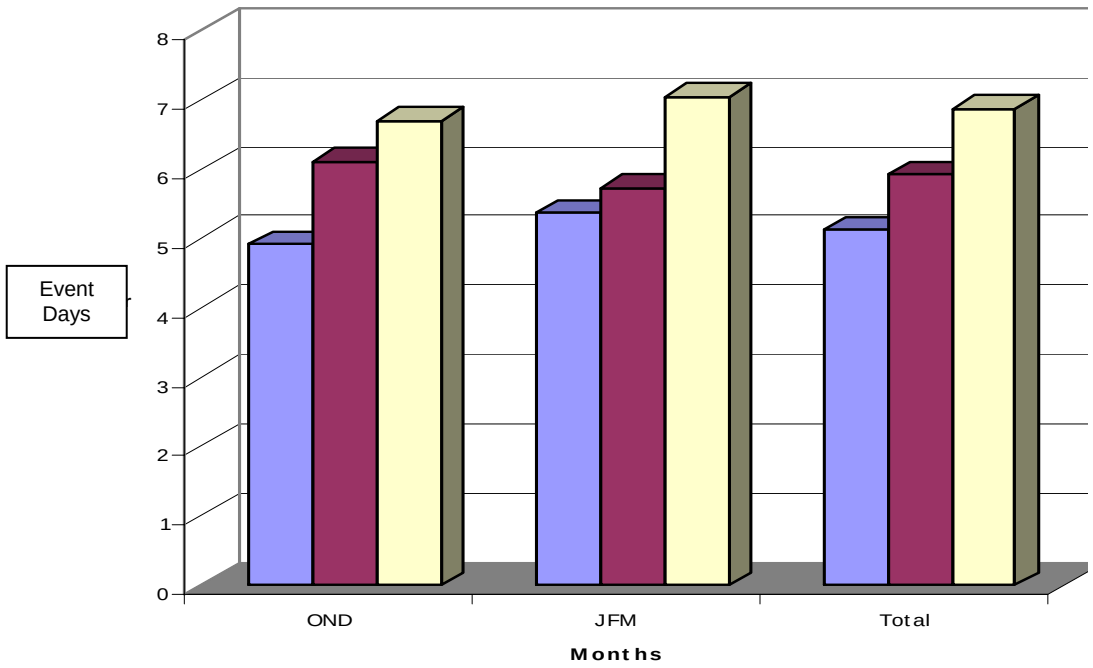

Figure 60. Average number of event days per phase, based on an average of all phases for MJO events with low amplitude (blue), medium amplitude (purple), and high amplitude (yellow), and analyzed by season: OND (left bars), JFM (middle bars), and October-March (right bars). In both fall and winter, stronger MJOs characteristically take 1-2 days longer to progress through a single MJO phase than do weaker MJOs.

The relationship between MJO amplitude and speed has obvious implications for extended range forecasting of the MJO and of the extratropical responses to the MJO. For example, knowledge of the MJO amplitude might be used to improve forecasts of when the MJO will be in a given phase, and how long it will be in that phase. These phase forecasts could then be used to forecast the NPNA response, based, for example, on guidelines that relate MJO phase to NPNA circulation and precipitation (e.g., Table 15).

4. Relationships between the MJO and Southwest Asia

Barlow et al. (2005) researched teleconnections between the MJO and anomalous weather conditions over southwest Asia (SWA). Vorhees (2006) analyzed the impacts of the MJO and several other climate variations on SWA. He found that when the convective and subsidence phases of the MJO were over the IO or Maritime Continent, there were pronounced anomalous upper-level and lower-level tropical Rossby waves over southern Asia, which led to large anomalies in SWA weather and climate. In our study, we found that conditions over SWA are highly sensitive to MJO events. Figures 6 and 59, for phases 3 and 1 of the MJO, illustrate this idea well. In phase 3, the convective component of the MJO is over the eastern IO, and the result is a tropical Rossby wave response centered over SWA in the form of an anomalous upper-level high. In phase 1, the subsidence component of the MJO is over the maritime continent, and the result is a tropical Rossby wave response centered over SWA in the form of an anomalous upper-level low. These MJO impacts on SWA are enhanced when there is a concurrent EN or LN event, and the MJO phase is such that there is constructive interference between the convective and subsidence components of the EN or LN and the MJO (see Table 6). For example, when an EN event is occurring and the MJO is in phases 7-8. In this case, both EN and the MJO cause anomalous subsidence over the maritime continent which sets up an anomalous upper-level cyclone over southern Asia. Vorhees (2006) has shown that enhanced subsidence over the Maritime Continent is associated with anomalously cool and dry conditions in SWA. On the other hand, when a LN event is occurring and the MJO is in phases 4-5, both the LN and MJO cause anomalous convection over the Maritime Continent, leading to an anomalous upper-level anticyclone over southern Asia. Vorhees (2006) showed that this situation lead to anomalously warm and wet conditions in SWA.

E. CONCLUSIONS

Our research has generated a number of preliminary guidelines for using the MJO as a forecast tool, particularly for extended range forecasts of precipitation forecasts in western North America.

We found that the NPNA response to the MJO is highly sensitive to three critical factors: (1) the phase of the MJO; (2) the season in which the MJO occurs and; (3) coexisting El Niño or La Niña conditions. By examining composites based on all possible combinations of these three critical factors, we identified the combinations of critical factors that are associated with positive and negative precipitation anomalies in four regions of western North America. By analyzing composites for which these critical factor these combinations existed, we identified the global and regional scale circulation patterns associated with anomalously wet and dry periods in the four regions. Figures 61-64 show the characteristic patterns that tend to produce anomalously high onshore flow and high precipitation, and offshore flow and low precipitation, for the four regions of western North America that we investigated CA-DSW, PNW, BC, and AK.

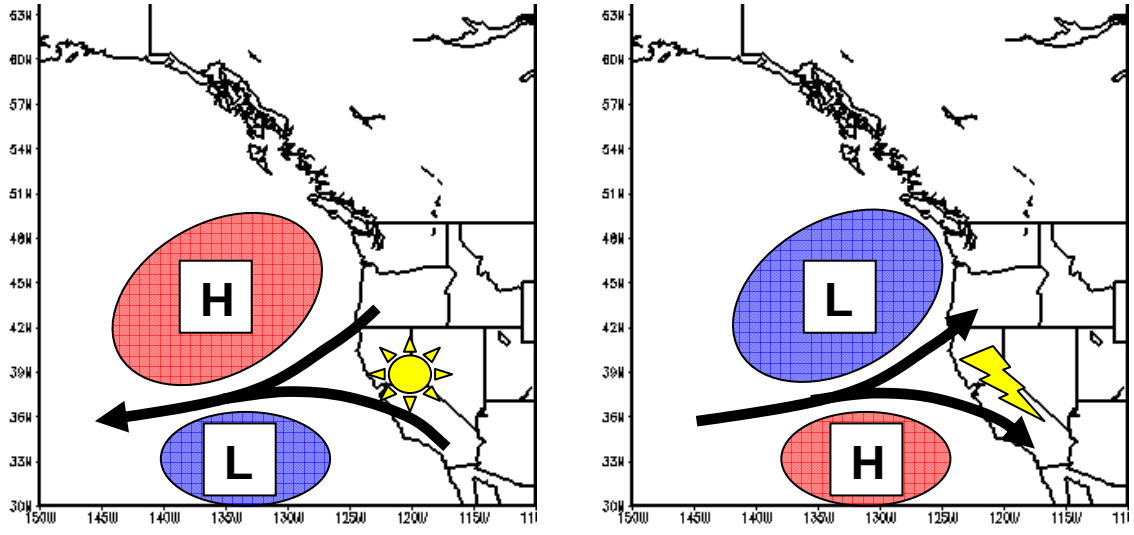

Figure 61. Schematics of low-level anomalous heights and winds flow associated with anomalously dry (left) and wet (right) periods for CA-DSW region.

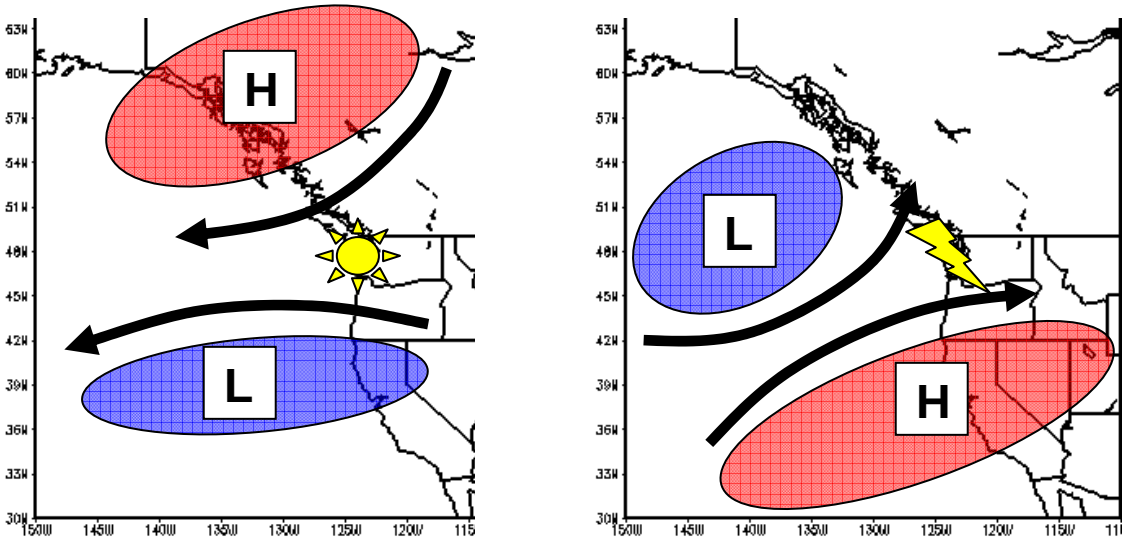

Figure 62. Schematics of low-level anomalous heights and winds flow associated with anomalously dry (left) and wet (right) periods for PNW region.

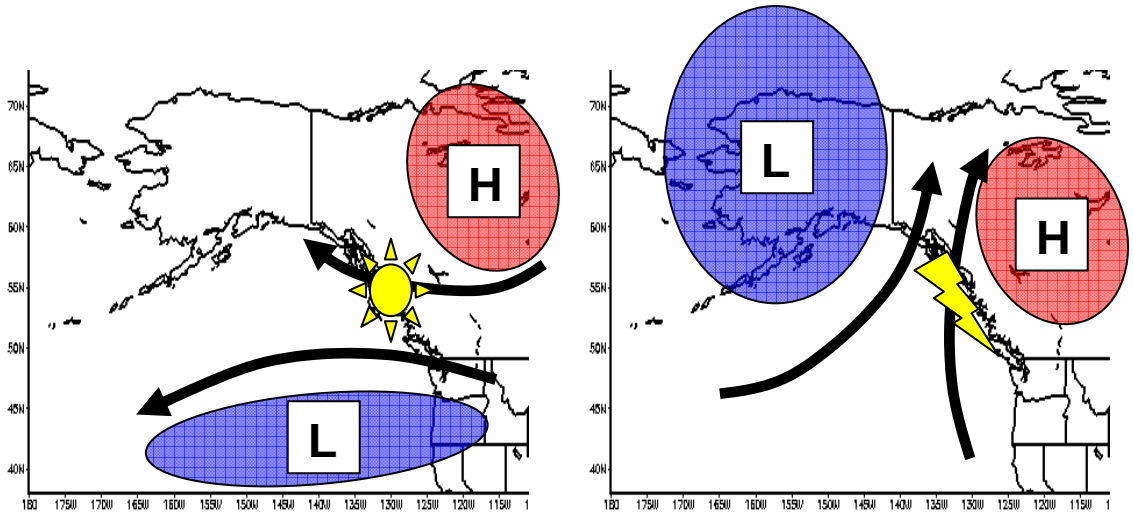

Figure 63. Schematics of low-level anomalous heights and winds flow associated with anomalously dry (left) and wet (right) periods for BC region.

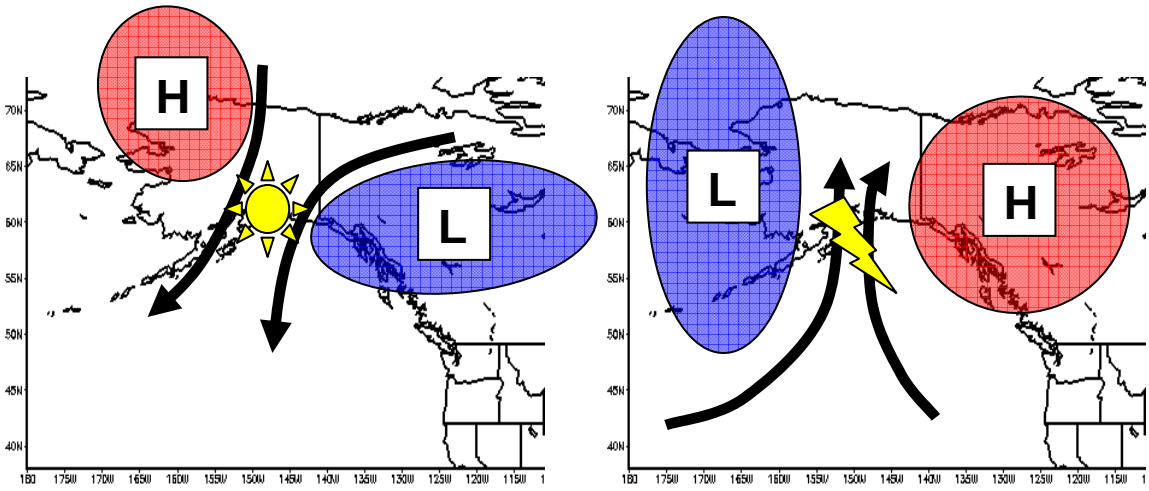

Figure 64. Schematics of low-level anomalous heights and winds flow associated with anomalously dry (left) and wet (right) periods for AK region.

We summarized our results for the four regions in the form of tables listing the MJO, seasonal, background state, and global and regional circulation anomalies that are favorable and unfavorable for anomalously wet and dry conditions in the four regions. These tables represent preliminary guidelines for using MJO information in preparing extended range forecasts. We tested these guidelines by analyzing three individual cases of anomalously high precipitation in the CA-DSW region. We found that the guidelines were consistent with the critical factors and circulation conditions that existed immediately before and during these three anomalously wet events.

Our results indicate that there is a relatively high potential for improving extended range forecast products for western North America through careful analysis and application of information about the state of the MJO, the season in which the MJO is occurring, concurrent background EN or LN conditions, and large scale and regional circulation patterns.

IV. SUMMARY AND CONCLUSIONS

A. SUMMARY

We have investigated atmospheric variables that play a critical role in determining the response of the NPNA circulation and precipitation anomalies to MJO activity. Our main data came from the NCEP/NCAR reanalysis dataset, and we used the Wheeler RMM1/RMM2 index to characterize MJO activity and the MEI index to identify EN, LN, and neutral periods. We constructed and analyzed a wide range of composites (e.g. all MJO events in phase 1 in the fall during a simultaneous El Nino event).

We identified MJO phase, season of MJO occurrence, and concurrent EN/LN/neutral background state as the three factors that are most critical in determining the NPNA response to the MJO. We identified the state of these critical factors, and associated large scale and regional circulation patterns, associated with anomalously wet and dry conditions in four regions of western North America. Individual case studies were then examined to test our results against real world events in which extreme precipitation was associated with MJO activity. For the four western North America regions, we developed and tested guidelines for use by researchers and forecasters in analyzing and forecasting the NPNA circulation and precipitation response to MJO activity.

B. TELECONNECTIONS BETWEEN THE MJO AND NPNA CIRCULATION AND PRECIPITATION

The following results were obtained from our analyses of MJO activity and NPNA circulation and precipitation.

1. MJO activity is highly sensitive to the phase of the MJO.
2. Both the MJO convective and subsidence components induce a tropical Rossby wave response. These Rossby wave responses contribute to anomalous extratropical wave trains.

3. NPNA circulation and precipitation anomalies are sensitive to the season in which the MJO is occurring. Alterations to the background flow characteristics cause the NPNA response to MJO events occurring during the fall season (OND) to differ from those occurring during the winter season (JFM). However, anomalously wet and dry conditions in western North America can occur in either season.
4. Coexisting ENLN conditions strongly affect NPNA response to the MJO. This occurs primarily through modifications of the tropical Rossby wave response to the MJO caused by constructive and destructive interference between the convective and subsidence components of the MJO and ENLN events.
5. Anomalous precipitation periods across western North America exhibit significant differences from region to region. Dipoles in anomalous precipitation are common, with a setup for anomalously high precipitation in one region resulting in anomalously low precipitation in regions to the north and/or south. This is related to the positioning of critical anomalous height patterns, which directly influence the onshore / offshore flow components.

C. DYNAMICAL MECHANISMS FOR MJO TELECONNECTIONS

A key goal of this study was to investigate the methods by which the MJO induces extratropical wave trains over the NPNA region that, in turn, generate anomalous precipitation over western North America. From our analyses, we have identified a chain of events that link the MJO to the NPNA region. Together, these events describe the primary mechanisms by which the MJO impacts the NPNA region.

1. The eastward propagation of the MJO includes the eastward motion of both a region of anomalously strong convection (convective component) and a region of anomalously strong subsidence (subsidence component). The position, extent, and

strength of this anomalous convection and subsidence are altered by the phase of the MJO, the season of MJO occurrence, and any concurrent EN/LN event.

2. Anomalously strong rising (sinking) motion in the convective (subsidence) component of the MJO leads to increased outflow to (inflow from) the poles at the equatorial tropopause.
3. Anomalously strong upper level outflow (inflow) leads to the development of a tropical Rossby wave response to the convective (subsidence) component in the form of an upper-level anticyclone (cyclone).
4. The tropical Rossby wave response helps initiate an anomalous extratropical wave train, leading to anomalous circulation patterns over the NPNA region.
5. The elements of the wave train over the northeast Pacific can create anomalously onshore (offshore) flow in western North America, leading to positive (negative) precipitation anomalies. The sign, areal extent, magnitude, and orientation, of the elements over the northeast Pacific determine the location, sign, and intensity of the western North American precipitation anomalies.
6. Depending on the orientation of the anomalous circulation pattern, anomalous onshore (offshore) flow may develop, leading to anomalously high (low) precipitation over coastal regions of North America, which are related to MJO activity.
7. EN or LN events, if present, set up circulation anomalies in the tropical northeast Pacific that can positively or negatively contribute to the MJO induced onshore and offshore flow anomalies, and to the MJO induced precipitation anomalies.

D. CONTRIBUTIONS OF THIS STUDY

Numerous prior studies have focused on the teleconnections associated with the MJO in various parts of the world, including across the western CONUS.

Our study has confirmed some of the findings of these previous studies. But we have developed a number of new findings about MJO impacts on NPNA circulation and precipitation, due to the many differences between this study and prior studies,. Some of these differences are described below.

1. We used the Wheeler RMM1/RMM2 index to identify MJO events, which is unique to this study. Other studies have simply used bandpass filtering of tropical data to isolate an intraseasonal or intraseasonal-interannual signal. The use of the near real time RMM1/RMM2 index provides a clearer and more detailed description of MJO activity while allowing other climate variations to be accounted for. It is also better suited for developing results that can be readily applied to forecasting processes.
2. We have based most of our analyses on an amplitude based method that allows us to distinguish the response to MJO events of any range of amplitudes (low, medium, high, all amplitudes, etc.). This helps identify a wider and more realistic range of NPNA responses.
3. We have identified critical factors in determining the NPNA response, and then constructed composites based on all possible combinations of those factors. This allowed us to identify the combinations of factors that are most commonly associated with precipitation extremes in western North America, and the large scale and regional circulation patterns associated with those extremes.
4. We used the MEI index to categorize MJO events according to the background El Nino / La Nina / Neutral state.
5. We created lagged composites of all days within each composite to account for the delay in the extratropical response, and to better investigate MJO impacts from a forecasting perspective
6. We investigated individual events for comparison to the composite events and to test our forecasting guidelines.

7. We investigated MJO events up to, and including, the year 2005, which is more recent than any current publication for our regions of interest.
8. We did not apply any filtering to our data. This allowed us to look at actual weather conditions that occurred during an MJO event, which of course is how the situation would appear to forecasters.

These approaches have allowed this study to make important contributions to the research into NPNA teleconnections associated with the MJO. We hope that our study will promote considerable future research into MJO teleconnections in an attempt to improve extended range forecasts for western North America.

E. IMPLICATIONS FOR DEPARTMENT OF DEFENSE FORECASTING

Chapter III, Section B identifies conditions associated with MJO activity that appear to be favorable and unfavorable for anomalous precipitation patterns in western North America. These favorable and unfavorable conditions can be used as preliminary guidelines for developing forecasts of western North American precipitation during or soon after MJO activity. Our investigations of individual cases suggest that these guidelines may be useful in analysis and forecasting. We hope that further research into this topic will lead to much improved guidelines and forecasting aids for both DoD and civilian forecasters.

F. RECOMMENDATIONS FOR FUTURE RESEARCH

In this study, we have applied a variety of new approaches to understanding the impacts of MJO teleconnections on NPNA weather conditions. However, considerable additional research is necessary before the MJO can be confidently utilized as a forecast tool for major western CONUS DoD operations. Specific recommendations for future research include the following:

1. This study has highlighted the potential of the background flow to have a profound effect on the NPNA circulation anomalies that

develop in conjunction with MJO activity. But, except for separating fall cases from winter cases, we did not explore methods through which to classify the background flow and determine its effects. A better understanding of the east Asian – north Pacific jet and other background flow characteristics that are present during MJO events would likely increase the understanding of how the MJO affects the NPNA region, and how and why those effects vary from one MJO to the next.

2. We recommend that additional research be conducted on the lag between a given state of the MJO and the corresponding response in the NPNA region. . In particular, highlighting the anomalously wet and dry periods across a region of interest and then looking back in time to determine the evolution of the important anomalous features would provide insights for improving extended range forecasts.
3. We have created new methodologies (ABM and CFM) through which to composite MJO events. Due to lack of time, we did not investigate all the potentially important amplitude ranges (e.g., extremely high amplitudes). It would be useful to do so, in part to assess the nonlinearity of the response to the MJO. With respect to the CFM, we were able to look at only phase 4 events due to time constraints. Investigating additional phases, primarily phase 3 and phase 5, and tracing each through the lifecycle of the MJO would likely result in a more robust dataset through which to make conjectures.
4. We have investigated the interactions between the MJO and ENLN, but looking into the role that other large-scale oscillations play in influencing the MJO signal across the NPNA region would be valuable. Other global-scale phenomena that should be considered in investigating the interactions of climate different variations

include the Indian Ocean Zonal Mode, intraseasonal variations of the Asian summer monsoon, Pacific Decadal Oscillation, and North Atlantic Oscillation.

5. We recommend that the investigation of MJO teleconnections be expanded to other parts of the globe, including eastern Asia and southwest Asia. Some research has been done by Vorhees (2006) on the impacts of MJO activity on the SWA region, but a more in-depth study focusing on the MJO is desirable.

We hope that this study will lead to more in-depth future studies of the implications of MJO activity for extended range forecast for regions of DoD interest, including the western CONUS. In particular, we hope that the research and findings contained within this study can be improved so that in the near future, DoD weather personnel and their customers can use MJO based forecasts in operational planning.

THIS PAGE INTENTIONALLY LEFT BLANK

LIST OF REFERENCES

Barlow, M. A., M. Wheeler, B. Lyon, and H. Cullen, 2005: Modulation of daily precipitation over southwest Asia by the Madden-Julian Oscillation. *Mon. Wea. Rev.*, **133**, 3579-3594.

Bond, N. A., and G. A. Vecchi, 2003: The influence of the Madden-Julian Oscillation on precipitation in Oregon and Washington. *Wea. Forecasting*, **18**, 600-613.

Gill, A. E., 1980: Some simple solutions for heat-induced tropical circulation. *Quart. J. Roy. Meteor. Soc.*, **106**, 447-462.

Hall, J. D., A. J. Matthews, and D. J. Karoly, 2001: The modulation of tropical cyclone activity in the Australian region by the Madden-Julian Oscillation. *Mon. Wea. Rev.*, **129**, 2970-2982.

Hendon, H. H., and B. Liebmann, 1990: The intraseasonal (30-50 day) oscillation of the Australian summer monsoon. *J. Atmos. Sci*, **47**, 2909-2924.

-------, and K. C. Mo, 1997: Persistent north Pacific circulation anomalies and the tropical intraseasonal oscillation. *J. Climate*, **10**, 223-244.

-------, J. –K. E. Schemm, W. Shi, and A. Leetma, 2000: Extreme precipitation events in the western United States related to tropical forcing. *J. Climate*, **13**, 793-820.

Horel, J. D., and J. M. Wallace, 1981: Planetary-scale atmospheric phenomena associated with the Southern Oscillation. *Mon. Wea. Rev.*, **109**, 813-829.

Jones, C., 2000: Occurrence of extreme precipitation events in California and relationships with the Madden Julian Oscillation. *J. Climate*, **13**, 3576-3587.

Kalnay, E. and Coauthors, 1996: The NCEP/NCAR 40-Year reanalysis project. *Bull. Amer. Meteor. Soc*., **77**, 437-471.

Kistler, R. and Coauthors, 2001: The NCEP-NCAR 50-Year reanalysis: monthly means CD-ROM and documentation. *Bull. Amer. Meteor. Soc*., **82**, 247-267.

Liebmann, B., and C. A. Smith, 1996: Description of a complete (interpolated) outgoing longwave radiation dataset. *Bull. Amer. Meteor. Soc.*, **77**, 1275-1277.

Lorenz, D. J., and D. L. Hartmann, 2006: The effect of the MJO on the North American Monsoon. *J. Climate*, **19**, 333-343.

Madden, R. A., and P. R. Julian, 1971: Detection of a 40-50 Day oscillation in the zonal wind in the tropical Pacific. *J. Atmos. Sci.*, **28**, 702-708.

-------, and P. R. Julian, 1994: Observations of the 40-50-Day tropical oscillation: A Review. *Mon. Wea Rev.*, **122**, 814-837.

Matsuno, T., 1966: Quasi-geostrophic motions in the equatorial area. *J. Meteorol. Soc. Jpn.*, **44**, 25-43.

Mo, K. C., and R. W. Higgins, 1998: Tropical convection and precipitation regimes in the western United States. *J. Climate*, **11**, 2404-2423.

-------, 1999: Alternating wet and dry Episodes over California and intraseasonal oscillations. *Mon. Wea. Rev.*, **127**, 2759-2776.

-------, 2000: Intraseasonal modulation of summer precipitation over North America. *Mon. Wea. Rev.*, **128**, 1490-1505.

Nogués-Paegle, J., and K. C. Mo, 1997: Alternating wet and dry conditions over South America during summer. *Mon. Wea. Rev.*, **125**, 279-291.

Paegle, J. N., L. A. Byerle, and K. C. Mo, 2000: Intraseasonal modulation of South American summer precipitation. *Mon. Wea. Rev*., **128**, 837-850.

Sardeshmukh, P. D., and B. J. Hoskins, 1988: The generation of global rotational flow by steady idealized tropical divergence. *J. Atmos. Sci*, **45**, 1228-1251.

Slingo, J. M., D. P. Rowell, K. R. Sperber, F. Nortley, 1999: On the predictablity of the interannual behavior of the Madden-Julian Oscillation and its relationship with El Niño. *Q. J. R. Meteorol. Soc.*, **125**, 583-610.

Wheeler, M. C., and H. H. Hendon, 2004: An all-season real-time multivariate MJO index: Development of an index for monitoring and prediction. *Mon. Wea. Rev.*, **132**, 1917-1932.

Whitaker, J. S., and K. M. Weickmann, 2001: Subseasonal variations of tropical convection and week-2 prediction of wintertime western North American rainfall. *J. Climate*, **14**, 3279-3288.

Wolter, K., and M. S. Timlin, 1993: Monitoring ENSO in COADS with a seasonally adjusted principal component index. *Proc. Of the 17th Climate Diagnostics Workshops*, Norman, OK, NOAA/N MC/CAC, NSSL, Oklahoma Clim. Survey, CIMMS and the School of Meteor., Univ. of Oklahoma, 52-57.

Zhang, C., 2005: Madden-Julian Oscillation. *Rev. Geophys*., 43, **RG2003**, 1-36.

THIS PAGE INTENTIONALLY LEFT BLANK

INITIAL DISTRIBUTION LIST

1. Defense Technical Information Center
   Ft. Belvoir, Virginia

2. Dudley Knox Library
   Naval Postgraduate School
   Monterey, California

3. Meteorology Department
   Code ME/WA
   Naval Postgraduate School
   Monterey, California

4. Dr. Tom Murphree
   Code MR/ME
   Naval Postgraduate School
   Monterey, California

5. Dr. Carlyle Wash
   Code MR/WX
   Naval Postgraduate School
   Monterey, California